Technical Report Documentation Page

1. Report No.	2. Government Accession No.	3. Recipient's Catalog No.
FHWA/TX-05/0-4203-3		

4. Title and Subtitle	5. Report Date
EVALUATION OF SELECTED LABORATORY PROCEDURES AND DEVELOPMENT OF DATABASES FOR HMA	January 2005
	6. Performing Organization Code

7. Author(s)	8. Performing Organization Report No.
Amit Bhasin, Joe W. Button, and Arif Chowdhury	Report 0-4203-3

9. Performing Organization Name and Address	10. Work Unit No. (TRAIS)
Texas Transportation Institute The Texas A&M University System College Station, Texas 77843-3135	11. Contract or Grant No. Project 0-4203

12. Sponsoring Agency Name and Address	13. Type of Report and Period Covered
Texas Department of Transportation Research and Technology Implementation Office P. O. Box 5080 Austin, Texas 78763-5080	Technical Report: September 2001 - August 2004
	14. Sponsoring Agency Code

15. Supplementary Notes

Project performed in cooperation with the Texas Department of Transportation and the Federal Highway Administration.

Project Title: Strategic Study for Resolving Hot Mix Asphalt Related Issues

16. Abstract

The objectives of this research project were to develop and validate laboratory test protocols for measuring rut-susceptibility of hot mix asphalt (HMA) mixtures; to identify the best available laboratory test protocol(s) for predicting moisture susceptibility of HMA paving mixtures; and to develop a TxDOT HMA test database to be used for evaluating and/or validating the proposed AASHTO mechanistic-empirical pavement design guide.

Twelve field mixes and three lab mixes were tested using Asphalt Pavement Analyzer (APA), Hamburg, Dynamic Modulus, Flow Time, Flow Number, and Simple Shear at Constant Height for the evaluation of rutting tests. Mixture parameters resulting from different tests were ranked and compared with APA rut depth as a base. Rankings of the different parameters were analyzed using statistical techniques. Findings indicate that flow time and flow number tests capture fundamental material properties and should be considered for inclusion in the mixture design and selection processes. Caution must be exercised in interpreting rut susceptibility of mixes based on the E* parameters, especially when evaluating mixtures containing polymer-modified asphalts.

Nine mixtures were tested using the Hamburg. Their individual aggregates and binders were tested for surface energy measurement using Universal Sorption Device and Wilhelmy plate method, respectively. Mixtures with and without antistripping agents like hydrated lime and commercially available liquid antistripping agents were tested. Within groups of controlled mixes, the calculated bond strength based on surface energy measurements relates well with the deformation data from the Hamburg test.

About 30 plant-produced mixes and 50 lab-produced field mixes were tested using the Hamburg and dynamic modulus devices. Plant-produced mixes were tested for production verification and lab-produced mixes were tested to develop a mixture database for future use, especially for the AASHTO design guide.

17. Key Words	18. Distribution Statement
Dynamic Modulus, Moisture Susceptibility, Rutting Resistance	No restrictions. This document is available to the public through NTIS: National Technical Information Service 5285 Port Royal Road Springfield, Virginia 22161 http://www.ntis.gov

19. Security Classif.(of this report)	20. Security Classif.(of this page)	21. No. of Pages	22. Price
Unclassified	Unclassified	163	

Form DOT F 1700.7 (8-72) **Reproduction of completed page authorized**

EVALUATION OF SELECTED LABORATORY PROCEDURES AND DEVELOPMENT OF DATABASES FOR HMA

by

Amit Bhasin
Graduate Research Assistant
Texas Transportation Institute

Joe W. Button
Research Engineer
Texas Transportation Institute

and

Arif Chowdhury
Associate Transportation Researcher
Texas Transportation Institute

Report 0-4203-3
Project Number 0-4203
Project Title: Strategic Study for Resolving Hot Mix Asphalt Related Issues

Performed in cooperation with the
Texas Department of Transportation
and the
Federal Highway Administration

January 2005

TEXAS TRANSPORTATION INSTITUTE
The Texas A&M University System
College Station, Texas 77843-3135

DISCLAIMER

The contents of this report reflect the views of the authors, who are responsible for the facts and the accuracy of the data presented herein. The contents do not necessarily reflect the official view or policies of the Federal Highway Administration (FHWA) or the Texas Department of Transportation (TxDOT). This report does not constitute a standard, specification, or regulation. The engineer in charge was Joe W. Button, P.E., (Texas, # 40874).

ACKNOWLEDGMENTS

Mr. Dale Rand, P.E., director of the Flexible Pavement Branch, was instrumental in developing and initiating this project. Mr. Gregory S. Cleveland, P.E., technical operations manager, Materials and Pavements Section of the TxDOT Construction Division, served as project director (PD) for this research effort. Mr. John Rantz, director of Construction, Lubbock District, served as program coordinator (PC). Their suggestions and support during the accomplishment of this project are hereby acknowledged. Several TxDOT districts supplied plant-mixed and raw materials and thus rendered significant help to this research project.

Appreciation is extended to the Texas Department of Transportation and the Federal Highway Administration for the financial support provided and to the Pavements and Design Research Management Committee.

TABLE OF CONTENTS

Page

LIST OF FIGURES

Page

LIST OF TABLES

Page

CHAPTER 1:
INTRODUCTION

GENERAL

Approximately 94 percent of paved roads in Texas are asphalt pavements. Each year, rehabilitation of these existing roads and construction of new roads require about 12 million tons of hot mix asphalt (HMA), which equates to approximately $500,000,000. The investment of the citizens of Texas in the current road networks is surely in the trillions of dollars. As pavement engineers it behooves us to employ the latest technology to manage and expand the system in the safest and most efficient manner possible.

BACKGROUND

Historically, most hot mix pavements in Texas have performed acceptably. Yet, in recent years, an increasing number of HMA pavements demonstrated unacceptable performance, particularly related to rutting, moisture damage, segregation, and high in-place air voids. Contributors to this apparent reduction in performance include increased traffic volumes, truck traffic and weight, and congestion. Some highways of Texas have experienced a 20 percent annual growth in truck traffic, and the number of equivalent single axle loads (ESALs) on these roads has increased 600 percent since 1970! Consequently, HMA mixtures and pavement design strategies that have historically performed well are now being decimated.

Relatively new protocols have been developed that have demonstrated improved ability to predict potential HMA pavement failures. The asphalt pavement analyzer (APA) and Hamburg wheel tracking device (HWTD) are two torture testing devices that are gaining popularity due to their ability to identify (and thus avoid) mixtures that may be susceptible to premature failure, particularly due to rutting and moisture damage. National Cooperative Highway Research Program (NCHRP) Project 9-19 developed a series of "Simple Performance Tests" (SPTs) to characterize and measure the fundamental properties of HMA mixture. Procedures recently developed at the Texas Transportation Institute for measuring surface energy of aggregate and asphalt have opened the door for predicting moisture susceptibility of asphalt mixtures.

The Texas Department of Transportation (TxDOT) initiated Research Project 0-4203 in 2001 with broad objectives to study selected HMA-related issues and create a mixture database

for future use. The portion of the project reported herein focuses primarily on rutting and moisture susceptibility of HMA mixtures. TxDOT is considering adoption of the mechanistic-empirical (M-E) pavement design procedure being developed by American Association of State Highway and Transportation Officials (AASHTO). Not all of the design inputs required for this pavement design guide are currently readily available to TxDOT.

OBJECTIVE

The overall objective of the research reported herein is to provide the tools for TxDOT to design and control HMA materials for pavements that will meet the increasing performance demands. Specific objectives of the tasks include:

- develop and validate laboratory test protocols for measuring rut-susceptibility of HMA mixtures,
- identify the best available laboratory test protocol(s) for predicting moisture susceptibility of HMA paving mixtures,
- analyze HMA plant production mixtures to determine if TxDOT specifications are adequate to produce mixtures that are resistant to different distresses, and
- measure dynamic modulus and other properties of TxDOT HMA mixtures to establish a database of mix properties that can be used as inputs for the mechanistic-empirical (proposed by AASHTO) pavement design guide.

SCOPE OF WORK REPORTED

Research Project 0-4203 contained several tasks that had little or no interconnection. Some tasks have previously been documented in other reports (Research Reports 0-4203-1, 0-4203-2, and 0-4203-4). This report mainly covers four different tasks performed under this project.

Chapter 1 provides a brief introduction, background, and specific objectives of Tasks 3, 5, and 7 of the project.

Chapter 2 documents the effort and results related to the evaluation of laboratory test protocols for predicting HMA rutting. Several appendices present the detailed results from this task.

Chapter 3 describes the research effort conducted to evaluate the laboratory test protocols for predicting the moisture susceptibility of HMA. Detailed results of this task are documented in the indicated appendices.

Chapter 4 summarizes the laboratory tests conducted with plant-produced and laboratory-produced HMA mixtures collected from different districts of TxDOT during the 3-year period of this research project. Raw and analyzed data from these laboratory tests are provided to TxDOT in electronic form copied onto a CD-ROM.

Chapter 5 discusses the conclusions and recommendations resulting from the tasks addressed in this report.

Appendices A through I contains the detailed results of the tests conducted to accomplish the stated objectives.

CHAPTER 2:
EXAMINATION OF LABORATORY TEST PROTOCOLS FOR PREDICTING RUTTING

BACKGROUND AND OBJECTIVE

The main objective of this subtask was to develop and validate laboratory test protocols for measuring rut-susceptibility of HMA mixtures. Specifically, the ability to accurately assess the rut-susceptibility of asphalt mixtures used in Texas is one of the primary goals of this project.

The research work presented in this report overlapped with some of the ongoing tests that were conducted as a part of the FHWA Project No. 9-558 (Bhasin et al., 2003) which had similar objectives for the south central region of the USA. Researchers felt that more conclusive inferences can be drawn if the data from both efforts are collectively analyzed, which indeed proved to be the case. The current report is therefore based on the analysis of 14 HMA mixes, of which, four are field mixes from Texas, three are laboratory designed mixes using aggregates from Texas, and seven are field mixes from neighboring states including Arkansas, Arizona, Oklahoma, Louisiana, and New Mexico. However, due to differences in the experiment design of both projects, not all tests were conducted on all 14 mixes. For the purpose of analysis, these mixes were divided into two groups of twelve and seven mixes with five mixes common to both groups. Similar analytical tools were used on both groups to draw conclusions. The following sections of this Chapter present more details about these mixtures and methods of analysis.

Material Selection

A total of fourteen mix designs were selected for this research. Four of these mix designs were field mixes from various districts in Texas. Three mix designs were developed in the Texas Transportation Institute (TTI) laboratory using aggregates from various districts in Texas to achieve certain desired properties for the purpose of this research. These mixes with their properties are listed below:

- a highly rut-susceptible mix using rounded siliceous river gravel and a PG 64-22 asphalt,
- a rut-resistant mix with low modulus using rhyolite aggregate and a highly polymer-modified asphalt, and

• a mix similar to the one above but using crushed siliceous river gravel aggregates in place of angular aggregates with the highly polymer-modified asphalt.

The highly polymer-modified asphalt mentioned above had a polymer content near 6 percent; whereas, a usual value is about 1 to 2 percent. Additionally, seven field mixes from the south central states were included. Table 2.1 summarizes these 14 mix designs. Appendix A details the gradations of the aggregates.

Note that the selected mix designs have widely different binder grades, maximum nominal aggregate size, and gradations. Typically, one would expect some kind of control over the binder grade or aggregate properties in selection of candidate materials. However, this is not the case for the present set of materials because the purpose of this experiment was not to evaluate rut resistance of a mixture as a function of its material properties but instead to evaluate the test procedures that are used to assess rut resistance of mixtures. Therefore, the factors that need to be controlled are the environmental and loading conditions of the test. It is also necessary to select a set of materials that demonstrate a broad range of physical properties that affect rut resistance to evaluate the test procedures over a broad range of values.

The selected mixtures were from a variety of geographic locations and designed for different traffic loads. It must be noted that, if a mix is ranked as poor-performing in this experiment, it does not necessarily imply that the mix will perform poorly in the field as well or vice versa. For example, when a mix designed for low-temperature application (say with PG 64-xx) is compared with a mix designed for high temperature application (say with PG 82-x) and both are compared based on test results at 130°F, it is imperative that the latter will outperform the former, but it does not necessarily imply that this will be the case in field. However, since the subject of the evaluation is the test procedure and not the material, it is important to maintain the same test environment for all mixtures in order to provide identical bases for comparing the results.

Table 2.1. Details of Selected Mixtures.

Sl. No.	Mix ID	Origin (Mix Code)	Max Nom. Agg. Size, mm	Type	Binder Grade	Additives	Design AC %	Design Air Voids, %	Remarks
1	9.5 mm Twin Lakes Gravel Tosco	Arkansas DOT (ARTL)	9.5	Creek Gravel	PG 64-22	Nil	6.0	4.5	
2	9.5 mm Granite Mountain Lyon	Arkansas DOT (ARLR)	9.5	Granite	PG 64-22	0.5% Morelife 300	5.8	4.5	
3	Basalt (below restricted zone)	Arizona DOT (AZ)	19	Basalt	PG 64-22	1.5% Type II Cement	5.0	5.0	
4	Nova Scotia Granite	Louisiana DOT (LA)	12.5	Granite	PG 70-22M	0.6% Anti-strip	4.7	4.0	Level 1 mix design
5	12.5 mm Crushed Gravel, Bingham	New Mexico DOT (NM Bingham)	12.5	Hard Rock Crushed Gravel	PG 70-22	1.5% Lime	4.3	4.0	
6	19 mm Monzonite Vado	New Mexico DOT (NMVado)	19	Monzo-nite	PG 82-16	None	4.8	4.0	
7	12.5 mm Granite/ Limestone	Oklahoma DOT (OK)	12.5	Granite + Limestone	PG 70-28	None	4.8	4.0	
8	12.5 mm Stone Filled Wichita Falls	Texas DOT (TXWF)	12.5	Limestone	PG 76-22	1% Lime	4.8	4.0	
9	CMHB-C Bryan	Texas DOT (TXBryan)	12.5	Limestone	PG 64-22	None	4.6	3.5	
10	Rounded Gravel Mix	Lab Mix (ROG)	9.5	Rounded River Gravel	PG 64-22	None	5.5	4.0	Lab Rut Susceptible
11	9.5 mm Crushed Gravel	Lab Mix (64-40RG)	9.5	Crushed River Gravel	PG 64-40	None	5.5	4.0	Low Modulus High Recovery
12	Rhyolite	Lab Mix (64-40RHY)	9.5	Rhyolite	PG 64-40	None	7.8	3.5	Low Modulus High Recovery
13	Traprock	Texas DOT (TXCO)	19 (3/4")	SMA	PG 70-22	None	5.5	4.0	Designed using TGC
14	Limestone	Texas DOT (TXYK)	19	Type C	PG 76-22	None	4.6	4.0	Designed using TGC

Experiment Design

This research includes the following test protocols:

- Hamburg wheel tracking device,
- Asphalt Pavement Analyzer,
- frequency sweep at constant height test (FSCH),
- dynamic modulus,
- flow time (static creep), and
- flow number (dynamic creep).

Hamburg and APA tests were selected to represent a simulative type of performance prediction test or torture test. As mentioned earlier, 12 mixtures were tested using the APA and seven using the Hamburg, including five mixes that were common to both tests. The dynamic modulus, flow time, and flow number tests comprised the "Simple Performance Tests" recommended by NCHRP Project 9-19 (Witczak et al., 2002). These three tests were conducted on all 14 mixes. FSCH was developed as a part of the original performance prediction model in the Strategic Highway Research Program (SHRP). All tests that were conducted on individual mix designs are summarized in Table 2.2.

A brief description of each of the selected test methods along with the parameters related to rutting are described in the following subsections. For the dynamic modulus, flow time, and flow number tests, the specimens were 4 inches in diameter and 6 inches in height with a gauge length of 4 inches. Technicians prepared the specimens by coring and sawing the ends of a 6-inch diameter and 7-inch height specimen, which was compacted using a Superpave gyratory compactor (SGC). Air voids in the cored and finished specimens were ensured to be between 6 and 8 percent. All APA and FSCH test specimens were also prepared using the SGC.

Hamburg Wheel Tracking Test

The Hamburg test was performed by oscillating an 8.0-inch diameter and 1.85-inch wide steel wheel loaded with 158 lb over a SGC compacted specimen 2.5 inches in height submerged in water at a temperature of 122°F. Permanent deformation of each specimen was recorded with reference to the number of passes of the loaded wheel. Mixtures exhibiting susceptibility to moisture damage tend to undergo stripping and usually exhibit a sudden increase in the slope of a

plot of rut depth versus the number of passes after a certain number of cycles. However, this phenomenon was not observed for any of the mixes.

Table 2.2. Matrix of Experiments for Task 3a.

Sl. #	Sample ID	APA	SST	DM	FN	FT	Hamburg
1	ARTL	X	X	X	X	X	
2	ARLR	X	X	X	X	X	
3	AZ	X	X	X	X	X	
4	LA	X	X	X	X	X	
5	NMBingham	X	X	X	X	X	
6	NMVado	X	X	X	X	X	
7	OK	X	X	X	X	X	
8	TXWF	X	X	X	X	X	X
9	TXBryan	X	X	X	X	X	X
10	ROG	X	X	X	X	X	X
11	64-40RG	X	X	X	X	X	X
12	64-40RHY	X	X	X	X	X	X
13	TXCO			X	X	X	X
14	TXYK			X	X	X	X

Final rut depth at 20,000 cycles was considered as a parameter representative of rut-susceptibility of the mix. This test was conducted until the specimen reached a rut depth of one-half inch or 20,000 cycles, whichever came first. For mixes that failed before 20,000 cycles, the final rut depth at 20,000 cycles was extrapolated from the test data.

Asphalt Pavement Analyzer

The APA is a loaded wheel tester that about 35 state Department of Transportations (DOT) have adopted as a torture test device to evaluate or qualify their HMA paving mixtures. The APA test typically involves oscillating a loaded grooved wheel back and forth (counted as one cycle) over a pressurized rubber hose that rests on the test specimen. The APA test was conducted in a dry condition at a temperature of 140°F with a hose pressure of 100 psi and a vertical load of 100 lb. Three pairs of specimens 3 inches in height and 6 inches in diameter were tested. Data from each pair were recorded to one channel resulting in three replicate data sets.

The parameters related to rutting from the APA test are:

- Final rut depth at 8000 cycles (the test is terminated if a rut depth of one-half inch is reached before 8000 cycles, in which case the value extrapolated to 8000 cycles is considered as the final rut depth).
- Creep slope of the linear portion of the rut depth versus number of cycles curve, expressed as of millimeters of rut depth/thousand cycles.

Dynamic Modulus Test

This test is used to estimate the dynamic modulus of a HMA mix at different temperatures and loading rates. For the present research, dynamic modulus tests were conducted in accordance with NCHRP 1-37A, "Draft Test Method for Dynamic Modulus Test," at 25, 10, 5, 1, 0.5, and 0.1 Hz (sinusoidal loading) and 14, 40, 70, 100, and 130°F. The peak stress level for measuring the dynamic modulus was chosen in order to maintain the total measured strain within 50 to 150 microstrain. All tests were conducted on two replicates with three axial linear variable differential transducers (LVDTs) on each replicate to record the strain. The order for conducting each test was from lowest to highest temperature and highest to lowest frequency of loading at each temperature to minimize specimen damage. The matrix of data generated from this test can be represented in the form of a single master curve which can then be used to estimate the modulus of the mix at any given loading rate or temperature (details covered in Chapter 4).

Witczak et al. (2002) compared the E* and E*/sin ϕ values from dynamic modulus tests with actual pavement rutting using the WesTrack and Accelerated Loading Facility (ALF) test data. Comparisons were made for a wide variety of frequencies, temperatures, and test conditions (confined and unconfined), and correlations of varying degrees were found. The parameters related to rutting that were measured in this project are:

- E* and E*/sin ϕ at 10 Hz and 130°F, and
- E* and E*/sin ϕ at 1 Hz and 130°F

where,

$$|E^*| = \frac{\sigma_0}{\varepsilon_0},$$

σ_o = axial stress,
ε_o = is the axial strain, and
ϕ = is the phase angle between measured strain and applied stress.

Rationale for selecting the high temperature was based on earlier research (Witczak et al., 2002). Rationale for selecting 10 Hz was based on the fact that this frequency most closely represents highway speeds of about 60 miles per hour based on equivalent pulse time conversion for sinusoidal loading (Barksdale, 1971). To compare these results with the APA results, a frequency of 1Hz was selected from the dynamic modulus test data. The frequency of 1Hz was arrived at using the aforementioned pulse time conversion for an APA loading arm that moves at 60 strokes per minute with a travel of 12 inches.

Flow Time (Static Creep)

In a static creep test the specimen is subjected to a constant stress level at a given temperature. Resulting strain is measured over a certain period of time or until the sample fails. Total compliance at any given point in time is calculated as the ratio of the measured strain to the applied stress. The flow time test is one of the simple performance tests that correlated well with the field rutting performance of mixes in the NCHRP Project 9-19 (Witczak et al., 2002). The test was performed under unconfined conditions at a single temperature of 130°F and stress of 30 psi. Two replicate specimens were tested using three axial LVDTs on each sample to record the strain.

The parameters related to rutting from the flow time test that are included in this project are:

- flow time value,
- flow time slope, and
- flow time intercept.

The flow time value is defined as the time at which the rate of change of compliance is minimum. The flow time value and flow time intercept can be obtained graphically from the log compliance versus log time plot. All three parameters are depicted in a typical plot, as shown in Figures 2.1 and 2.2. Bhasin et al. (2003) provide more details about the origin and interpretation of these parameters.

Two important aspects of this test are selecting the test temperature and stress level. In practice, it is recommended that, when comparing mix designs for a specific location, the effective temperature, T_{eff}, for that location be used as the test temperature. The effective temperature is based on historical temperature data for the location where the HMA is to be placed. The selected stress level must not be very high as this might cause rapid sample failure rendering the test insensitive to differences between mixes. Conversely, the stress level should be large enough so that the sample reaches the tertiary flow zone (as shown in Figure 2.1) within a reasonable testing time.

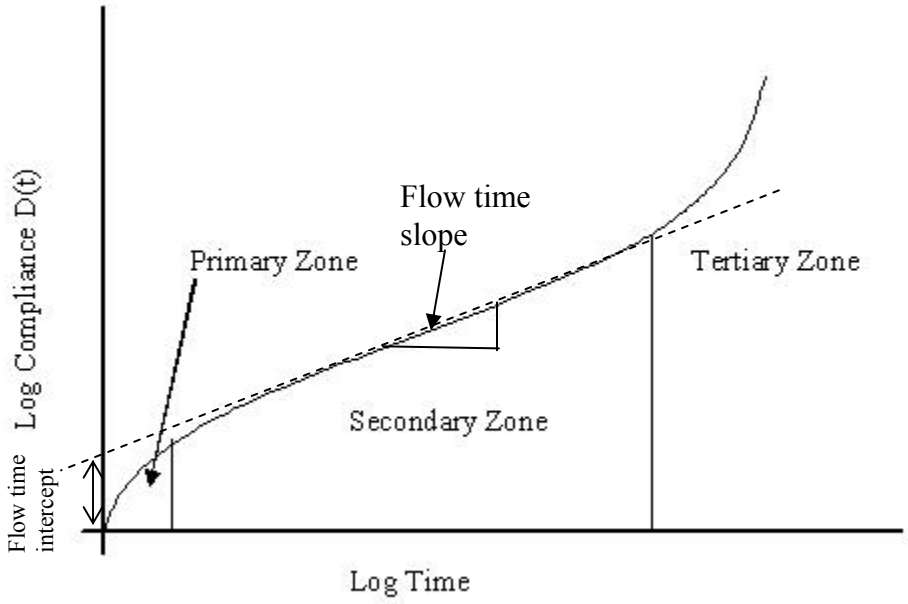

Figure 2.1. Compliance versus Time Curve on Log Scale.

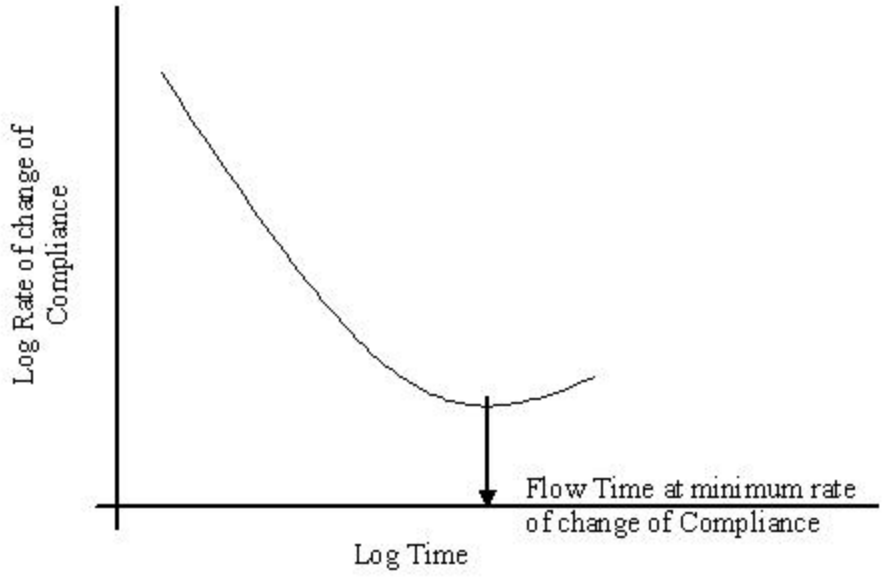

Figure 2.2. Rate of Change of Compliance versus Time on Log Scale.

Flow Number (Dynamic Creep)

The basic difference between this test and the static creep test is that it involves application of stress in a dynamic form. The stress is applied in a haversine wave form with a wavelength of 0.1 seconds followed by a rest or dwell period of 0.9 seconds. Each load cycle (lasting 1.0 second) is therefore composed of a stress application and a rest period. In terms of sample response, this test allows for periodic recovery of the sample. All tests were conducted at a temperature of 130°F with a peak stress level of 30 psi using two replicates with three axial LVDTs on each replicate to record the strain.

The parameters related to rutting from the flow number test included in this project are:

- flow number value, and
- flow number slope.

The flow number value and slope are derived in exactly the same way as the flow time value and flow time slope with the exception that the number of load cycles is plotted on the x-axis in place of the loading time. The flow number intercept was not included in the analysis,

as other studies have demonstrated that this parameter does not correlate well with field performance (Witczak et al., 2002).

Frequency Sweep at Constant Height Test. Frequency sweep at constant height was performed at 14, 60, and 104°F over a range of frequencies (10, 5, 2, 1, 0.5, 0.2, 0.1, 0.05, 0.02, and 0.01 Hz). Other researchers (Zhang et al., 2002; Chowdhury and Button, 2003) have confirmed a sound correlation between the repeated shear at constant height test and laboratory rutting tests (APA and Hamburg, respectively).

Parameters related to rutting that are included in the analysis are:

- G* and G*/sin δ at 10 Hz at a temperature of 104°F, and
- G* and G*/sin δ at 1 Hz at a temperature of 104°F.

Where,

$$|G^*| = \frac{\tau_0}{\gamma_0},$$

τ_o = shear stress,

γ_o = shear strain, and

δ = phase angle between measured strain and applied stress.

The rationale for selecting frequencies of 10 Hz and 1Hz are the same as those described for the dynamic modulus test, i.e., these frequencies represent the loading of samples due to typical highway speeds and the APA arm, respectively.

TEST RESULTS

A total of six tests were selected for mutual comparison. Some of the tests, such as the dynamic modulus and FSCH, were conducted at a number of frequencies and temperatures. However, only data for the selected parameters, as described earlier, are reported in this section. Remaining data are reported in Appendix B of this report. Data for the selected parameters are provided in Tables 2.3 to 2.18.

Table 2.3. Summary of APA Rut Depth Results.

Mix No.	Mix Identity	Final Permanent Deformation (mm)				CV, %	Final Count
		Left	Middle	Right	Average		
1	ARTL	8.6	8.0	7.9	8.2	5	8000
2	ARLR	11.5	12.1	10.5	11.3 (18.9)[1]	7	3865 (8000)
3	AZ	4.2	4.3	4.7	4.4	6	8000
4	LA	7.5	7.9	6.2	7.2	12	8000
5	NMBingham	2.6	2.9	2.1	2.5	16	8000
6	NMVado	---	2.3	1.8	2.0	18	8000
7	OK	4.7	4.3	3.8	4.2	11	8000
8	TXWF	3.3	4.0	3.5	3.6	10	8000
9	TXBryan	5.3	4.9	3.9	4.7	15	8000
10	ROG	19.8	17.0	16.8	17.9 (19.1)[1]	9	6201 (8000)
11	64-40RG	6.4	6.5	6.1	6.3	3	8000
12	64-40RHY	3.8	3.7	3.8	3.8	1	8000

CV – Coefficient of Variation

[1] Value in brackets is an extrapolated value

Table 2.4. Summary of APA Creep Slope Values.

Mix No.	Mix Identity	Slope (mm/thousand cycles)				CV, %
		Left	Middle	Right	Average	
1	ARTL	0.528	0.438	0.491	0.49	9.4
2	ARLR	2.011	1.741	1.554	1.77	13.0
3	AZ	0.207	0.158	0.248	0.20	21.9
4	LA	0.268	0.282	0.302	0.28	5.9
5	NMBingham	0.147	0.292	0.151	0.20	41.9
6	NMVado	---	0.100	0.079	0.09	16.4
7	OK	0.281	0.299	0.202	0.26	19.7
8	TXWF	0.273	0.284	0.330	0.30	10.2
9	TXBryan	0.181	0.113	0.134	0.14	24.1
10	ROG	0.622	0.703	0.628	0.65	6.9
11	64-40RG	0.557	0.422	0.468	0.48	14.2
12	64-40RHY	0.155	0.189	0.242	0.19	22.6

CV – Coefficient of Variation

Table 2.5. Summary of Hamburg Wheel Tracking Test Results.

Sample No.	Mix Quality	Hamburg Rut Depth (mm)	Number of Passes
8	TXWF	8.9	20,000
9	TXBryan	4.6	20,000
10	ROG	12.1 (47.6)[1]	4541 (20,000)
11	64-40RG	9.2 (38.1)[1]	4300 (20,000)
12	64-40RHY	5.4	20,000
13	TXCO	2.17	20,000
14	TXYK	3.72	20,000

[1] Value in brackets is an extrapolated value assuming no stripping occurred

Table 2.6. Summary of E* at 54.4°C and 10 Hz.

Mix No.	Mix Quality	E* (MPa)			CV, %
		Sample 1	Sample 2	Average 1000 MPa	
1	ARTL	1323	848	1.1	31
2	ARLR	390	480	0.4	15
3	AZ	826	913	0.9	7
4	LA	712	794	0.8	8
5	NMBingham	1518	1771	1.6	11
6	NMVado	1625	1978	1.8	14
7	OK	629	406	0.5	31
8	TXWF	1120	1035	1.1	6
9	TXBryan	1145	1312	1.2	10
10	ROG	591	786	0.7	20
11	64-40RG	211	231	0.2	6
12	64-40RHY	507	405	0.5	16
13	TXCO	2156	1997	2.1	5
14	TXYK	2204	1858	2.0	12

CV – Coefficient of Variation

Table 2.7. Summary of E*/sin ϕ at 54.4°C and 10 Hz.

Mix No.	Mix Quality	E*/sin ϕ (MPa)			CV, %
		Sample 1	Sample 2	Average 1000 MPa	
1	ARTL	2753	1475	2.1	43
2	ARLR	734	864	0.8	12
3	AZ	1792	1798	1.8	0.2
4	LA	1402	1367	1.4	2
5	NMBingham	3896	4982	4.4	17
6	NMVado	4915	5159	5.0	3
7	OK	1140	855	1.0	20
8	TXWF	3037	2327	2.7	19
9	TXBryan	2421	2517	2.5	3
10	ROG	1180	1773	1.5	28
11	64-40RG	872	729	0.8	13
12	64-40RHY	1673	1250	1.5	21
13	TXCO	3130	3190	3.2	1
14	TXYK	5097	4086	4.6	16

CV – Coefficient of Variation

Table 2.8. Summary of E* at 54.4°C and 1 Hz.

Mix No.	Mix Quality	E* (MPa)			CV, %
		Sample 1	Sample 2	Average 1000 MPa	
1	ARTL	453	263	0.4	37
2	ARLR	135	147	0.1	6
3	AZ	333	347	0.3	3
4	LA	239	272	0.3	9
5	NMBingham	769	894	0.8	11
6	NMVado	854	992	0.9	11
7	OK	228	181	0.2	16
8	TXWF	544	430	0.5	17
9	TXBryan	528	503	0.5	3
10	TXCO	594	530	0.6	8
11	64-40RG	152	145	0.1	3
12	64-40RHY	311	218	0.3	25
13	TXYK	1077	821	0.9	19
14	ROG	231	323	0.3	23

CV – Coefficient of Variation

Table 2.9. Summary of E*/sin ϕ at 54.4°C and 1 Hz.

Mix No.	Mix Quality	E*/sin ϕ (MPa)			CV, %
		Sample 1	Sample 2	Average 1000 MPa	
1	ARTL	876	413	0.6	51
2	ARLR	274	312	0.3	9
3	AZ	649	622	0.6	3
4	LA	417	511	0.5	14
5	NMBingham	1512	1810	1.7	13
6	NMVado	1792	1869	1.8	3
7	OK	427	411	0.4	3
8	TXWF	1158	799	1.0	26
9	TXBryan	1079	900	1.0	13
10	ROG	420	613	0.5	26
11	64-40RG	678	460	0.6	27
12	64-40RHY	845	628	0.7	21
13	TXCO	1071	1003	1.0	5
14	TXYK	2039	1425	1.7	25

CV – Coefficient of Variation

Table 2.10. Summary of Flow Time Values.

Mix No.	Mix Quality	Flow Time (sec)			CV, %
		Sample 1	Sample 2	Average	
1	ARTL	44	51	48	10
2	ARLR	24	20	22	13
3	AZ	298	297	298	0.2
4	LA	56	125	91	54
5	NMBingham	29950	21445	25698	23
6	NMVado	30942	25585	28263	13
7	OK	1849	1224	1537	29
8	TXWF	997	489	743	48
9	TXBryan	2824	3108	2966	7
10	ROG	7	9	8	18
11	64-40RG	136	84	110	33
12	64-40RHY	164	62	113	64
13	TXCO	23247	21968	22608	4
14	TXYK	28764	26348	27556	6

CV – Coefficient of Variation

Table 2.11. Summary of Flow Time Slope Values.

Mix No.	Mix Quality	Flow Time Slope: m			CV, %
		Sample 1	Sample 2	Average	
1	ARTL	0.243	0.282	0.26	10
2	ARLR	0.378	0.323	0.35	11
3	AZ	0.229	0.235	0.23	2
4	LA	0.361	0.267	0.31	21
5	NMBingham	0.149	0.156	0.15	3
6	NMVado	0.200	0.117	0.16	37
7	OK	0.225	0.189	0.21	12
8	TXWF	0.181	0.225	0.20	15
9	TXBryan	0.192	0.178	0.18	5
10	ROG	0.682	0.556	0.62	14
11	64-40RG	0.295	0.312	0.30	3
12	64-40RHY	0.176	0.246	0.21	23
13	TXCO	0.152	0.163	0.16	5
14	TXYK	0.168	0.174	0.17	2

CV – Coefficient of Variation

Table 2.12. Summary of Flow Time Intercept a Values.

Mix No.	Mix Quality	Flow Time Intercept: a			CV, %
		Sample 1	Sample 2	Average 0.001x	
1	ARTL	0.01410	0.01310	14	5
2	ARLR	0.01220	0.01370	13	8
3	AZ	0.01450	0.00920	12	32
4	LA	0.00830	0.01390	11	36
5	NMBingham	0.00750	0.00820	8	6
6	NMVado	0.00460	0.01290	9	67
7	OK	0.00333	0.01160	8	78
8	TXWF	0.01060	0.00780	9	22
9	TXBryan	0.00830	0.00700	8	12
10	ROG	0.00940	0.01410	12	28
11	64-40RG	0.00960	0.01230	11	17
12	64-40RHY	0.01370	0.01320	13	3
13	TXCO	0.00629	0.00592	6	4
14	TXYK	0.00476	0.00538	5	9

CV – Coefficient of Variation

Table 2.13. Summary of Flow Number Values.

Mix No.	Mix Quality	Flow Number			CV, %
		Sample 1	Sample 2	Average 1000x	
1	ARTL	235	201	0.2	11
2	ARLR	227	111	0.2	49
3	AZ	667	401	0.5	35
4	LA	395	461	0.4	11
5	NMBingham	15000	15001	15.0	--
6	NMVado	15001	15001	15.0	--
7	OK	3455	3663	3.6	4
8	TXWF	1527	4791	3.2	73
9	TXBryan	2495	9119	5.8	81
10	ROG	225	179	0.2	16
11	64-40RG	227	167	0.2	22
12	64-40RHY	2119	1115	1.6	44
13	TXCO	4999	7067	6.0	24
14	TXYK	6343	7167	6.8	9

CV – Coefficient of Variation

Typically, the flow time test was conducted for 30,000 seconds or until the sample failed due to crack initiation in the tertiary zone. Mixtures NMBingham and NMVado demonstrated relatively much higher flow time values for reaching the tertiary flow stage as compared to the remainder of the mixes. In most cases, the samples failed when the strain approached 1.5 to 2 percent.

Table 2.14. Summary of Flow Number Slope Parameter Values.

Mix No.	Mix Quality	Flow Number Slope: b			CV, %
		Sample 1	Sample 2	Average	
1	ARTL	0.4120	0.4561	0.43	7
2	ARLR	0.5367	0.5480	0.54	1
3	AZ	0.4740	0.4165	0.44	9
4	LA	0.4753	0.3909	0.43	14
5	NMBingham	0.2710	0.3157	0.29	11
6	NMVado	0.3043	0.3254	0.31	5
7	OK	0.2810	0.3437	0.31	14
8	TXWF	0.4328	0.3695	0.40	11
9	TXBryan	0.2933	0.4180	0.36	25
10	ROG	0.5578	0.6004	0.58	5
11	64-40RG	0.3805	0.3657	0.37	3
12	64-40RHY	0.1758	0.2611	0.22	28
13	TXCO	0.2461	0.315	0.28	17
14	TXYK	0.2021	0.286	0.24	24

CV – Coefficient of Variation

Flow number tests continued until the sample failed in the tertiary zone or until 15,000 cycles. In the case of the NMBingham and NMVado mixes, no tertiary flow was observed even at 15,000 cycles; therefore, the test was stopped. Because of this occurrence, the exact flow numbers for these mixtures could not be ascertained. At this stage, the total strain in these mixtures was less than 1.5 percent.

Table 2.15. Summary of G* at 40°C and 10 Hz.

Mix No.	Mix Quality	G* (MPa)			CV, %
		Sample 1	Sample 2	Average 1000 MPa	
1	ARTL	29865	56629	43	44
2	ARLR	29524	34174	32	10
3	AZ	36884	35757	36	2
4	LA	46393	41339	44	8
5	NMBingham	72198	54706	63	19
6	NMVado	151066	110063	131	22
7	OK	49815	56280	53	9
8	TXWF	51645	44354	48	11
9	TXBryan	67367	65693	67	2
10	ROG	45657	43436	45	4
11	64-40RG	35757	15221	25	57
12	64-40RHY	8181	15276	12	43

CV – Coefficient of Variation

Table 2.16. Summary of G*/sin δ at 40°C and 10 Hz.

Mix No.	Mix Quality	G*/sin δ (MPa)			CV, %
		Sample 1	Sample 2	Average 1000 MPa	
1	ARTL	34867	73665	54	51
2	ARLR	33792	39601	37	11
3	AZ	45949	44254	45	3
4	LA	55816	52829	54	4
5	NMBingham	119995	84338	102	25
6	NMVado	330153	257258	294	18
7	OK	74840	84125	79	8
8	TXWF	74889	62336	69	13
9	TXBryan	92369	82246	87	8
10	ROG	65690	60608	63	6
11	64-40RG	44254	23990	34	42
12	64-40RHY	10752	28981	20	65

CV – Coefficient of Variation

Table 2.17. Summary of G* at 40°C and 1 Hz.

Mix No.	Mix Quality	G* (MPa)			CV, %
		Sample 1	Sample 2	Average 1000 MPa	
1	ARTL	10407	19075	15	42
2	ARLR	8528	9913	9	11
3	AZ	14296	12039	13	12
4	LA	14141	15308	15	6
5	NMBingham	34118	33910	34	0.4
6	NMVado	86288	63868	75	21
7	OK	22695	24005	23	4
8	TXWF	19880	17087	18	11
9	TXBryan	24934	22102	24	9
10	ROG	17410	17674	18	1
11	64-40RG	12039	8999	11	20
12	64-40RHY	4227	11145	8	64

CV – Coefficient of Variation

Table 2.18. Summary of G*/sin δ at 40°C and 1 Hz.

Mix No.	Mix Quality	G*/sin δ (MPa)			CV, %
		Sample 1	Sample 2	Average 1000 MPa	
1	ARTL	12945	23527	18	41
2	ARLR	10272	11784	11	10
3	AZ	18326	14517	16	16
4	LA	18276	21848	20	13
5	NMBingham	60528	63813	62	4
6	NMVado	187691	137994	163	22
7	OK	38127	41603	40	6
8	TXWF	29254	24056	27	14
9	TXBryan	36336	30250	33	13
10	ROG	26125	24891	26	3
11	64-40RG	14517	17063	16	11
12	64-40RHY	5694	30222	18	97

CV – Coefficient of Variation

High variability in results was observed, particularly (but not necessarily) when the shear modulus values were toward the lower end (i.e., at high temperatures and/or low frequencies).

This observation indicates that the test is not as sensitive to mixtures with lower shear moduli. This variability was exhibited in spite of the fact that the air voids for the tested specimens were within 7±0.5%.

Comparison of Test Results

The main objective of this research was to compare the different tests used to predict the rutting performance of HMA mixes. In an ideal experiment design, the test results must be correlated with field performance, and the merit of each test parameter should be based on the strength of this correlation. But in order to do so, precise qualitative field performance data, together with the field traffic data must be available. However, this information was not available for the mixes used in this research. The alternative way to compare test results is by using a torture test, such as Hamburg or APA, as a reference in place of field performance. This assumption leads to two arguments. Firstly, can the torture test be considered as representative of field performance, and secondly, if such a test is a suitable indicator of field performance, then why there is a need to explore other test methods, which would essentially do the same task, i.e., predict field performance.

To address the first argument, one can provide evidence from literature (Zhang et al., 2002; Williams and Prowell, 1999) to substantiate that torture tests can be used to obtain a fair estimate of field performance. If this is the case, then it is required to justify the need for a SPT in addition to the HWTD. There is a two-fold answer to the second argument. Firstly, when comparing a set of, say, 10 parameters with the rut depth of a torture test, it is possible that, for a certain class of mixtures, the torture test may contradict the results from the rest of the parameters, in which case, one might question the efficacy of torture tests for this class of mixtures. Secondly, while the torture test can rate the performance of a mix, it cannot provide information about fundamental material properties of the mix, as compared to the simple performance tests or the FSCH. These material properties are an important part of the mechanistic design tools. It is therefore worthwhile to research test methods that can not only substantiate or improve the prediction accuracy of a torture test but can also be used for obtaining fundamental material properties.

Methods of Analysis

As mentioned earlier, not all tests were conducted on all mixes. In order to analyze and compare results, the mixtures were divided into two groups. The first group of mixtures is referred to as the APA mixes. Results from this group were analyzed with the APA torture test as the reference. The second group of mixtures is referred to as Hamburg mixes. Results from this group were analyzed with the Hamburg test as the reference.

The following are some of the techniques by which the results from different tests were analyzed and compared:

- comparison of ranks based on different test parameters,
- comparison of rank correlation coefficient of different test parameters with the APA or Hamburg as the basis,
- statistical grouping and ranking of different mixtures to compare sensitivity for both APA mixes and Hamburg mixes, and
- direct correlation of different test parameters with the APA and Hamburg as the basis.

All of these techniques along with the analyzed data are presented in the following subsections.

Comparison of Ranks

One of the direct methods of comparing results from two different tests is by comparing the rankings of the different mixes by these test methods. Tables 2.19 and 2.20 represent the ranks of mixtures from the APA and Hamburg groups, respectively.

Although the exact flow number values for the two mixtures from New Mexico could not be ascertained, a value of 15,000 and 15,001 was assigned to the mixtures NMBingham and NMVado, respectively, for the purpose of the ranking analysis.

Table 2.19 shows that, in the case of the PG 64-40 mixture designed using rhyolite, the APA rut depth and creep slope indicate a relatively sound mix in terms of rutting resistance. However, the dynamic modulus and the shear modulus tests indicate a relatively poor mix when the rankings are compared at 10 Hz. Further, dynamic modulus at 1 Hz ranks the mixture similar to the APA result. Furthermore, the flow time slope, flow number, and flow number intercept

parameters rank the rhyolite mixture more closely to the APA rut depth than the other parameters. These differences are not evident from the data presented in Table 2.19. One of the reasons for this could be the small size of the group and the mixtures being relatively similar in performance.

Table 2.19. Comparisons of Rankings by Parameters from Different Tests for APA Mixes.

Mixture Number	APA Rut Depth	APA Creep Slope	G* at 10 Hz	G*/sin δ at 10 Hz	G* at 1Hz	G*/sin δ at 1Hz	E* at 10 Hz	E*/sin ϕ at 10 Hz	E* at 1 Hz	E*/sin ϕ at 1 Hz	Flow Time	Flow Time Intercept	Flow Time Slope	Flow Number	Flow Number Slope
NMVado	1	1	1	1	1	1	1	1	1	1	1	4	2	1	4
NMBingham	2	4	3	2	2	2	2	2	2	2	2	3	1	2	2
TXWF	3	8	5	5	5	5	5	3	4	4	5	5	4	5	7
64-40RHY	4	3	12	12	12	9	10	8	8	5	7	11	6	6	1
OK	5	6	4	4	4	3	9	10	10	11	4	1	5	4	3
AZ	6	5	9	9	9	10	6	6	6	7	6	9	7	7	10
TXBryan	7	2	2	3	3	4	3	4	3	3	3	2	3	3	5
64-40RG	8	9	11	11	10	11	12	11	11	8	8	6	9	11	6
LA	9	7	7	7	8	7	7	9	9	10	9	7	10	8	8
ARTL	10	10	8	8	7	8	4	5	5	6	10	12	8	9	9
ARLR	11	12	10	10	11	12	11	12	12	12	11	10	11	12	11
ROG	12	11	6	6	6	6	8	7	7	9	12	8	12	10	12

Table 2.20. Comparison of Rankings by Parameters from Different Tests for Hamburg Mixes.

Mixture Number	Hamburg rut depth	E* at 10 Hz	E*/sin ϕ at 10 Hz	E* at 1 Hz	E*/sin ϕ at 1 Hz	Flow Time	Flow Time Slope	Flow Time Intercept	Flow Number	Flow Number Slope
TXCO	1	1	2	2	2	2	1	2	2	3
TXYK	2	2	1	1	1	1	2	1	1	2
TXBryan	3	3	4	3	3	3	3	3	3	4
64-40RHY	4	6	6	6	5	5	5	7	5	1
TXWF	5	4	3	4	4	4	4	4	4	6
64-40RG	6	7	7	7	6	6	6	5	7	5
ROG	7	5	5	5	7	7	7	6	6	7

This method of comparing ranks suffers from the drawback that the conclusions drawn are mostly qualitative. A more quantitative tool for comparing ranks is the Kendall tau rank correlation coefficient described in the next subsection.

Comparisons of Rank Correlation Coefficients

A correlation coefficient for each test parameter with respect to the APA or Hamburg test was computed by comparing their respective ranks. The Kendall tau rank correlation method was used for this purpose (Kendall and Dickinson, 1990). The value of this coefficient ranges from -1 to +1, where -1 indicates that the rankings are perfectly inverse of each other, and +1 indicates that the rankings are perfectly correlated with each other. A coefficient value of 0 means that there is absolutely no correlation between the rankings. This coefficient can be determined for any two pairs of ranks. In general, a coefficient value of about 0.6 or higher or - 0.6 or lower would indicate a good relationship between the two systems of ranking. Tables 2.21 and 2.22 list out the values of these coefficients with APA and Hamburg tests as a basis, respectively.

Table 2.21. Kendall Tau Coefficients of Correlation – All Test Parameters versus APA Rut Depth or Creep Slope (APA Group).

Sample No.	Test Parameter	APA Rut Depth	APA Creep Slope
1	Flow Time	0.79	0.70
2	Flow Time Slope m	-0.76	-0.61
3	Flow Number	0.70	0.73
4	Flow Number Slope b	-0.64	-0.55
5	E*/sin ϕ at 1 Hz	0.55	0.58
6	G*/sin δ at 1 Hz	0.49	0.46
7	E*/sin ϕ at 10 Hz	0.49	0.46
8	E* at 1 Hz	0.46	0.49
9	G*/sin δ at 10 Hz	0.39	0.36
10	E* at 10 Hz	0.39	0.39
11	Flow Time Intercept a	-0.36	-0.33
12	G* at 1 Hz	0.33	0.36
13	G* at 10 Hz	0.30	0.42

Table 2.22. Kendall Tau Coefficients of Correlation – All Test Parameters versus Hamburg Rut Depth (Hamburg Group).

Sample No.	Test Parameter	Rank Coeff
1	Flow Time Slope m	-0.90
2	Flow Time	0.81
3	E*/sin ϕ at 1 Hz	0.81
4	Flow Number	0.71
5	E* at 10 Hz	0.71
6	E* at 1 Hz	0.62
7	Flow Time Intercept a	-0.62
8	E*/sin ϕ at 10 Hz	0.52
9	Flow Number Slope	-0.52

The correlation coefficients (Table 2.21) show that the flow number and flow time values predict rutting performance most closely to predictions based on the APA rut depth and APA creep slope. Dynamic modulus and shear modulus exhibit notably weaker correlations than the flow tests. The poorer correlations may be due, in part, to the different predictions for the mixtures containing the PG 64-40. Also note that, since there were only two mixtures using highly modified asphalt, the difference in strength of correlations cannot be attributed to this factor alone. However, at the same time, it should be remembered that the PG 64-40 amplifies the affect of polymer modification in an HMA mixture. It is also possible that mixtures containing asphalt with lower polymer content would exhibit similar trends but probably with less intensity. With the exception of flow number slope, similar trends are seen for the rank correlation coefficients with Hamburg as the basis in Table 2.22. The contrast in the strength of relationships between various test parameters in Table 2.22 is less than that in Table 2.21. This may be due, in part, to the smaller size of mixture group.

Apparently, dynamic modulus may be recommended in the new national Mechanistic Design Guide as the main test to characterize HMA. This experiment was designed, in part, to evaluate the ability of the dynamic modulus test to properly characterize or rank HMA mixtures containing polymer-modified binders. The test yielded a dynamic modulus for the gravel and rhyolite mixtures containing PG 64-40 but did not account for the recovery of the deformation due primarily to the polymer. Therefore, the dynamic modulus test ranked the PG 64-40 mixtures as relatively poor while both torture tests (APA and Hamburg) ranked them as rut

resistant. The only parameter from the dynamic modulus test that has better correlation with the torture tests is the E*/sin ϕ at 1Hz. This observation can be explained by the fact that the lower loading frequency and the phase angle are able to better account for the viscoelastic properties of the mix. However, it must also be noted that the phase angle, ϕ, is not one of the inputs in the forthcoming design guide, that is, thickness design and rutting predictions are based on the E* value alone.

Groupings of Statistically Similar Mixes

Analyses based on rankings are associated with the drawback that rankings are not representative of the range of the data. For example, the difference between the values of any two consecutive rankings is not necessarily the same as the difference between any other two consecutive rankings. Therefore, when mixture properties are relatively similar, the rankings may change for such sets of mixtures based on the sensitivity (or lack thereof) of the test being conducted. To address this limitation, a Duncan grouping was performed for each of the test parameters using all the test replicates at a significance level of $\alpha = 0.05$ and assuming equal variance of the particular mixture property. Appendix C presents details of the statistical analysis.

As is common with the Duncan Multiple Range Test, the number of groups formed for each parameter varied (depending on sensitivity of the test). For example, APA rut depth classified the 12 samples into six groups of statistically equivalent values; whereas, APA creep slope data classified the same 12 samples into only four groups.

Each test parameter and its ranking based on Duncan groupings are shown in Tables 2.23 and 2.24 for the APA and Hamburg mixes, respectively. The total at the bottom of the table indicates the total number of significant groups into which the mixes were divided. The mix designs were ranked in the order of their resistance to rutting. Note that the same rank is shared by mixes that are found to be statistically indifferent. In some cases, a mix design is assigned more than one rank. For example, a ranking of 2-3 means that this particular mix belongs to both the second and third groups.

The Duncan groupings show that flow time and flow number classify all the mixes into only two to three groups of statistically similar values, as compared to the APA rut depth test, which classifies the mixtures into six different groups (Table 2.23). This outcome shows that the

APA is comparatively more sensitive to differences in mixture properties than flow time and flow number values. Similarly, Hamburg classifies seven mixes in five different groups; whereas, the number of groups for other tests is smaller (Table 2.24).

Table 2.23. Rankings Based on Duncan Groups for Each Test Parameter for APA Group.

Mixture Number	APA Rut Depth	APA Creep Slope	G* at 10 Hz	G*/sin δ at 10 Hz	G* at 1 Hz	G*/sin δ at 1 Hz	E* at 10 Hz	E*/sin ϕ at 10 Hz	E* at 1 Hz	E*/sin ϕ at 1 Hz	Flow Time	Flow Time Intercept	Flow Time Slope	Flow Number	Flow Number Slope
NMVado	1	1	1	1	1	1	1	1	1	1	1	1	1-2	1	1-3
NMBingham	1-2	1-2	2-3	2	2	2	1	1	1	1	1	1	1	1	1-2
64-40RHY	2-3	1-2	5	5	4	3	5-6	3-4	4-5	2-3	2	1	1-3	3	1
TXWF	2-3	2	2-4	2-4	3-4	3	2-3	2	2-3	2	2	1	1-3	2-3	3-4
AZ	3	1-2	3-5	3-5	3-4	3	2-4	2-4	3-4	2-4	2	1	1-4	3	4-5
OK	3	1-2	2-4	2-4	2-3	2-3	4-6	4	4-5	3-4	2	1	1-3	2-3	1-3
TXBryan	3	1-2	2	2-3	2-3	3	2	2	2	2	2	1	1-2	2	2-4
64-40RG	4	3	4-5	4-5	4	3	6	4	5	3-4	2	1	3-5	3	2-4
LA	4-5	2	2-4	3-5	3-4	3	3-5	2-4	4-5	3-4	2	1	4-5	3	4
ARTL	5	3	2-4	3-5	3-4	3	2-3	2-3	3-4	2-4	2	1	2-5	3	4
ARLR	6	4	4-5	4-5	4	3	5-6	4	5	4	2	1	5	3	5-6
ROG	6	3	2-4	2-5	3-4	3	4-5	3-4	4-5	3-4	2	1	6	3	6
TOTAL Groups	**6**	**4**	**5**	**5**	**4**	**3**	**6**	**4**	**5**	**4**	**2**	**1**	**6**	**3**	**6**

Table 2.24. Rankings Based on Duncan Groups for Each Test Parameter for Hamburg Group.

Mixture ID	Hamburg	E* at 10Hz	E*/sinφ at 10Hz	E*/sinφ at 1Hz	E* at 1Hz	Flow Time Value	Flow Time Slope	Flow Time Intercept	Flow Number Value	Flow Number Slope
TXCO	1	1	2	2	2	2	1	1	1	1-3
TXYK	2	1	1	1	1	1	1	1	1	1-2
TXBR	2-3	2	2	2	2	3	1	1-2	1	2-3
64-40RHY	3	3-4	3	2	3	4	1-2	3	1-2	1
TXWF	4	2	2	2	2	4	1	1-2	1-2	3
64-40RG	4	4	3	2	3	4	2	2-3	2	2-3
ROG	5	3	3	2	3	4	3	2-3	2	4
TOTAL	**5**	**4**	**3**	**3**	**3**	**4**	**3**	**3**	**2**	**4**

Based on the above analysis, some of the observations that can be inferred are as follows:

- The number of groups for flow time value, flow time intercept, and flow number value were very few (one to three). Following are two potential reasons: (1) The mixtures selected had a wide range of resulting values from very low to very high, thus minimizing the number of groups of statistically equivalent values. Further, the difference between the performance levels of some of the mixtures (specifically those from New Mexico) was much higher than those of other mixtures. For example, the flow time value for the two mixtures from New Mexico was about 30,000, and the flow time value for the rest of the mixtures was below about 3000. Therefore, the results were "cluttered" at the lower end of the rankings for most of the mixes. This reasoning is substantiated by the groupings for the Hamburg mixes. For example, based on the same test data, groupings of flow time value place TXBryan and TXWF in the same group for APA mixes but in a different group for Hamburg mixes. (2) Researchers were trying to capture the tertiary flow phenomenon for all the mixes (PG 64 to PG 82) in the same reasonable stress and temperature window. This could only be done, as the results indicated, by sacrificing some sensitivity of the test. Consider the analogy of using the same measuring scale to measure different objects ranging from a few inches in length to a few miles. If the measuring scale were too small then the measurements would be accurate but would take considerable time to complete, or, if the measuring scale is large then it would take reasonable time to measure but by sacrificing some accuracy for objects in the smaller length scale. The latter analogy holds here. Conversely, by selecting mixes that are not this widely apart in their properties and an appropriate stress level, one can achieve adequate sensitivity for this test.
- For the APA mixes, flow time slope and flow number slope separated the mixes into six groups, which was much better than the flow time or flow number values. For the Hamburg mixes, a similar trend with flow number value and flow number slope was observed, with the former dividing the mixes in only two groups and the latter in four groups. Flow time value yielded four groups while flow time slope yielded three.

- Based on APA rut depth, the PG 64-40 rhyolite mix was ranked in the second and third of the six groups. The mix can, therefore, be said to perform better than most of the other mixes, since it is in the top 33 to 50 percent of the mixtures. The PG 64-40 river gravel, on the other hand, was ranked in the fourth of six groups. Among the Hamburg mixes, the PG 64-40 rhyolite mix was placed in the third, and PG 64-40 river gravel was placed in the fourth group out of five groups based on rut depth.
- Among the APA mixtures, based on the dynamic modulus grouping, the PG 64-40 rhyolite is placed in the fifth and sixth of the six groups when E* values are compared at 10 Hz and in the fourth and fifth of the five groups when the values are compared at 1 Hz. This means that the E* values placed this mix in the last 33 percent (i.e., 67 to 100 percent from the top) of the mixtures. The PG 64-40 river gravel was placed in sixth of the six groups and fifth of the five groups when E* values are compared at 10 and 1 Hz, respectively. Among the Hamburg mixes, E* values placed the PG 64-40 rhyolite mix in the last group (with the exception of $E^*/\sin \phi$ at 1 Hz, where it was in the second to the last group).
- For the SST results on the APA mixes, the PG 64-40 mixes were placed in the latter groups.
- Flow time slope and flow number slope categorized the PG 64-40 rhyolite mixes in the top groups, similar to APA rut depth. Based on this finding and assuming that APA relates reasonably well to pavement rutting, flow number slope and flow time slope appear to relate well to predicted rutting in a pavement. For the Hamburg group, Hamburg rut depth, flow number slope, flow time slope, and $E^*/\sin \phi$ at 1Hz ranked this mix as average, while other parameters ranked it in the poorest group. Once again, it must be noted that these distinctions are not very predominant due to the small size of the Hamburg group.

Correlation with Torture Tests

One of the direct methods for comparing results from torture tests to other test parameters is by direct correlation and computation of coefficient of correlation (R^2). For determining R^2 values, a power function was used for all the parameters. This was because the permanent deformations observed in the APA or Hamburg tests are related to the viscoelastic properties of the HMA mixtures, which are most commonly expressed in terms of a power function in

mechanistic analyses of these mixtures. The correlation for the flow number value with the APA results was developed based on only 10 mixture designs. The two mixture designs from New Mexico were excluded because these samples never reached the point of tertiary flow within the tested range of 15,000 cycles. Tables 2.25 and 2.26 summarize the R^2 values obtained. The graphs showing the correlations with APA and Hamburg are included in Appendix D and E, respectively.

Table 2.25. R^2 Values for Correlations between Various Parameters with APA Results.

Parameter	R^2 Values	
	versus APA rut depth	versus APA creep slope
Flow time slope	0.84	0.56
Flow number value	0.63	0.56
E*/sin ϕ @ 1Hz	0.63	0.59
Flow number slope	0.62	0.46
Flow time value	0.61	0.55
E* @ 1 Hz	0.48	0.53
G*/sin δ @ 1 Hz	0.46	0.50
E*/sin ϕ @ 10 Hz	0.45	0.48
Flow time intercept	0.34	0.31
G* @ 1 Hz	0.33	0.38
E* @ 10 Hz	0.24	0.32
G*/sin δ @ 10 Hz	0.22	0.28
G* @ 10 Hz	0.11	0.16

Table 2.26. Correlation Coefficients between Various Parameters and Hamburg Rut Depth.

Parameter	R^2 Values
Flow Number Value	0.88
Flow Time Slope	0.82
Flow Time Value	0.74
E*/sin ϕ at 1 Hz	0.65
Flow Number Slope	0.60
E*/sin ϕ at 10 Hz	0.59
E* at 1 Hz	0.56
E* at 10 Hz	0.54
Flow Time intercept	0.44

The following observations are made from the data in Tables 2.25 and 2.26.

- Flow time slope and flow number value provided the best correlations with both the Hamburg and APA rut depths. Generally, Hamburg provided higher R^2 values than APA. In general, rut depth from the APA at 8000 strokes correlated better than creep slope with the remaining parameters.
- Correlations of the APA test parameters with dynamic modulus and FSCH tests were not as good as correlations of the APA test parameters with the flow time and flow number test parameters. Similar results were found in other studies Zhou and Scullion (2001), where relatively low dynamic modulus values were observed for heavy duty asphalt mixes in contradiction of the field performance, APA, and permanent strain test results. For the Hamburg mixes, with the exception of E*/sin ϕ at 1 Hz, the R^2 values for all other E* parameters were less than those for the flow time or flow number parameters.
- Correlations of E*/sin ϕ or G*/sin δ were relatively better than correlations of E* and G* alone with the APA or Hamburg test parameters. This difference is likely because the phase angle captures the viscoelastic behavior of the mix, which is also responsible for the permanent deformation rather than the resilient modulus values alone.

- Correlations of E* or G* were relatively better when a lower frequency such as 1 Hz was considered in place of a higher frequency such as 10 Hz. However, even the lower frequency values did not show any strong correlations.

DISCUSSIONS AND CONCLUSIONS

Twelve field mixes and three laboratory mixes were included in this part of the research project. Four of the 12 mixtures tested were obtained from Texas DOT districts and eight from neighboring states. Two laboratory mixes were prepared using a highly polymer-modified binder with crushed rhyolite (9.5 mm angular) and crushed river gravel aggregates. A third laboratory mix contained uncrushed river gravel and was intentionally designed using conventional asphalt to be rut susceptible. All 15 of these mixes were tested using the simple performance tests (dynamic modulus, flow time, and flow number). Researchers tested 12 of the mixtures using the APA and FSCH, and seven mixtures using the Hamburg wheel tracking device.

Objectives included: evaluate applicability of current test procedures and equipment for measuring HMA mixture properties with particular emphasis on the complex modulus tests and gap-graded and polymer-modified mixtures. The findings from this work are briefly summarized below:

- Flow time slope and flow number value provided the best correlations with both the APA and Hamburg rut depth.
- APA rut depth correlated with the flow number and flow time parameters better than the APA creep slope correlated with these values.
- The correlations of the APA test parameters with dynamic modulus and FSCH tests were not as good as correlations of the APA test parameters with the flow time and flow number test parameters. Zhou and Scullion (2001) reported similar findings where relatively low dynamic modulus values were observed for heavy duty asphalt mixes in contradiction to the field performance, APA, and permanent strain test results.

- Correlations of Hamburg test results with dynamic moduli were poorer than correlations of Hamburg with flow time and flow number parameters, with the exception of E*/sin ϕ at 1 Hz.
- Correlations of E*/sin ϕ or G*/sin δ with the Hamburg and APA test parameters were better than correlations of E* and G* alone with these parameters. This is likely because the phase angle represents the viscoelastic behavior of the mix, which is responsible for the permanent deformation rather than the resilient modulus. This difference is important because, currently, the phase angle from the dynamic modulus test is not a vital input in the mechanistic-empirical design guide that is under development.
- Correlations of E* or G* with the APA parameters were better at lower test frequencies than at higher frequencies. However, these values did not show strong correlations.
- The overall rut depth from the APA test at 8000 strokes correlated better with all other parameters as compared to the APA creep slope.
- Correlations of Hamburg rutting with the other test parameters were similar to the correlations between the APA rut depth and those same parameters. Flow number value, flow time slope, E*/sin ϕ at 1 Hz, flow number slope, and flow time value were among the best five correlations both with Hamburg and the APA rut depths.
- Using the Duncan multiple range test, flow time slope and flow number slope were able to separate the mixes into six Duncan groups of statistically equivalent values, which was much better than the flow time or flow number values. However, comparing results from Hamburg and APA groups, it is concluded that the sensitivity of the flow time or flow number tests can be improved by (1) selecting the appropriate temperature and stress levels for the mixes being compared and (2) comparing mixes that have similar properties unlike a broad range as seen in the APA mixes selected for this research.
- Based on the APA rut depth, the PG 64-40 + rhyolite mix can be placed in the second and third of the six Duncan groups in terms of ranking. The mix can therefore be said

to perform better than most of the other mixes since it is in the top 33 to 50 percent of the mixtures. In contrast, the PG 64-40 + river gravel mix was ranked in the fourth of the six Duncan groups.

- Based on the Duncan grouping for dynamic modulus, the PG 64-40 + rhyolite mix was placed in the fifth or sixth of the six groups when E* values are compared at 10 Hz and in the fourth and fifth of the five groups when the values are compared at 1 Hz. This means that the E* values placed this mix in the worst 33 percent of the mixtures. The PG 64-40 + river gravel mix was placed in the sixth of 6 groups and fifth of 5 groups when E* values are compared at 10 and 1 Hz, respectively. These groupings are quite contrary to those for the APA parameters. Similarly, for the Hamburg mixes, this mix was rated in the last group by E* parameters (except E*/sin ϕ at 1 Hz) and in the second from the last group by most other parameters.
- The results from this research indicate that caution must be exercised in interpreting the rut susceptibility of mixes based on the E* parameters, especially when evaluating mixtures containing polymer-modified asphalts.
- These findings indicate that flow time and flow number tests capture fundamental material properties and should be considered for inclusion in the mixture design and selection process.

CHAPTER 3:
MOISTURE SUSCEPTIBILITY OF HMA

BACKGROUND AND OBJECTIVE

Moisture damage is regarded as one of the major forms of HMA pavement distress. Earlier studies present several theories that explain different moisture susceptibility of mixes based on differences in adhesion at the asphalt-aggregate interface. These theories ascribe the adhesive strength of the asphalt-aggregate interface to one or more of the following three mechanisms:

- loss of adhesion due to poor mechanical interlocking of asphalt binder and aggregate,
- physical adhesion between asphalt and aggregate in the presence of moisture (surface energy), and
- adhesion due to chemical interactions between the asphalt and minerals on the aggregate surface in dry and wet conditions.

Over the past few decades, most researchers have recognized these three mechanisms (Ishai and Craus, 1976; Scott, 1977; Taylor and Khosla, 1983; Terrel and Al-Swailm, 1994; Curtis et al., 1991; Kanitpong and Bahia, 2003).

In earlier studies (Majidzadra and Brovold, 1968) explained adhesive failure in the presence of moisture based on the reasoning that water reduces free energy of an asphalt-aggregate interface and is therefore thermodynamically more favorable. The amount of free energy released depends on the surface properties of the asphalt and the aggregate. This release of free energy in a three-component system can also be quantitatively calculated if the surface energies of the three components, namely, asphalt, aggregate, and water are known. Recent studies (Cheng, 2002; Kim and Little, 2003) have demonstrated that the calculated fracture bond energies correlate well with the moisture susceptibility of HMA mixes. Based on this understanding, surface energies of aggregate and asphalt can be used to quantitatively estimate the moisture damage in hot mix asphalt on the basis of adhesive bond energy at the asphalt-aggregate interface in the presence of water.

Material Selection and Experiment Design

In order to assess the validity of a test procedure to predict moisture damage, an ideal experiment design would be to test field mixes and compare the laboratory predictions to field performance. In order to execute such an experiment design, a wide spectrum of mixes with quantitative field data will be required. Since the current project was aimed at exploratory investigations of new test methods, researchers decided to use laboratory mixes instead of field mixes. The most evident advantage of this change is that well-controlled mixes with various types of treatments can be used in the study. This, in turn, can facilitate a more fundamental understanding of mixture behavior.

The two main candidate tests included for this study are the Hamburg wheel tracking test and tests to measure surface energy of aggregates and asphalts. While the former is a torture test that is commonly used to identify rut-susceptible and moisture-susceptible mixes, the latter aims at measuring fundamental surface properties of aggregates and asphalts. These tests appear quite complementary.

The Universal Sorption Device (USD) and Wilhelmy plate (WP) method were selected for measuring the surface energy of aggregates and asphalts, respectively. The measured surface energy values can be used for the following purposes:

- calculating cohesive bond strength of asphalt, which is related to the fatigue cracking and healing of asphalt in hot mix;
- calculating adhesive bond strength between asphalt and aggregate, which is related to adhesive fracture between asphalt and aggregate; and
- calculating adhesive bond strength between asphalt and aggregate in the presence of water, which is related to the propensity of the asphalt-aggregate bond to fail due to moisture.

Nine HMA mixture designs were selected for this research. Tables 3-1 and 3-2 summarize the selected mix designs and tests selected for this research. Appendix F includes gradations for individual mixes.

Mix 1 was adopted based on a design by Colorado Materials Company located in San Marcos, Texas. This mix utilizes Colorado Type C, Colorado Type D, Colorado Type F, Colorado manufactured sand, and field sand, which was obtained from the Brazos County,

Texas, area. This mix also serves as a control mix for Mixes 2 and 3 that have the same design with the exception of the addition of 1 percent hydrated lime by weight of mix and 1.5 percent liquid antistrip agent by weight of asphalt, respectively.

Mix 4 is a laboratory designed mix using crushed river gravel from Fordyce at Victoria, Texas, and a polymer modified PG 64-40 asphalt. This mix also serves as a control for Mixes 5 and 6 to investigate the influence of lime and liquid antistrip agent, respectively. Apart from these two groups of three mixes each, three other mixes were designed using rounded gravel, limestone, and granite aggregates.

Table 3.1. Summary of Mix Designs for Task 3b.

Mix No.	Mix Type	Aggregate Description	Asphalt	OAC (%)	Additives
1	Type C	Limestone from Colorado Materials, San Marcos, Texas	PG 64-22	4.4	None
2					1% Hydrated Lime[1]
3					1.5% Perma–Tac[2]
4	9.5 mm Superpave Mix	Crushed Gravel from Fordyce, Victoria, Texas	PG 64-40 polymer modified asphalt	5.5	None
5					1% Hydrated Lime[1]
6					1.5% Perma-Tac[2]
7	SMA Mix (Marshall)	Granite from Vulcan Materials, Georgia	PG 76-22	5.9	None
8	Lab Mix	Rounded Brazos River Valley gravel	PG 64-22	5.5	None
9	Type C	Limestone from Brownwood	PG 64-22	4.3	None

[2] By weight of aggregate
[1] Liquid antistripping agent (by weight of asphalt)

Hamburg wheel tracking tests were conducted on all nine mixes. To determine adhesive bond strength for each mixture, surface energy of both asphalt and aggregate must be known. For a mix without additive, the surface energy value of aggregate and neat asphalt was determined. For a mix with additives, the liquid antistripping agent or hydrated lime is added to the asphalt cement, and surface energy of the modified asphalt was determined and used for calculating bond strength. For example, in Mixes 1 through 3, surface energies of the aggregates

were determined only once and combined with surface energy of the neat asphalt, asphalt + hydrated lime, and asphalt + liquid antistripping agent to determine the bond strength of the three mixes, respectively.

Table 3.2. Experiment Matrix for Task 3b.

Mix No.	Design Number	Remarks	Tests		
			HW	U S D	WP
1	Colorado Limestone	PG 64-22, Aggregate from Colorado Materials, San Marcos, Texas	X	X	X
2	Colorado Limestone + 1% Lime		X		X
3	Colorado Limestone + Liquid Additive		X		X
4	Fordyce Crushed Gravel	PG 64-40 (Polymer Modified), Aggregate from Fordyce, Victoria, Texas	X	X	X
5	Fordyce Crushed Gravel + 1% Lime		X		X
6	Fordyce Crushed Gravel + Liquid Additive		X		X
7	Georgia Granite	PG 76-22 SMA, Aggregate from Vulcan Materials, Georgia	X	X	X
8	Brazos Uncrushed Gravel	PG 64-22, Aggregate from Brazos River Valley, Texas	X	X	[1]
9	Brownwood Limestone	PG 64-22, Aggregate from Brownwood, Texas	X	X	

[1] Same asphalt as in case of mix 1 used

HW = Hamburg wheel load test (mix)

USD: Universal Sorption Device (aggregate)

WP = Wilhelmy plate method (asphalt)

DATA INTERPRETATION AND TEST RESULTS

Hamburg - Data Interpretation

The Hamburg wheel-tracking test is a torture test that is used to assess the rutting and moisture damage susceptibility of HMA. This test is performed by oscillating an 8.0-inch diameter and 1.85-inch wide steel wheel loaded with 158 lb over a SGC compacted specimen, 2.5 inches in height submerged in water at 122°F. Permanent deformation of each specimen is recorded with reference to the number of passes of the loaded wheel. For this research, the test was conducted for 20,000 passes or until the sample reached a maximum deformation of about

10 mm. Mixtures showing excessive susceptibility to moisture damage tend to undergo stripping and usually exhibit a sudden increase in the slope of the curve for rut depth versus number of passes after a certain number of cycles. Figure 3.1 shows typical deformation curves for samples that exhibit and do not exhibit significant moisture damage in a Hamburg test.

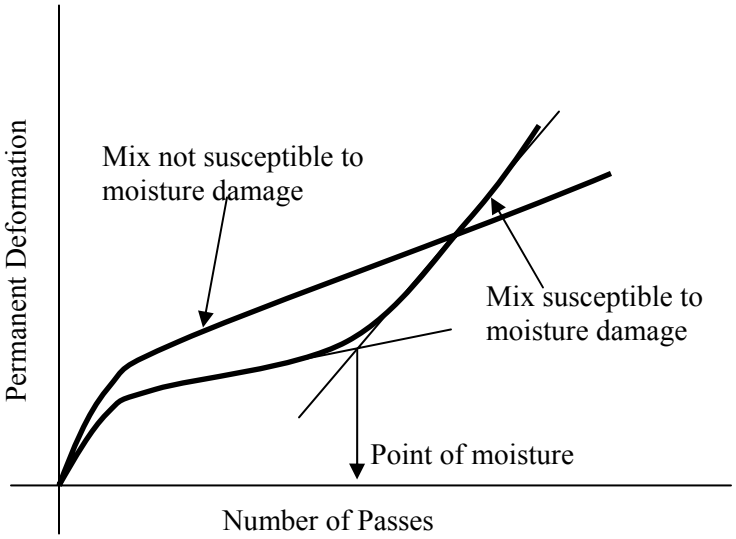

Figure 3.1. Typical Output of Hamburg Wheel Tracking Test.

For the mixes that undergo moisture damage, the following method was adopted to determine the number of passes at which moisture damage commenced. After a number of initial passes (typically ranging from 200 to 300), the rate of deformation of the mix became constant. Failure due to moisture damage is identified by a sudden increase in the rate of deformation as the test progresses. Equations of the two best-fit lines corresponding to each linear zone (before and after incipient moisture damage) are determined. The abscissa of the point of intersection of these two lines is considered as an estimate of the number of passes at which moisture damage begins. In the following sections of this report, this will be referred to as the point at which moisture damage starts, although in reality this point refers to the number of cycles when the effect of moisture damage is apparent; because damage may have started several cycles earlier.

If equations of the two lines are

$y = m_1 x + c_1$, and

$y = m_2 x + c_2$

where,

m_1 and m_2 are slopes of the straight lines, and

c_1 and c_2 are intercepts of the straight lines,

then the number of passes at which moisture damage begins is calculated as:

$$\frac{c_2 - c_1}{m_1 - m_2}$$

Also, the rut depth (ordinate of the point of intersection of the two lines) at which the moisture damage begins is calculated as,

$$\frac{m_1 c_2 - m_2 c_1}{m_1 - m_2}$$

Hamburg - Test Results

Tables 3.3 and 3.4 summarize results from the Hamburg test. Graphs for the test data are included in Appendix G. Note that in Table 3.4, only five mixes that showed moisture damage were included.

Hamburg - Discussion

Mixes 1 through 3 were designed using limestone aggregates from Colorado Materials. Mix 1 was a control mix without any additive. Mixes 2 and 3 were similar to Mix 1 with the exception that they were treated with 1 percent hydrated lime by weight and 1.5 percent liquid antistripping agent (Perma-Tac), respectively. Mix 1 reached a maximum average rut depth of 11 mm at 15,000 passes. Mixes 2 and 3 reached a maximum average rut depth of 8.3 mm at 7,500 and 6,500 passes, respectively. Further, all three mixes exhibited significant moisture damage during the test. While moisture damage for Mix 1 commenced after 9,700 cycles, moisture damage for Mixes 2 and 3 commenced after 4,300 and 3,500 cycles, respectively. The average rut depth at which moisture damage started in all three mixes is approximately the same (i.e., 2.5 mm). These observations indicate that addition of hydrated lime or liquid antistripping agent actually reduced resistance to moisture damage of the Colorado Limestone mix.

Table 3.3. Final Hamburg Rut Depth of Mixes.

Mix No.	Mix Design	Total no. of Passes (x1000)	Rut Depth (mm)			CV (%)
			Left	Right	Average	
1	Colorado Limestone	15.0	11.6	10.4	11.0	8
2	Colorado Limestone + 1% Lime	7.5	8.2	8.3	8.3	1
3	Colorado Limestone + Liquid Additive	6.5	7.5	9.0	8.3	13
4	Fordyce Crushed Gravel	4.5	9.9	9.0	9.5	7
5	Fordyce Crushed Gravel + 1% Lime	20.0	9.3	9.2	9.3	1
6	Fordyce Crushed Gravel + Liquid Additive	20.0	7.6	10.1	8.9	20
7	Georgia Granite	20.0	7.0	7.0	7.0	0
8	Brazos Uncrushed Gravel	6.0	10.0	11.0	10.5	7
9	Brownwood Limestone	20.0	7.3	--[1]	7.3	

[1] Data from second channel was not generated

Table 3.4. Point of Moisture Damage in Hamburg Test for Mixes.

No.	Design Number	Passes at Imminent Moisture damage (x1000)			CV (%)	Rut Depth at Imminent Moisture damage (mm)			CV (%)
		Left	Right	Avg.		Left	Right	Avg.	
1	Colorado Limestone	9.6	9.7	9.7	1	2.9	2.2	2.5	18
2	Colorado Limestone + 1% Lime	4.3	4.3	4.3	0	2.5	2.7	2.6	6
3	Colorado Limestone + Liquid Additive	3.2	3.8	3.5	12	2.4	3.0	2.7	16
4	Fordyce Crushed Gravel	2.7	3.4	3.1	16	6.8	4.8	5.8	24
8	Brazos Uncrushed Gravel	3	2	2.5	28	1.9	1.6	1.7	13

Researchers designed Mixes 4 through 6 using crushed gravel aggregates from Fordyce. Similar to Mixes 1 through 3, Mix 4 was a control mix without any additive while Mixes 5 and 6 were treated with 1 percent lime by weight and 1.5 percent liquid antistripping agent (Perma-Tac), respectively. Mix 4 reached a maximum average rut depth of 9.5 mm at 4,500 passes. Mixes 5 and 6 reached a maximum average rut depth of 9.3 mm and 8.9 mm at 20,000 passes, respectively. Further, only Mix 4 demonstrated significant moisture damage at 3,500 cycles at an average rut depth of 5.4 mm. Comparison of Mixes 4 through 6 indicates that addition of liquid antistripping agent or hydrated lime significantly improved the performance of the mixes containing gravel aggregates.

Mixes 7 through 9 were designed using granite, gravel, and limestone aggregates. While Mixes 8 and 9 were designed with a PG 64-22 asphalt, Mix 9 was designed using a PG 76-22 asphalt. The final average rut depth for the granite and limestone mixes (7 and 9) was about 7 mm after 20,000 passes. These mixes did not show any sign of moisture damage. The average permanent deformation for the gravel mix was 10.5 mm after only 6,000 passes. Moisture damage was observed for this mix after 2,500 passes and at 1.7 mm of rut depth.

While the first six mixes are useful for evaluating the moisture damage characteristics for well-controlled mix designs, Mixes 7 through 9 are intended to provide some feedback about the global variability of comparisons between Hamburg performance and surface energy tests.

Surface Energy - Data Interpretation

The three-component theory of surface energy (Van Oss et al., 1988) was used as the basis for various calculations in the present research. According to this theory, the total surface energy of a material can be divided into three components namely, Lifschitz van der Waals component or the dispersive component, the acid component, and the base component. Surface energy of asphalts and aggregates can be used to calculate adhesive bond strength at the asphalt-aggregate interface in dry and wet conditions as well as the cohesive bond strength of asphalt. The cohesive bond strength of asphalt can be used to estimate the cracking and healing characteristics of asphalt in a hot mix. Details about the cohesive bond strength are beyond the scope of this project and are not included in this report.

The adhesive bond strength at the asphalt-aggregate interface in dry conditions is determined by combining the surface energy components of asphalt and aggregate using the following formulae:

$$\Delta G_{12}^{a} = \Gamma_1 + \Gamma_2 - \Gamma_{12}$$

$$\Gamma_i = \Gamma_i^{LW} + \Gamma_i^{AB} = \Gamma_i^{LW} + 2\sqrt{\Gamma_i^{+}\Gamma_i^{-}}$$

$$\Gamma_{ij} = \Gamma_{ij}^{LW} + \Gamma_{ij}^{AB}$$

$$\Gamma_{ij}^{LW} = \left(\sqrt{\Gamma_i^{LW}} - \sqrt{\Gamma_j^{LW}}\right)^2$$

$$\Gamma_{ij}^{AB} = 2\left(\sqrt{\Gamma_i^{+}} - \sqrt{\Gamma_j^{+}}\right)\left(\sqrt{\Gamma_i^{-}} - \sqrt{\Gamma_j^{-}}\right)$$

where,

ΔG_{12}^{a} is the adhesive bond energy between asphalt and aggregate,

Γ_1 is the total surface energy of the asphalt,

Γ_2 is the total surface energy of the aggregate, and

Γ_{12} is the surface energy of the asphalt aggregate interface,

superscript LW refers to the Lifschitz van der Waals component,

superscript AB refers to the acid-base component,

superscript + refers to the acid component, and

superscript - refers to the base component.

The three surface energy components, Γ^{LW}, Γ^{+}, and Γ^{-}, which form the basic input of the adhesion calculations, are determined from the USD and WP tests for aggregate and asphalt, respectively.

Similarly, the adhesive bond strength at the asphalt-aggregate interface in wet conditions is determined using the following formula:

$$\Delta G_{132}^{a} = \Gamma_{13} + \Gamma_{23} - \Gamma_{12}$$

where,

ΔG_{132}^{a} is the adhesive bond energy between the asphalt and the aggregate in the presence of water,

subscript 1 refers to asphalt,

subscript 2 refers to aggregate,

subscript 3 refers to water, and

Γ_{ij} can be determined using the equations shown above.

The adhesive bond energy between the asphalt and aggregate in the presence of water, ΔG_{132}^{a} is typically negative. This phenomenon indicates that moisture damage is thermodynamically favorable since there is a release of free energy when water displaces asphalt at the asphalt-aggregate interface. The greater the magnitude of free energy release the stronger will be the drive for water to displace asphalt and cause stripping. Further, low adhesive bond strength at the asphalt-aggregate interface in dry conditions can increase the number of sites for water to break into the interface and aggravate moisture damage.

Surface Energy - Test Results

The USD and WP tests were used to determine the three surface energy components of aggregates and asphalts, respectively. Both of these test methods are currently being developed under the NCHRP Project 9-37, "Using Surface Energy Measurements to Select Materials for Asphalt Pavements." Aggregates passing the No. 4 sieve and retained on No. 8 sieve were used for testing with the USD. Two replicate aggregate samples were tested using three different probe vapors (n-hexane, methyl propyl ketone [MPK], and water).

Glass slides coated with asphalt were used for testing with the WP method. Six slides were prepared for obtaining two replicate data points using each of the three probe liquids. The three probe liquids used with the WP test were diiodomethane, ethylene glycol, and water. Appendix H describes in detail the test procedures and theoretical basis for these tests.

The USD measures spreading pressure of various probe liquids on an aggregate surface, which are then used to calculate surface energy components of the aggregates. Table 3.5 presents spreading pressures of various probe vapors on the aggregate surfaces that were tested in this research. The uncrushed gravel from the Brazos Valley and the crushed gravel from Victoria were mineralogically similar. Since surface energy is an intrinsic material property dictated by the type of mineral surface of the aggregate it is reasonable to expect similar surface energy values for both these two aggregates. Based on this reasoning and the extensive test time involved for testing aggregates, researchers decided to use the same surface properties for both the gravel aggregates.

Table 3.6 summarizes the calculated surface energy components for various aggregates based on the spreading pressures shown in Table 3.5. Appendix H contains the theoretical basis

for these calculations. The WP device was developed to measure the advancing and receding contact angle of various probe liquids on an asphalt surface. Table 3.7 summarizes the advancing contact angles for different asphalts, and Table 3.8 summarizes the calculated surface energy components based on the advancing contact angles. Appendix H contains the theoretical basis for these calculations.

Once the surface energy of asphalts and aggregates are known, the adhesive bond strength with and without the presence of water can be calculated using the equations shown in the previous section. Table 3.9 shows the calculated bond energy at the asphalt-aggregate interface in dry and wet conditions. Note that the matrix of values was calculated for all combinations of aggregates and asphalts including hypothetical mixtures that were not actually tested in the experiment design (those shown in gray).

Table 3.5. Spreading Pressure of Vapors on Aggregates and Specific Surface Areas.

Aggregate (Abbreviation)	SSA (m^2/gm)		Spreading Pressure (ergs/cm^2)					
			Hexane		MPK		Water	
	Avg.	CV (%)	Avg.	CV (%)	Avg.	CV (%)	Avg.	CV (%)
Colorado Materials Limestone (CLLS)	1.47	4	28.4	7	49.4	22	135.3	10
Gravel	1.00	9	30.4	7	72.5	3	302.3	2
Brownwood Limestone (BW LS)	2.15	4	32.7	4	50.5	10	159.8	3
Georgia Granite (GG)	0.12	28	23.2	2	23.2	2	124.7	23

Table 3.6. Surface Energy Components of Aggregates.

Aggregate	Surface Energy Components (ergs/cm^2)			
	Γ^{LW}	Γ^{+}	Γ^{-}	Γ^{Total}
CLLS	57.7	5.5	340.4	144.1
Gravel	61.4	19.6	1067.6	350.8
BW LS	65.6	3.8	432.6	146.7
GG	50.0	0.1	399.6	59.5

Table 3.7. Contact Angle of Probe Liquids on Asphalt Slides.

Asphalt	Contact Angle (°)					
	Diiodomethane		Ethylene Glycol		Water	
	Avg.	CV (%)	Avg.	CV (%)	Avg.	CV (%)
64-40 N	85.8	0	66.1	1	101.7	1
64-40 HL	94.7	1	65.4	1	101.6	1
64-40 AS	77.7	1	51.9	5	87.7	2
64-22 N	88.6	1	67.1	2	102.9	0
64-22 HL	65.9	1	66.2	1	100.0	1
64-22 AS	65.1	3	58.7	1	85.4	3
76-22 N	86.8	1	60.7	2	98.8	1

Table 3.8. Surface Energy Components of Asphalts.

Asphalt (Abbreviation)	Surface Energy Components (ergs/cm^2)			
	Γ^{LW}	Γ^{+}	Γ^{-}	Γ^{Total}
PG 64-40 Neat (64-40 N)	14.6	3.3	0.2	16.3
PG 64-40 + Hydrated Lime (64-40 HL)	10.7	5.4	0.1	12.3
PG 64-40 + Liquid Antistrip (64-40 AS)	18.7	4.0	1.7	24.0
PG 64-22 Neat (64-22 N)	13.3	3.7	0.1	14.6
PG 64-22 + Hydrated Lime (64-22 HL)	25.2	0.8	0.1	25.8
PG 64-22 + Liquid Antistrip (64-22 AS)	25.6	0.7	6.0	29.8
PG 76-22 Neat (76-22 N)	14.2	4.7	0.2	15.9

Table 3.9. Bond Energy at Asphalt-Aggregate Interface.

Aggregate / Asphalt	CM LS		Gravel		BW LS		GG	
	Dry	Water	Dry	Water	Dry	Water	Dry	Water
64-40 N	127.4	-66.4	183.0	-177.9	139.5	-78.8	127.1	-56.1
64-40 HL	136.9	-55.8	205.9	-153.7	150.9	-66.3	139.2	-42.9
64-40 AS	145.9	-63.3	210.7	-165.5	158.7	-74.9	142.0	-56.6
64-22 N	128.3	-63.8	186.4	-172. 7	140.8	-75.7	129.1	-52.4
64-22 HL	111.6	-82.9	141.4	-220.1	120.7	-98.3	107.8	-76.1
64-22 AS	119.6	-96.2	156.3	-226.4	126.8	-113.4	106.6	-98.6
76-22 N	139.3	-57.2	204.7	-158.8	153.1	-67.9	140.3	-45.6

Surface Energy - Discussion

Bond energy without the presence of water is positive, which means that energy must be supplied to the system to cause debonding between the asphalt and aggregate. However, in the presence of water, this energy is negative, which means that there is a release of free energy when water displaces asphalt from the asphalt-aggregate interface. Therefore, water damage is

normally a thermodynamically favorable phenomenon. The greater the magnitude of the released free energy, the greater will be the drive for water to displace asphalt and cause debonding at the interface. It is important to note that the magnitude of energy released in the presence of water must not be considered as a global parameter, that is, comparisons of free energy released are more appropriate when limited to similar mixes. This is because other mix parameters such as aggregate gradation, asphalt film thickness distribution, and ability of an asphalt film to hold and transfer moisture (diffusivity) can also influence the propensity of the mix to undergo moisture damage.

Table 3.10 compares results from the Hamburg test and the bond energy calculations based on the measured surface energy. For Mixes 1 through 3 addition of lime or antistrip agent reduces performance of the mix with limestone in terms of rutting and moisture damage. The bond energy calculations indicate a similar trend. Addition of hydrated lime and liquid antistrip to the mix caused a reduction in the dry adhesive bond strength and an increase in the free energy released when water displaces asphalt at the aggregate-asphalt interface. Similar consistency between Hamburg and surface energy results is seen in Mixes 4 through 6. However, in these mixes, addition of lime and antistrip agent improved resistance to moisture damage based on both Hamburg data and bond energy calculations.

Mixes 7 through 9 were different in terms of type and gradation of aggregates and asphalt type. Bond energy calculations indicate that the gravel mix is most likely to fail among the three mixes, which corresponds with the Hamburg test results. In the absence of comprehensive material performance based mechanistic models, it is not recommended to compare the values of free energy released universally among different types of mix designs. For example, when the release of free energy in the presence of water for Mix 9 is compared with Mixes 1, 2, and 3, one would expect Mix 9 to undergo a similar level of moisture damage as Mixes 2 and 3. But this was not the case. Some of the possible reasons for this happening could be the difference in the specific surface area of aggregates, film thickness distribution, and very likely, the adhesive bond strength in the absence of water. Since Mix 9 has a dry adhesive bond energy that is higher than that of Mixes 2 and 3, it is possible that adhesive "defects" for Mix 9 that also act as initiation sites for moisture damage are fewer as compared to Mixes 2 and 3.

Table 3.10. Comparison of Bond Energy Calculations with Hamburg Data.

No.	Mix Design	Total		Moisture Damage		Adhesive Bond Strength (ergs/cm^2)	
		Passes (x1000)	Rut Depth (mm)	Passes (x1000)	Rut depth (mm)	Dry	Wet
1	Colorado Limestone	15.0	11.0	9.7	2.5	128.3	-63.8
2	Colorado Limestone + 1% Lime	7.5	8.3	4.3	2.6	111.6	-82.9
3	Colorado Limestone + Liquid Additive	6.5	8.3	3.5	2.7	119.6	-96.2
4	Fordyce Gravel	4.5	9.5	3.1	5.8	183.0	-177.9
5	Fordyce Gravel + 1% Lime	20.0	9.3	none	none	205.9	-153.7
6	Fordyce Gravel + Liquid Additive	20.0	8.9	none	none	210.7	-165.5
7	Georgia Granite	20.0	7.0	none	none	140.3	-45.6
8	Brazos Uncrushed Gravel	6.0	10.5	2.5	1.7	186.4	-172. 7
9	Brownwood Limestone	20.0	7.3	none	none	140.8	-75.7

Conclusions Related to Moisture Testing

Within groups of controlled mixes, the calculated bond strength based on surface energy measurements relates well with the deformation data from the Hamburg wheel load test.

Typically, one expects the moisture susceptibility of a mix to decrease with the addition of agents such as hydrated lime or liquid antistripping agent. However, for the mix design with limestone aggregate the moisture susceptibility of the mix increased when hydrated lime or liquid antistripping agent was added. This increase in moisture susceptibility was observed consistently in both the Hamburg test and bond energy calculations.

Measuring surface energy of asphalts is a relatively fast technique as compared to measuring surface energy of aggregates. The precision of measurement of the WP test is also

much greater than that of the USD test. Further, one can expect similar surface energy components for aggregates of similar mineralogical composition. This is seen by comparing the surface energy values of the two different types of limestone included in this research.

The aim of this project was to conduct exploratory research on more fundamental methods and techniques for evaluating moisture damage. It was not the purpose of this project to evaluate or validate the Hamburg test with respect to fundamental tests such as measurement of surface energy or vice versa. While the Hamburg test is an attractive tool to get quick estimates about the moisture susceptibility of mixes, it is not capable of informing the user about the mechanisms affecting moisture resistance. As a practicing engineer, one will rarely find a situation where a large number of choices are available for selection of aggregate and/or asphalt. In such cases, knowledge of the mechanisms influencing mixture performance can be used to accurately predict potential problems and modify the mix to meet the requirements. Knowledge of fundamental properties, such as surface energy, improves the engineer's ability to properly address these issues during the mixture design and analysis stage.

During mix preparation in the lab, hydrated lime is added by spraying slurry in the required proportion onto the aggregate surface. However, for surface energy calculations, hydrated lime was added to the asphalt and surface energy of the modified asphalt was determined using the WP test. Therefore, for a lab mix, increased concentration of lime at the aggregate-asphalt interface can result in a much larger release of free energy as compared to the calculated values where hydrated lime is added to the asphalt.

Various factors such as gradation, asphalt film thickness distribution, and diffusivity of asphalt can affect the propensity of a mix to undergo moisture damage. Therefore, the bond strength calculated from surface energy measurements must not be applied universally to all mixes without considering these and other influencing factors. However, results from tests conducted on controlled HMA mixtures indicate that fundamental materials properties are consistent with large-scale mechanical properties of the mix. Further research is needed to incorporate the effect of differences in specific surface area and aggregate gradation in the mix.

CHAPTER 4:
TEXAS HMA MIXTURE CHARACTERIZATION

INTRODUCTION

TxDOT uses a very large number of HMA mixtures in its vast highway network. They widely vary from the mixtures types, aggregate types, and asphalt types. Several types of new generation mixtures like permeable friction course, and stone mastic asphalt have been introduced to meet the current demand. A mixture database can aid the engineers during the mixture selection process and/or pavement design. Developing a mixture test database for Texas is a huge task. In this project, researchers attempted to test and document the results of some field mixtures using different tests. Both plant-produced and lab-produced mixtures were tested. In some cases results of the tests conducted under other tasks were also documented.

LAB-PRODUCED MIXTURE

The proposed AASHTO Design Guide adopts a mechanistic-empirical approach for the structural design of asphalt pavement (2002 Design Guide). The basic inputs for pavement design include environment, material, and traffic data. There are two major aspects of M-E based material characterization: pavement response properties and major distress/transfer functions. Pavement response properties are required to predict states of stress, strain, and displacement within the pavement structure when subjected to external wheel loads. These properties for assumed elastic material behavior are the elastic modulus and Poisson's ratio. The major distress/transfer functions for asphalt pavements are load-related fatigue fracture, permanent deformation, and thermal cracking.

The new design guide suggests a hierarchical system for materials characterization. Three input levels comprise the system. Level 1 represents a design philosophy of the highest practically achievable reliability, while Levels 2 and 3 represent successively lower reliability. The proposed AASHTO mechanistic-empirical design method offers several levels of design based on the traffic level.

NCHRP Project 9-19 researchers suggest constructing a dynamic modulus master curve for all mixtures. The master curve is developed by conducting frequency sweeps at five different temperatures and six frequencies. The same master curve can be used as an input for predicting rutting and fatigue damage. Level 1 material characterization requires actual testing to measure

the dynamic modulus of an asphalt mixture, Level 2 allows for an estimated value, and Level 3 provides a default value. Developing a database for the asphalt mixtures commonly used by an agency will benefit Level 2 and Level 3 mixture designs and provide initial data for Level 1 designs.

Dynamic Modulus Test

Dynamic modulus tests (Figure 4.1) conducted on the selected mixtures followed the method recommended by NCHRP Project 1-37A, "Draft Test Method for Dynamic Modulus Test" (Witczak et al., 2002). Later AASHTO adopted this test procedure as "Standard Method of Test for Determining Dynamic Modulus of Hot-Mix Asphalt Concrete" with AASHTO Designation TP 62-03 (AASHTO Provisional Standards, 2003). The dynamic modulus test procedure applies a sinusoidal axial compressive stress to a HMA specimen at a given spectrum of temperatures and loading frequencies. The applied stress and resulting recoverable strain responses are used to calculate the dynamic modulus and phase angle. Complex modulus, expressed as E*, is a complex number defining the relationship between stress and strain for a linear viscoelastic material. Dynamic modulus, expressed as $|E^*|$, is the absolute value of complex modulus. Dynamic modulus is calculated by dividing the peak-to-peak stress by the peak-to-peak strain for a material subjected to sinusoidal loading. Phase angle (δ) is the lag time measured in degrees between a sinusoidally applied stress and resulting strain in a stress-controlled test.

The results obtained from this test can be used to construct a master curve using the dynamic modulus value measured at different temperatures and frequencies. This master curve can be used for characterizing HMA mixtures for pavement layer thickness design and performance analyses. This master curve, in fact, characterizes both the rutting and fatigue performance of HMA mixtures.

Specimen Preparation

Dynamic modulus test is conducted on a 4-inch (100 mm) diameter and 6-inch (150 mm) high compacted specimen. Initially, the specimens were compacted using a SGC with dimensions of 6 inches in diameter and 7 inches in height. The final specimen was obtained by coring from the 6-inch diameter specimen and sawing the two ends. The final air void contents of the cored specimens were maintained within 7±0.5 percent. Incidentally, air void contents of

the cored specimens used for testing was typically 1.5 to 2 percent lower than those in the larger size SGC compacted specimen. The 6-inch diameter specimens were therefore compacted to approximately 9 to 10 percent air void content.

Two replicate specimens from each mixture were fabricated. Coring and sawing made the specimen process somewhat complicated and time consuming, but the cored and sawed specimens typically have more uniform air void distribution than their 6-inch diameter counterparts (Witczak et al., 2002). The smooth sawn cylindrical surface was very conducive for attaching LVDTs.

Testing

Testing was performed on two replicates, each with three LVDTs for recording specimen strains. The LVDTs were fixed to the specimen using fastening clamps that were glued to the specimen surface. A spacing of 4 inches (100 mm) between the studs was maintained which left about 1 inch (25 mm) from either face of the specimen. Care was taken to ensure that the studs were vertically aligned. Each LVDT was placed at an equal distance (120°) around the cylindrical surface.

Each specimen was tested at six different loading frequencies and four different temperatures. Witczak et al. (2002) proposed five different temperatures for conducting this test including 14°F (-10°C). The stress required to cause measurable strain at 14°F was beyond the capacity of the test equipment available at TTI at the beginning of this project; so a few mixtures tested during that period excluded testing at 14°F.

The loads selected for each frequency were such that the total strain in the specimen would be 50 to 150 microstrains. Witczak et al. (2002) suggested this range of strain to keep sample deformation within the linear range. Loads causing smaller strains would not give accurate readings, and loads causing larger strains would cause the sample to deform permanently, thereby altering its properties. Sometimes a preliminary (or "dummy") specimen was used to determine the load required to keep the strain within these limits. Then, technicians performed the actual tests using two replicate specimens. Other cases experience dictated the stress used to cause suggested range of deformation.

All specimens were wrapped with cellophane and stored at room temperature to reduce unwanted aging before testing. To minimize specimen damage, researchers performed tests

starting at the highest frequency and progressing to the lowest frequency at each temperature while increasing the temperature from the lowest to the highest level. The test specimens were brought to the required test temperature by placing them in an environmental test chamber for a minimum of four hours for 70, 100, and 130°F and overnight for 40 and 14°F. To minimize shear stresses at the specimen ends, two thick latex sheets with silicone grease between them was placed between each end of the specimen and loading platens.

Data Acquisition and Data Analysis

The pneumatic testing system used for a few tests during the early stages of this project produced "noise" in some cases during the recording of deformation. Due to this equipment deficiency, researchers screened selected data manually and discarded any outliers. TTI purchased a hydraulic system which performed the SPTs more effectively and efficiently.

A data acquisition system and a desktop computer recorded associated stresses and strains of the replicate tests. Phase angle (δ) and dynamic modulus ($|E^*|$) were calculated using the average of the results from the last five loading cycles in accordance with recommendations of NCHRP Project 9-19. Measurement of phase angle (δ) was found to be more sensitive at higher loading frequencies and temperatures. In certain cases, the variation in the last five values of δ was so extensive that it was not possible for the computer to select a reasonable value of δ. If so, a δ value was computed manually. This trend was more prominent for very high loading frequencies, e.g., 25 Hz, and less prominent for the new hydraulic machine.

Averages of the modulus values obtained from each of the two replicate tests were used to plot the master curves. Different shifting techniques can be used to construct a master curve using time-temperature superposition. In this project, a sigmoidal function was employed for construction of the master curve. Pellinen et al. (2002) showed that, for the wide range of temperatures used to obtain the compressive dynamic modulus data, the sigmoidal function fit the data well because it followed the physical form of the measured data. Moreover, the proposed AASHTO guide utilizes the sigmoidal fitting function for the characterization of a HMA mixture. A master curve was plotted for each mix using a sigmoidal function described as follows (Pellinen et al., 2002):

Figure 4.1. Dynamic Modulus Testing Setup.

$$\log(|E^*|) = \delta + \frac{\alpha}{1 + e^{\beta - \gamma \log \xi}}$$

where,

|E∗| = dynamic modulus,

ξ = reduced frequency,

δ = minimum modulus value,

α = span of modulus values,

γ = shape parameter governing slope, and

β = shape parameter governing horizontal position of turning point.

This model typically represents a curve that becomes flat at very high and very low values of log (t) and typically represents the behavior of a viscoelastic material. The four variables involved in the model, i.e., δ, α, γ, and β along with the shift factors for the other three

temperature ranges are derived simultaneously using a nonlinear regression analysis supported by the "solver function" in the Microsoft Excel spreadsheet.

The reference temperature assumed in this case was 70°F (21.1°C). This temperature was selected in accordance with AASHTO TP 63-03. With the raw data available, a master curve can be created at different base temperatures. Dynamic modulus values for other temperatures were shifted to this value for plotting the master curve.

Presentation of Results in Database

Thirty average dynamic modulus, $|E^*|$, values (five temperatures × six frequencies) based on two replicates reported in tabular form along with raw data, analyzed data (Table 4.1), and master curve (Figure 4.2) for each mixture were recorded on a CD-ROM. The master file, describing general information about each mixture, was copied onto the CD-ROM in Microsoft® Excel® format. Each mixture has one or more links to separate Excel files describing the detailed test results and pertinent mixture information. This CD-ROM has been provided to TxDOT.

Table I.2 in Appendix I summarizes mixture properties and lists the tests performed on the lab-produced mixtures.

Table 4.1. Typical Dynamic Modulus Test Results.

Temperature (°F)	Dynamic Modulus Value at Different Frequencies, (psi)					
	25.0 Hz	10.0 Hz	5.0 Hz	1.0 Hz	0.5 Hz	0.1 Hz
14	5001708	4779002	4564926	4165926	3989053	3536679
40	3903553	3635377	3428988	2913088	2713879	2210742
70	1855906	1550964	1367998	983285	842453	583923
100	863629	619747	477683	277240	217049	142210
130	331267	221110	171000	101599	82454	60481

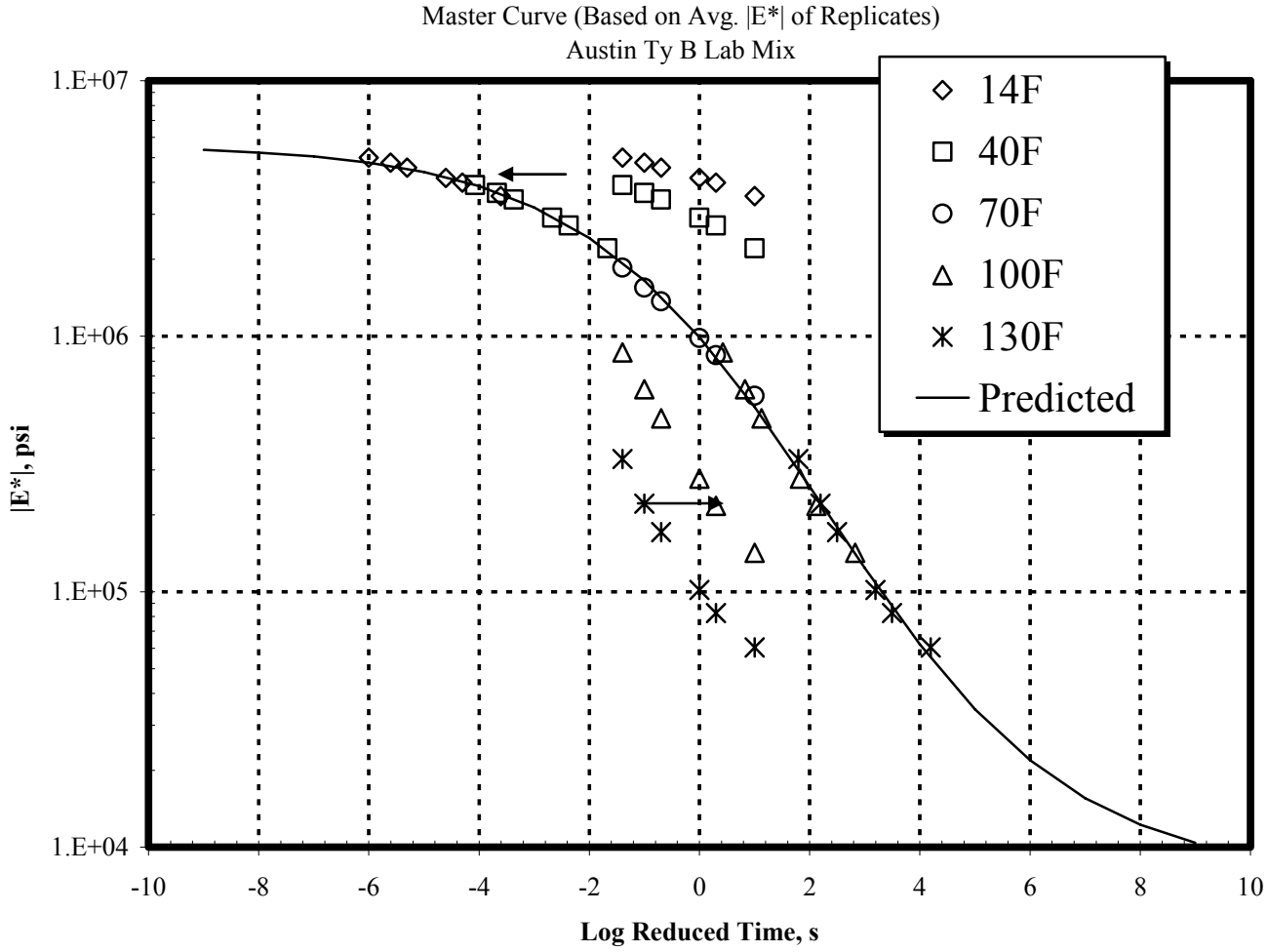

Figure 4.2. Typical Master Curve Developed from Dynamic Modulus Tests.

Hamburg Testing

Most of the mixtures tested with the dynamic modulus test were also tested with the Hamburg device. TxDOT Method Tex-242-F was followed during these tests. In most cases, the both raw and analyzed Hamburg data are presented in electronic format on the CD-ROM. The raw data obtained from this test were again analyzed using an Excel macro spreadsheet developed by TxDOT.

Flow Time and Flow Number Test

Few mixtures were tested with flow time and flow number tests. The descriptions of these two tests have already been mentioned in Chapter 3. These two tests can provide the fundamental properties of HMA mixture's rutting behavior. Results are documented on the CD-ROM.

PLANT-PRODUCED MIXTURE

The objective of this task was to test HMA plant production mixtures to determine if TxDOT specification requirements are adequate to produce mixtures that are resistant to several distresses. Researchers obtained about 30 plant-produced mixtures. They were tested dynamic modulus and Hamburg tests. Some mixtures were tested with APA as well. Few of the mixtures were collected from more than one production lot. Researchers reheated the mixtures in the lab before compacting to certain air voids content. During transportation from the construction site to the TTI laboratory and storage before compaction, and the reheating of mixtures may have attributed to further oxidation. All mixtures tested with Hamburg met the TxDOT criteria. Currently, TxDOT does not have any criteria for dynamic modulus or APA tests. For identical mixture, plant-produced mixture appeared to show stiffer modulus than their counter part produced in the laboratory.

Table I.1 documents the mixtures tested under this task. Detailed results can be obtained from the CD-ROM.

CHAPTER 5:
CONCLUSIONS AND RECOMMENDATIONS

GENERAL

Research Project 0-4203 was a large effort designed to study several HMA related issues in Texas. Results from other tasks of this project are published in three other reports (4203-1, 4203-2, and 4203-4). This report concentrates on the research effort to identify and validate best available laboratory test procedures to characterize permanent deformation and moisture susceptibility of HMA mixtures and to develop Texas mixture databases for both plant-produced mixes and lab-produced mixes.

Twelve field mixes and three laboratory mixes were included in the rutting characterization of mixtures. Four of the 12 mixtures tested were obtained from Texas DOT districts and eight were obtained from neighboring states. Two of the laboratory mixes were prepared using a highly polymer-modified binder with crushed rhyolite aggregate and crushed river gravel aggregates. A third laboratory mix contained uncrushed river gravel and conventional asphalt and was intentionally designed to be rut susceptible. All 15 of these mixes were tested using the simple performance tests (dynamic modulus, flow time, and flow number). Twelve of the mixtures were tested using the APA and SST-FSCH, and seven mixtures were tested using the Hamburg wheel-tracking device.

During the moisture susceptibility study, the researchers tested nine HMA mixtures using the Hamburg test. The Universal Sorption Device and Wilhelmy plate method were selected for measuring the surface energy of aggregates and asphalts, respectively. Mixtures were tested with and without antistripping agents.

Researchers obtained about 30 plant-produced mixtures from different parts of the state and tested using the Hamburg and dynamic modulus devices. Some of the plant-produced mixtures were tested using the flow time and flow number protocols, and APA device. Raw materials of 49 mixtures used in Texas were collected and then mixed and molded in the laboratory and tested to develop a database for TxDOT.

CONCLUSIONS

As mentioned earlier, the tasks documented in this report were not interrelated; the following conclusions based on their results are reported under separate headings.

Permanent Deformation

- Correlations of Hamburg test results with dynamic moduli were poorer than correlations of Hamburg with flow time and flow number parameters, with the exception of E*/sin ϕ at 1 Hz.
- Flow time slope and flow number value provided the best correlations with both the Hamburg and APA rut depth measurements.
- Correlations of E*/sin ϕ or G*/sin δ with the Hamburg and APA test parameters were better than correlations of E* and G* alone with these parameters. This is likely because phase angle represents the viscoelastic behavior of the mix, which is responsible for permanent deformation and not resilient modulus. This is significant because the phase angle from the dynamic modulus test is not a vital input in the mechanistic-empirical design guide that is currently under development.
- Correlations of Hamburg rutting with the other test parameters were similar to the correlations between the APA rut depth and those same parameters. Flow number value, flow time slope, E*/sin ϕ at 1 Hz, flow number slope, and flow time value were among the best five correlations both with Hamburg and the APA rut depths.
- APA rut depth correlated with the flow number and flow time parameters better than the APA creep slope correlated with these values.
- The correlations of the APA test parameters with dynamic modulus and FSCH tests were not as good as correlations of the APA test parameters with the flow time and flow number test parameters.
- Correlations of E* or G* with the APA parameters were better at lower test frequencies than at higher frequencies. However, these values did not show strong correlations.
- The overall rut depth from the APA test at 8000 strokes correlated better with all other parameters as compared to the APA creep slope.
- By applying the Duncan multiple range test procedure with the value of flow time slope and flow number slope, the research team was able to separate the mixes into

six Duncan groups of statistically equivalent values, which was much better than the flow time or flow number values. However, comparing results from Hamburg and APA groups, it is concluded that the sensitivity of the flow time or flow number tests can be improved by (1) selecting the appropriate temperature and stress levels for the mixes being compared and (2) comparing mixes that have similar properties unlike a broad range as seen in the APA mixes selected for this research.

- Based on the APA rut depth, the PG 64-40 + rhyolite mix can be placed in the second and third of the six Duncan groups in terms of ranking. The mix can therefore be said to perform better than most of the other mixes since it is in the top 33 to 50 percent of the mixtures. In contrast, the PG 64-40 + river gravel mix was ranked in the fourth of the six Duncan groups.
- Based on Duncan grouping for dynamic modulus, the PG 64-40 + rhyolite mix was placed in the fifth or sixth of the six groups when E* values are compared at 10 Hz and in the fourth and fifth of the five groups when the values are compared at 1 Hz. This means that the E* values placed this mix in the worst 33 percent of the mixtures. The PG 64-40 + river gravel mix was placed in the sixth of six groups and fifth of five groups when E* values are compared at 10 and 1 Hz, respectively. These groupings are quite contrary to those for the APA parameters. Similarly, for the Hamburg mixes, this mix was rated in the last group by E* parameters (except E*/sin ϕ at 1 Hz) and in the second from the last group by most other parameters.
- The results from this research indicate that caution must be exercised in interpreting the rut susceptibility of mixes based on the E* parameters, especially when evaluating mixtures containing polymer-modified asphalts.
- These findings indicate that flow time and flow number tests capture fundamental material properties and should be considered for inclusion in the mixture design and selection process.

Moisture Susceptibility

- Within groups of controlled mixes, the calculated bond strengths based on surface energy measurements relate well with the deformation data from the Hamburg wheel load test.
- Moisture susceptibility of mixtures designed using limestone aggregate increased when hydrated lime or liquid antistrip agent was added. This increase in moisture susceptibility was observed consistently in both the Hamburg test and bond energy calculations. The opposite was true for mixtures made using gravel aggregates.
- Measuring surface energy of asphalts is a relatively fast technique as compared to measuring surface energy of aggregates. Precision of measurements using the WP test is much greater than those from the USD test. Typically, one can expect similar surface energy components for aggregates of similar mineralogical composition. This observation is seen by comparing the surface energy values of the two different types of limestone included in this research.

Mixture Database

- All plant-produced mixtures passed TxDOT Hamburg criteria.
- In most cases, plant-produced mixtures yielded higher dynamic moduli (stiffer mix) than their corresponding lab mixtures. The likely reason for this is additional oxidative aging of asphalt in plant-produced mixtures during transportation, storage, and particularly reheating before molding of specimens.
- TxDOT does not have any criteria for APA, dynamic modulus, flow time, or flow number test. So these tests results could be compared for production verification.

RECOMMENDATIONS

- Exercise caution when estimating rut susceptibility of mixtures based on the E* parameters, particularly when evaluating mixtures containing polymer-modified asphalts.
- Consider using flow time and flow number tests in the mixture design and selection process since they can also be used to acquire fundamental material properties that relate better to rutting than dynamic modulus.

- Various factors such as gradation, asphalt film thickness distribution, and diffusivity of asphalt can affect the propensity of a mix to undergo moisture damage. Therefore, do not universally apply the bond strengths calculated from surface energy measurements to all mixes without considering these and other influencing factors. Results from bond strength tests conducted on controlled HMA mixtures indicate that fundamental materials properties are generally consistent with large-scale mechanical properties of the mix.
- Further research is needed to incorporate the effect of differences in specific surface area and aggregate gradation in an HMA mixture on bond energy.
- Since dynamic modulus is a key input for the proposed mechanistic-empirical pavement design guide, the dynamic modulus database should be expanded to include a wide variety of HMA mixtures from all parts of the state.

REFERENCES

AASHTO, *Provisional Standards*, American Association of State Highway and Transportation Officials, Washington, D.C., 2003.

Barksdale, R.G., "Compressive Stress Pulse Times in Flexible Pavements for Use in Dynamic Testing," Highway Research Record 335, Highway Research Board, 1971.

Bhasin, A., J.W. Button, and A. Chowdhury, "Evaluation of Simple Performance Tests on HMA Mixtures from the South Central United States," Research Report No. FHWA/TX-03/9-558-1, Texas Transportation Institute, Texas A&M University College Station, 2003.

Cheng, D., "Surface Free Energy of Asphalt-Aggregate Systems and Performance Analysis of Asphalt Concrete Based on Surface Free Energy," Ph.D. Dissertation at Texas A&M University, College Station, Texas, 2002.

Chowdhury, A. and J.W. Button, "Best Superpave Shear Test Protocol for Predicting Rutting," Research Report No. FHWA/TX-02/0-1819-S, Texas Transportation Institute, Texas A&M University, College Station, Texas, 2003.

Curtis, C.W., R.L Terrel, L.M. Perry, S. Al-Swailm, and C.J. Braanan, "Importance of Asphalt-Aggregate Interactions in Adhesion," Association of Asphalt Paving Technologists, Proceedings Volume 60, 1991.

Ishai, I. and J. Craus, "Effect of Filler on Aggregate-Bitumen Adhesion Properties in Bituminous Mixtures," Association of Asphalt Paving Technologists, Proceedings Volume 46, 1976.

Kanitpong, K. and H.U. Bahia, "Role of Adhesion and Thin Film Tackiness of Asphalt Binders in Moisture Damage of HMA," Association of Asphalt Paving Technologists, Proceedings Volume 72, 2003.

Kendall, M.G. and J.G. Dickinson, "Rank Correlation Methods," 5th Edition, Oxford University Press, 1990.

Kim, Y.R. and D.N. Little, "Development of Specification Type Tests to Assess Damage and Healing Properties of Bitumens and Mastics," FHWA/473630, Federal Highway Administration, pp. 163, 2003.

Little, D.N., D.R. Jones, and S. Logaraj, "Chemical and Mechanical Mechanisms of Moisture Damage in Hot Mix," National Seminar on Moisture Sensitivity, San Diego, California, 2002.

Majidzadra, K. and F.N. Brovold, "State of the Art: Effect of Water on Bitumen-Aggregate Mixtures," Highway Research Board, Special Report, 1968.

Pellinen, T.K., M.W. Witczak, and R.F. Bonaquist, "Asphalt Mix Master Curve Construction Using Sigmoidal Fitting Function with Non-linear Least Squares Optimization," 15th ASCE Engineering Mechanics Conference, Columbia University, New York, June 2002.

Scott, J.A.N., "Adhesion and Disbanding Mechanisms of Asphalt Used in Highway Construction and Maintenance," Association of Asphalt Paving Technologists, Proceedings Volume 47, pp. 19, 1977.

Taylor, M.A. and N.P. Khosla, "Stripping of Asphalt Pavements: State of the Art," Transportation Research Record 911, pp. 150-158, 1983.

Terrel, R.L., and S. Al-Swailm, "Water Sensitivity of Asphalt Aggregate Mixes: Test Selection," SHRP Report No. A-403, Strategic Highway Research Program, National Research Council, Washington D.C., 1994.

Van Oss, C.J., R.J. Good, and M.K. Chaudhury, "Additive and non-Additive Surface Tension Components and Interpretation of Contact Angles," Langmuir, No. 4, pp. 884-891, 1988.

Williams, R.C., and B.D. Prowell, "Comparison of Wheel Tracking Test Results with WesTrack Performance," Transportation Research Record 1681, 1999.

Witczak, M.W., K. Kaloush, T. Pellinen, M.E. Basyouny, and H. V. Quintus, "Simple Performance Test for Superpave Mix Design," NCHRP Report No. 465, 2002.

Zhang, J., L.A. Cooley, Jr., and P.S. Kandhal, "Comparison of Fundamental and Simulative Test Methods for Evaluating Permanent Deformation of Hot Mix Asphalt," Transportation Research Record 1789, 2002.

Zhou, F. and T. Scullion, "Laboratory Results from Heavy Duty Asphalt Mixes," Technical Memorandum to TxDOT, 2001.

2002 Design Guide. http://www.trb.org/mepdg/guide.htm .

APPENDIX A:
GRADATIONS OF HMA MIXES

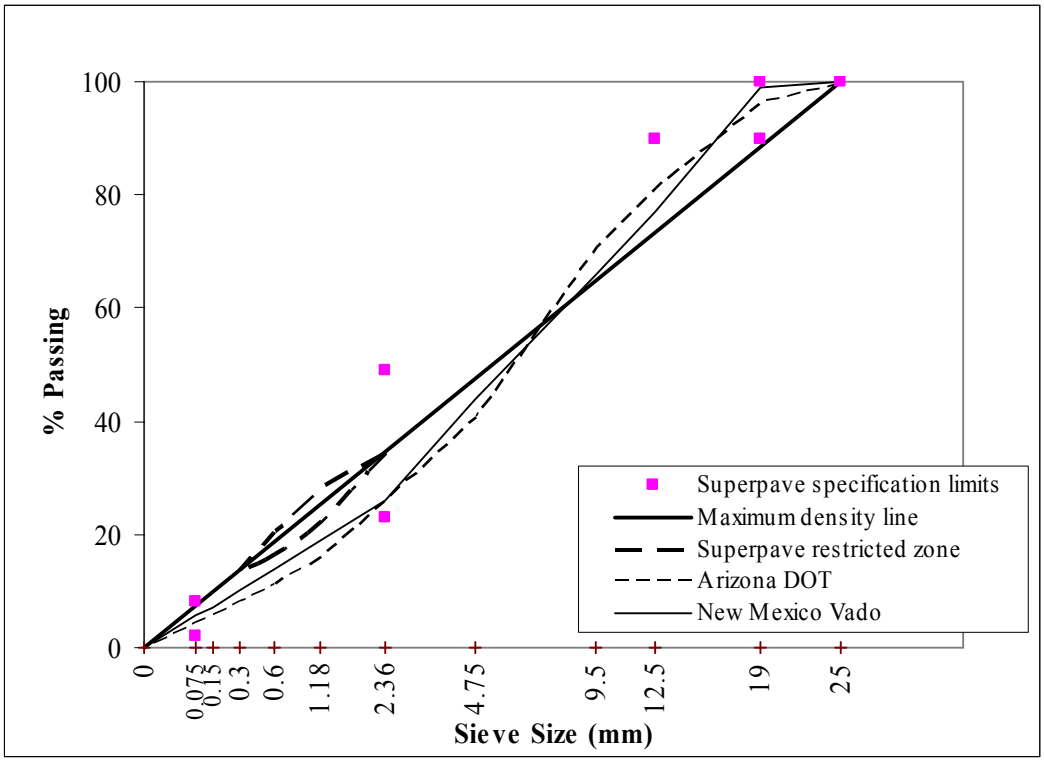

Figure A.1. Gradation of Mixes with 19 mm Maximum Nominal Aggregate Size.

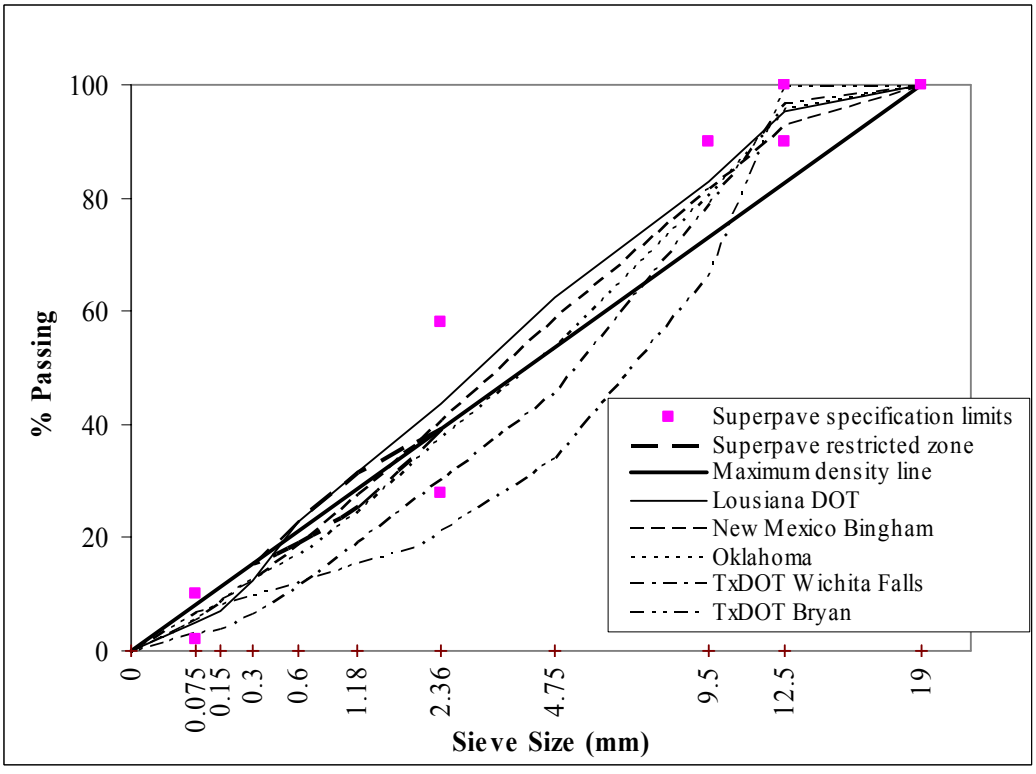

Figure A.2. Gradation of Mixes with 12.5 mm Maximum Nominal Aggregate Size.

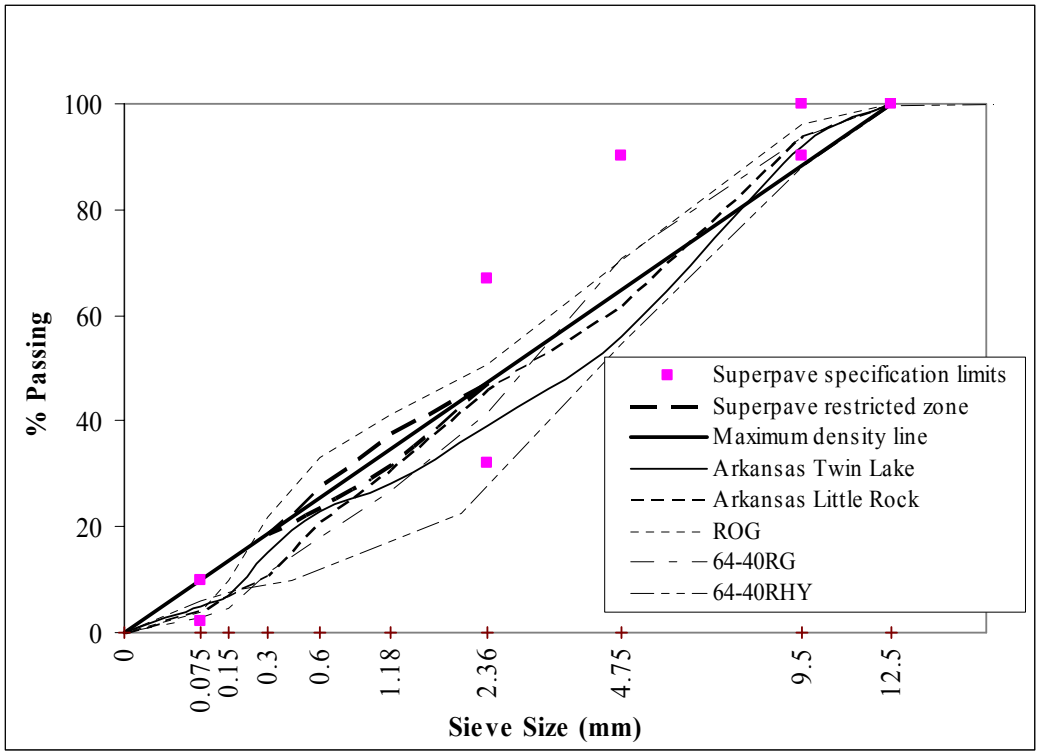

Figure A.3. Gradation of Mixes with 9.5 mm Maximum Nominal Aggregate Size.

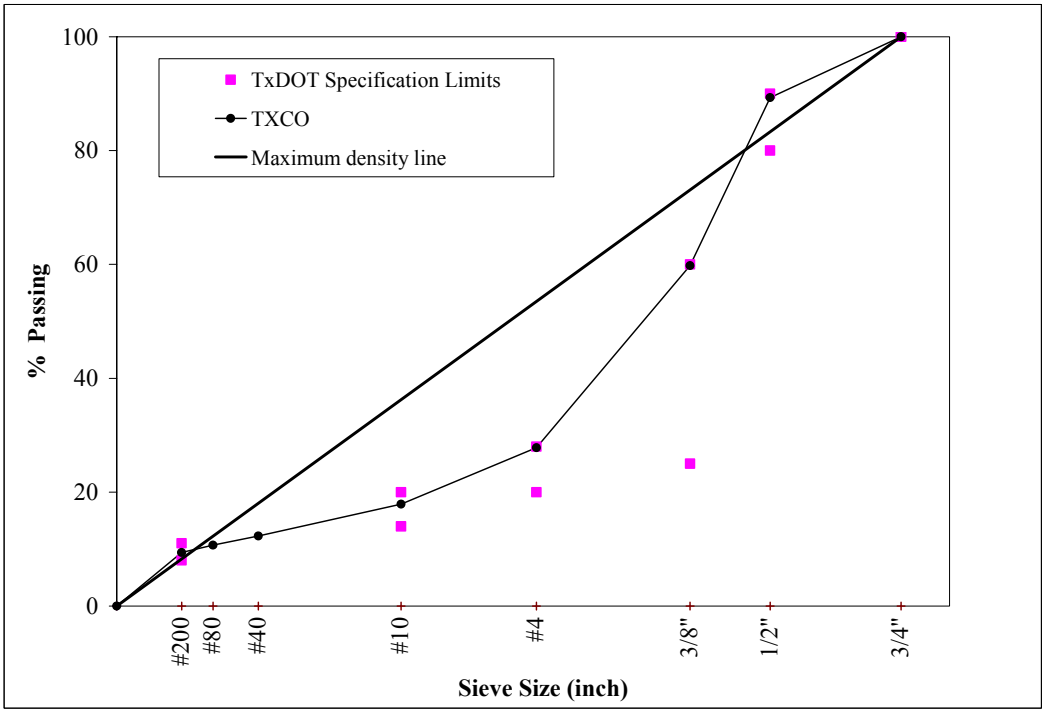

Figure A.4. Gradation of SMA Mix from Cotulla, Texas.

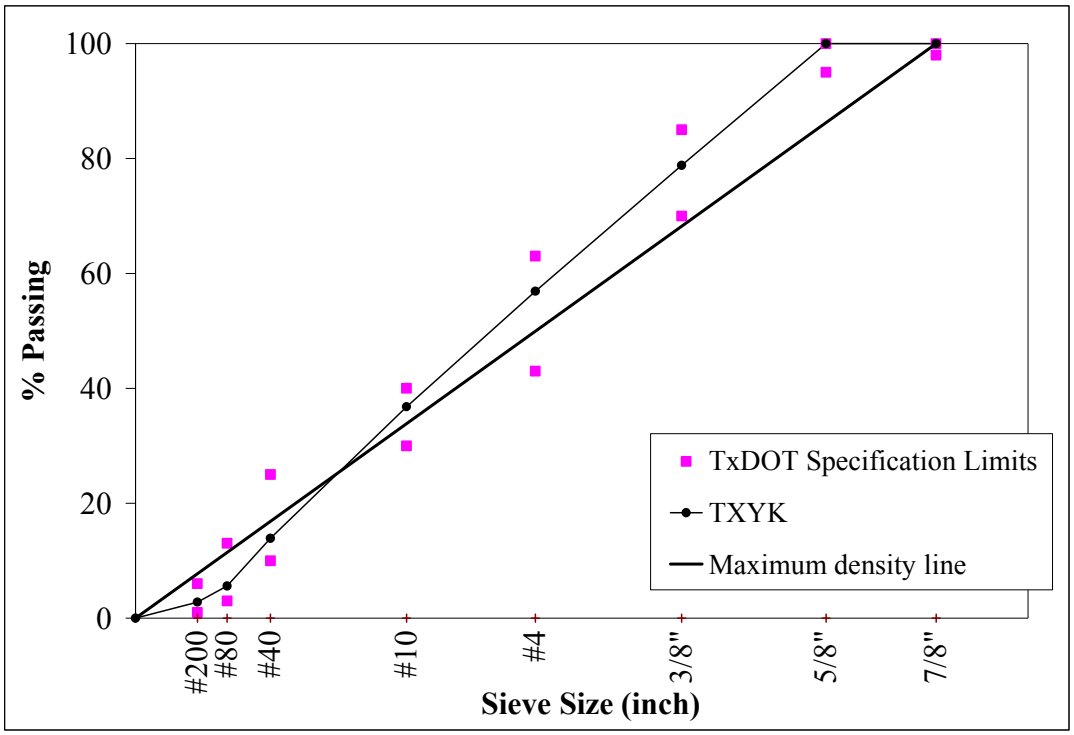

Figure A.5. Gradation of Type C Mix from Yoakum, Texas.

APPENDIX B:
SST DATA FOR ALL TEMPERATURES AND FREQUENCIES

Table B.1. FSCH Data for ARTL Mixture.

Freq. Hz	Test at 20°C						Test at 40°C					
	G* (MPa)			δ (Degrees)			G* (MPa)			δ (Degrees)		
	#1	#2	Avg.	#1	#2	Avg.	#1	#2	Avg.	#1	#2	Avg.
10	287934	227059	257497	30.32	23.28	26.8	29865	56629	43247	58.93	50.24	54.6
5	239059	200666	219863	29.74	23.03	26.4	21620	40633	31127	56.77	52.14	54.5
2	181788	165572	173680	33.01	24.21	28.6	13988	26722	20355	54.45	53.72	54.1
1	144886	140227	142557	35.66	25.9	30.8	10407	19075	14741	53.51	54.17	53.8
0.5	110291	117549	113920	38.69	28.33	33.5	7550	14338	10944	48.77	52.94	50.9
0.2	73248	89968	81608	42.39	31.25	36.8	5770	9631	7701	52.34	52.83	52.6
0.1	52896	71216	62056	44.88	33.85	39.4	4754	7867	6311	45.86	49.34	47.6
0.05	38317	56218	47268	46.52	35.87	41.2	3848	6236	5042	34.38	48.00	41.2
0.02	25162	39714	32438	50.35	39.13	44.7	3242	5162	4202	37.91	44.95	41.4
0.01	17658	29948	23803	53.01	41.11	47.1	3533	4953	4243	35.27	40.63	38.0

Table B.2. FSCH Data for ARLR Mixture.

Freq. Hz	Test at 20°C						Test at 40°C					
	G* (MPa)			δ (Degrees)			G* (MPa)			δ (Degrees)		
	#1	#2	Avg.	#1	#2	Avg.	#1	#2	Avg.	#1	#2	Avg.
10	268908	282415	275662	28.27	28.1	28.2	29524	34174	31849	60.89	59.65	60.3
5	224572	236267	230420	28.25	28.89	28.6	20585	23005	21795	60.2	61.02	60.6
2	176265	181211	178738	31.41	32.23	31.8	12511	14112	13312	61.3	59.76	60.5
1	141022	142185	141604	33.59	36.06	34.8	8528	9913	9221	56.12	57.27	56.7
0.5	109105	108975	109040	37.01	39.66	38.3	6956	7095	7026	53.99	55.87	54.9
0.2	75008	72740	73874	41.25	44.22	42.7	5284	4840	5062	44.55	52.42	48.5
0.1	54390	51919	53155	44.75	47.1	45.9	4096	4562	4329	39.79	53.7	46.7
0.05	39306	36423	37865	46.64	49.74	48.2	3773	3400	3587	39.33	49.39	44.4
0.02	25312	23049	24181	49.41	53.14	51.3	3277	3241	3259	43.97	48.8	46.4
0.01	18244	16414	17329	52.16	56.49	54.3	3431	2929	3180	38.41	50.99	44.7

Table B.3. FSCH Data for AZ Mixture.

Freq. Hz	Test at 20°C						Test at 40°C					
	G* (MPa)			δ (Degrees)			G* (MPa)			δ (Degrees)		
	#1	#2	Avg.	#1	#2	Avg.	#1	#2	Avg.	#1	#2	Avg.
10	216007	232332	224170	27.86	31.36	29.6	36884	35757	36321	53.39	53.9	53.6
5	184308	195937	190123	26.78	30.5	28.6	27617	26433	27025	53.51	54.61	54.1
2	145513	156628	151071	28.78	30.17	29.5	18316	17191	17754	53.09	54.94	54.0
1	116912	129882	123397	31.19	30.95	31.1	14296	12039	13168	51.27	56.03	53.7
0.5	93589	105233	99411	33.16	32.38	32.8	11005	9541	10273	50.18	54.48	52.3
0.2	66762	77624	72193	36.31	34.57	35.4	8389	6973	7681	46.76	52.22	49.5
0.1	51536	61696	56616	38.9	36.02	37.5	6869	5782	6326	43.91	48.86	46.4
0.05	38800	48456	43628	41.76	37.43	39.6	5892	4799	5346	42.58	47.27	44.9
0.02	26955	34686	30821	45.58	39.08	42.3	5251	4336	4794	40.67	47.24	44.0
0.01	20112	26524	23318	48.25	39.45	43.9	5089	4432	4761	38.56	44.86	41.7

Table B.4. FSCH Data for LA Mixture.

Freq. Hz	Test at 20°C						Test at 40°C					
	G* (MPa)			δ (Degrees)			G* (MPa)			δ (Degrees)		
	#1	#2	Avg.	#1	#2	Avg.	#1	#2	Avg.	#1	#2	Avg.
10	272570	259255	265913	29.29	29.54	29.4	46393	41339	43866	56.22	51.49	53.9
5	224736	213100	218918	31	30.14	30.6	31535	29378	30457	55.83	49.11	52.5
2	169114	158865	163990	34.16	33.22	33.7	20154	20123	20139	52.37	47.55	50.0
1	132332	126383	129358	36.66	35.06	35.9	14141	15308	14725	50.69	44.48	47.6
0.5	103077	99185	101131	39.82	37.45	38.6	10929	12048	11489	49.93	41.33	45.6
0.2	72046	71321	71684	42.94	40.07	41.5	7726	9154	8440	41.34	39.63	40.5
0.1	55088	55122	55105	44.94	41.31	43.1	6110	7939	7025	35.59	35.72	35.7
0.05	42266	43082	42674	45.64	42.49	44.1	5497	6826	6162	34.62	33.91	34.3
0.02	29989	31625	30807	46.72	43.14	44.9	4227	6137	5182	33.06	37.46	35.3
0.01	23588	24627	24108	46.44	43.90	45.2	4069	5334	4702	33.2	39.17	36.2

Table B.5. FSCH Data for NMBingham Mixture.

Freq. Hz	Test at 20°C						Test at 40°C					
	G* (MPa)			δ (Degrees)			G* (MPa)			δ (Degrees)		
	#1	#2	Avg.	#1	#2	Avg.	#1	#2	Avg.	#1	#2	Avg.
10	273758	379079	326419	30.41	21.96	26.2	72198	54706	63452	36.99	40.44	38.7
5	215222	309136	262179	29.55	23.66	26.6	58664	47077	52871	36.55	37.03	36.8
2	187310	244326	215818	26.99	24.42	25.7	42895	35636	39266	37.6	32.93	35.3
1	164551	206501	185526	27.43	25.44	26.4	34118	33910	34014	34.31	32.1	33.2
0.5	142697	174729	158713	27.62	26.26	26.9	28468	27658	28063	32.35	34.42	33.4
0.2	115700	138902	127301	29.21	27.27	28.2	23349	24310	23830	30.8	32.09	31.4
0.1	96398	115476	105937	29.94	28.06	29.0	19537	21236	20387	30.94	32.96	32.0
0.05	79981	96510	88246	31.66	28.6	30.1	16794	18378	17586	30.59	33.79	32.2
0.02	62393	75910	69152	34.07	30.41	32.2	14118	16227	15173	30.14	35.2	32.7
0.01	51185	62564	56875	35.85	31.35	33.6	12124	14907	13516	32.22	37.18	34.7

Table B.6. FSCH Data for NMVado Mixture.

Freq. Hz	Test at 20°C						Test at 40°C					
	G* (MPa)			δ (Degrees)			G* (MPa)			δ (Degrees)		
	#1	#2	Avg.	#1	#2	Avg.	#1	#2	Avg.	#1	#2	Avg.
10	328813	273245	301029	17.97	14.60	16.3	151066	110063	130565	27.23	25.33	26.3
5	313213	253672	283443	15.46	13.27	14.4	127054	94732	110893	26.93	25.46	26.2
2	284647	229052	256850	14.58	13.49	14.0	102809	75898	89354	26.32	25.98	26.2
1	264239	210958	237599	14.57	13.99	14.3	86288	63868	75078	27.37	27.57	27.5
0.5	243885	193745	218815	14.87	14.95	14.9	72738	53108	62923	28.28	28.42	28.4
0.2	215360	172540	193950	15.87	15.79	15.8	56443	41113	48778	28.85	30.71	29.8
0.1	196462	158284	177373	16.85	16.99	16.9	46783	33572	40178	30.41	31.04	30.7
0.05	176874	144311	160593	18.25	18.34	18.3	38694	27322	33008	32.33	33.43	32.9
0.02	153572	126152	139862	21.4	20.09	20.7	29926	20360	25143	34.47	36.01	35.2
0.01	134771	114222	124497	25.01	22.19	23.6	24349	16123	20236	36.6	38.22	37.4

Table B.7. FSCH Data for OK Mixture.

Freq. Hz	Test at 20°C						Test at 40°C					
	G* (MPa)			δ (Degrees)			G* (MPa)			δ (Degrees)		
	#1	#2	Avg.	#1	#2	Avg.	#1	#2	Avg.	#1	#2	Avg.
10	206533	228349	217441	32.41	29.91	31.2	49815	56280	53048	41.73	41.99	41.9
5	169299	190136	179718	31.28	29.09	30.2	39345	41870	40608	39.94	39.17	39.6
2	126994	148697	137846	32.01	29.93	31.0	28962	31139	30051	38.42	36.73	37.6
1	101887	121772	111830	32.79	31.19	32.0	22695	24005	23350	36.53	35.24	35.9
0.5	81609	98138	89874	33.48	32.03	32.8	17397	20988	19193	34.97	32.71	33.8
0.2	60617	74135	67376	33.32	32.78	33.1	15375	16266	15821	29.23	30.05	29.6
0.1	48882	59881	54382	33.17	32.94	33.1	12983	13431	13207	27.65	28.58	28.1
0.05	39366	49097	44232	33.38	33.64	33.5	11652	11732	11692	27.43	28.4	27.9
0.02	30314	37966	34140	33.57	34.36	34.0	10223	9644	9934	25.49	27.9	26.7
0.01	24522	31720	28121	35.61	35.78	35.7	9016	8877	8947	26.34	28.7	27.5

Table B.8. FSCH Data for TXWF Mixture.

Freq. Hz	Test at 20°C						Test at 40°C					
	G* (MPa)			δ (Degrees)			G* (MPa)			δ (Degrees)		
	#1	#2	Avg.	#1	#2	Avg.	#1	#2	Avg.	#1	#2	Avg.
10	176216	243264	209740	26.09	27.4	26.7	51645	44354	48000	43.6	45.36	44.5
5	150490	202942	176716	24.8	26.27	25.5	40027	34444	37236	41.86	44.45	43.2
2	125621	162840	144231	24.25	26.83	25.5	27693	23191	25442	44.7	46.14	45.4
1	108360	134927	121644	24.8	27.74	26.3	19880	17087	18484	42.81	45.26	44.0
0.5	91715	111269	101492	25.77	28.85	27.3	15920	13027	14474	44.8	45.51	45.2
0.2	73678	85788	79733	27.99	30.74	29.4	11415	9891	10653	42.86	44.07	43.5
0.1	62400	69936	66168	29.79	31.81	30.8	8811	8020	8416	42.39	42.67	42.5
0.05	52126	57732	54929	31.33	33.74	32.5	7127	6652	6890	41.64	41.98	41.8
0.02	40805	44378	42592	34.61	36.53	35.6	5791	5275	5533	41.45	43.23	42.3
0.01	34038	36403	35221	37.84	38.94	38.4	5209	4693	4951	42.43	43.81	43.1

Table B.9. FSCH Data for TXBryan Mixture.

Freq. Hz	Test at 20°C						Test at 40°C					
	G* (MPa)			δ (Degrees)			G* (MPa)			δ (Degrees)		
	#1	#2	Avg.	#1	#2	Avg.	#1	#2	Avg.	#1	#2	Avg.
10	356004	123570	239787	22.32	27.69	25.0	67367	65693	66530	46.83	53.01	49.9
5	299804	99263	199534	24.11	29.44	26.8	48408	45195	46802	47.21	52.74	50.0
2	243717	77018	160368	26.06	32.54	29.3	32461	29462	30962	45.69	49.65	47.7
1	202166	61566	131866	28.55	33.13	30.8	24934	22102	23518	43.33	46.94	45.1
0.5	165982	50406	108194	30.85	34.20	32.5	19097	17528	18313	39.55	44.16	41.9
0.2	126340	39342	82841	33.63	34.66	34.1	14650	12381	13516	37.13	37.15	37.1
0.1	101296	32207	66752	35.55	35.59	35.6	11621	10984	11303	36.03	34.61	35.3
0.05	81383	27518	54451	36.75	35.69	36.2	9999	9236	9618	32.09	31.99	32.0
0.02	61235	22872	42054	38.01	38.04	38.0	8854	8197	8526	32.88	34.08	33.5
0.01	49557	19754	34656	38.95	40.62	39.8	7836	7468	7652	32.16	33.92	33.0

Table B.10. FSCH Data for 64-22ROG Mixture.

Freq. Hz	Test at 20°C						Test at 40°C					
	G* (MPa)			δ (Degrees)			G* (MPa)			δ (Degrees)		
	#1	#2	Avg.	#1	#2	Avg.	#1	#2	Avg.	#1	#2	
10	252285	246605	249445	26.62	31.2	28.9	45657	43436	44547	44.03	45.78	44.9
5	207808	201048	204428	27.79	30.5	29.1	35023	33533	34278	42.98	45.46	44.2
2	162613	157045	159829	29.63	30.94	30.3	24082	23419	23751	45.83	46.83	46.3
1	131895	125295	128595	31.04	32.62	31.8	17410	17674	17542	41.79	45.24	43.5
0.5	106392	100799	103596	32.71	33.64	33.2	13464	13380	13422	43.78	45.94	44.9
0.2	79072	73495	76284	34.78	34.81	34.8	10158	10607	10383	41.93	43.66	42.8
0.1	62421	57871	60146	36.62	36.39	36.5	8395	8359	8377	41.69	41.64	41.7
0.05	49603	45431	47517	37.4	38.25	37.8	6880	7139	7010	39.19	40.25	39.7
0.02	36083	32890	34487	40.12	40.14	40.1	5790	6267	6029	37.6	37.75	37.7
0.01	28313	25892	27103	41.48	42.2	41.8	4992	5638	5315	41.78	36.33	39.1

Table B.11. FSCH Data for 64-40RG Mixture.

Freq. Hz	Test at 20°C						Test at 40°C					
	G* (MPa)			δ (Degrees)			G* (MPa)			δ (Degrees)		
	#1	#2	Avg.	#1	#2	Avg.	#1	#2	Avg.	#1	#2	Avg.
10	69840	55079	62460	40.56	42.6	41.6	35757	15221	25489	53.9	39.38	46.6
5	53863	41418	47641	38.17	42.1	40.1	26433	12880	19657	54.61	34.97	44.8
2	38532	29230	33881	35.96	41.04	38.5	17191	10533	13862	54.94	28.3	41.6
1	30658	23132	26895	34.85	40.63	37.7	12039	8999	10519	56.03	31.83	43.9
0.5	25149	17964	21557	33.52	38.61	36.1	9541	7791	8666	54.48	26.95	40.7
0.2	19662	13566	16614	31.46	35.92	33.7	6973	7002	6988	52.22	24.61	38.4
0.1	16204	11069	13637	31.28	36.09	33.7	5782	6687	6235	48.86	23.39	36.1
0.05	13789	9358	11574	30.03	35.95	33.0	4799	6221	5510	47.27	19.27	33.3
0.02	11515	7561	9538	31.74	37.65	34.7	4336	5442	4889	47.24	22.82	35.0
0.01	10127	6817	8472	31.47	39.96	35.7	4432	5208	4820	44.86	22.59	33.7

Table B.12. FSCH Data for 64-40RHY Mixture.

Freq. Hz	Test at 20°C						Test at 40°C					
	G* (MPa)			δ (Degrees)			G* (MPa)			δ (Degrees)		
	#1	#2	Avg.	#1	#2	Avg.	#1	#2	Avg.	#1	#2	Avg.
10	50195	73960	62078	43.17	40.04	41.6	8181	15276	11729	49.54	31.81	40.7
5	37561	57974	47768	41.66	38.31	40.0	6444	13832	10138	46.51	27.11	36.8
2	26719	41241	33980	40.12	37.46	38.8	4659	11827	8243	44.63	23.11	33.9
1	21290	32699	26995	39.4	36.12	37.8	4227	11145	7686	47.93	21.64	34.8
0.5	16880	26461	21671	39.16	34.44	36.8	3827	10317	7072	45.43	20.89	33.2
0.2	12407	19825	16116	36.53	32.93	34.7	3327	9585	6456	45.43	20.64	33.0
0.1	10402	16225	13314	35.69	33.06	34.4	3097	8983	6040	45.87	19.89	32.9
0.05	8510	14156	11333	33.34	31.96	32.7	2957	8676	5817	38.45	19.21	28.8
0.02	6892	11702	9297	32.83	32.71	32.8	2912	8039	5476	42.63	19.76	31.2
0.01	5696	9843	7770	31.83	34.16	33.0	3303	7757	5530	45.74	20.59	33.2

APPENDIX C:
STATISTICAL GROUPINGS OF DIFFERENT TEST RESULTS

All groupings were generated using the Duncan method with a significance level of $\alpha = 0.05$.

Table C.1. Grouping of Data Based on APA Rut Depth (APA Mixes).

Mix Type	N	1	2	3	4	5	6
NMVado	2	2.0					
NMBingham	3	2.6	2.6				
TXWF	3		3.6	3.6			
64-40RHY	3		3.8	3.8			
OK	3			4.3			
AZ	3			4.4			
TXBryan	3			4.7			
64-40RG	3				6.4		
LA	3				7.2	7.2	
ARTL	3					8.2	
ARLR	3						18.7
ROG	3						19.0
Significance		0.433	0.090	0.159	0.203	0.156	0.594

Uses Harmonic Mean Sample Size = 2.880

The group sizes are unequal. The harmonic mean of the group sizes is used. Type I error levels are not guaranteed.

Table C.2. Grouping of Data Based on APA Creep Slope (APA Mixes).

Mix Type	N	1	2	3	4
NMVado	2	0.090			
TXBryan	3	0.149	0.149		
64-40RHY	3	0.197	0.197		
NMBingham	3	0.198	0.198		
AZ	3	0.206	0.206		
OK	3	0.265	0.265		
LA	3		0.285		
TXWF	3		0.299		
64-40RG	3			0.483	
ARTL	3			0.483	
ROG	3			0.646	
ARLR	3				1.637
Significance		0.0507	0.0945	0.0514	1.0000

Uses Harmonic Mean Sample Size = 2.880.

The group sizes are unequal. The harmonic mean of the group sizes is used. Type I error levels are not guaranteed.

Table C.3. Grouping of Data Based on E* at 10 Hz, 54.4°C (APA Mixes).

Mix Type	N	1.00	2.00	3.00	4.00	5.00	6.00
64-40RG	2	221.00					
ARLR	2	435.00	435.00				
64-40RHY	2	456.00	456.00				
OK	2	517.50	517.50	517.50			
ROG	2		688.50	688.50			
LA	2		753.00	753.00	753.00		
AZ	2			869.50	869.50	869.50	
TXWF	2				1077.50	1077.50	
ARTL	2				1085.50	1085.50	
TXBryan	2					1228.50	
NMBingham	2						1644.50
NMVado	2						1801.50
Significance		0.10	0.08	0.06	0.07	0.05	0.33

Table C.4. Grouping of Data Based on E* at 1 Hz, 54.4°C (APA Mixes).

Mix Type	N	1	2	3	4	5
ARLR	2	141.00				
64-40RG	2	148.50				
OK	2	204.25	204.25			
LA	2	255.35	255.35			
64-40RHY	2	264.50	264.50			
ROG	2	277.00	277.00			
AZ	2		340.00	340.00		
ARTL	2		358.00	358.00		
TXWF	2			487.05	487.05	
TXBryan	2				515.40	
NMBingham	2					831.40
NMVado	2					923.05
Significance		0.09	0.06	0.06	0.68	0.19

Table C.5. Grouping of Data Based on E* /sin ϕ at 10 Hz, 54.4°C (APA Mixes).

Mix Type	N	1	2	3	4
ARLR	2	799.27			
64-40RG	2	800.17			
OK	2	997.70			
LA	2	1384.34	1384.34		
64-40RHY	2	1461.70	1461.70		
ROG	2	1476.12	1476.12		
AZ	2	1794.84	1794.84	1794.84	
ARTL	2		2114.17	2114.17	
TXBryan	2			2468.92	
TXWF	2			2682.20	
NMBingham	2				4438.63
NMVado	2				5036.86
Significance		0.05	0.13	0.07	0.17

Table C.6. Grouping of Data Based on E* /sin ϕ at 1 Hz, 54.4°C (APA Mixes).

Mix Type	N	1	2	3	4
ARLR	2	292.83			
OK	2	418.75	418.75		
LA	2	463.99	463.99		
ROG	2	516.86	516.86		
64-40RG	2	569.04	569.04		
AZ	2	635.59	635.59	635.59	
ARTL	2	644.81	644.81	644.81	
64-40RHY	2		736.48	736.48	
TXWF	2			978.47	
TXBryan	2			989.77	
NMBingham	2				1661.18
NMVado	2				1830.82
Significance		0.07	0.10	0.07	0.31

Table C.7. Grouping of Data Based on G* at 10 Hz, 40°C (APA Mixes).

Mix Type	N	1	2	3	4	5
64-40RHY	2	11728.50				
64-40RG	2	25489.00	25489.00			
ARLR	2	31849.00	31849.00			
AZ	2	36320.50	36320.50	36320.50		
ARTL	2		43247.00	43247.00	43247.00	
LA	2		43866.00	43866.00	43866.00	
ROG	2		44546.50	44546.50	44546.50	
TXWF	2		47999.50	47999.50	47999.50	
OK	2		53047.50	53047.50	53047.50	
NMBingham	2			63452.00	63452.00	
TXBryan	2				66530.00	
NMVado	2					130564.50
Significance		0.08	0.06	0.06	0.10	1.00

Table C.8. Grouping of Data Based on G* at 1 Hz, 40°C (APA Mixes).

Mix Type	N	1	2	3	4
64-40RHY	2	7686.00			
ARLR	2	9220.50			
64-40RG	2	10519.00			
AZ	2	13167.50	13167.50		
LA	2	14724.50	14724.50		
ARTL	2	14741.00	14741.00		
ROG	2	17542.00	17542.00		
TXWF	2	18483.50	18483.50		
OK	2		23350.00	23350.00	
TXBryan	2		23518.00	23518.00	
NMBingham	2			34014.00	
NMVado	2				75078.00
Significance		0.09	0.10	0.08	1.00

Table C.9. Grouping of Data Based on G* /sin δ at 10 Hz, 40°C (APA Mixes).

Mix Type	N	1	2	3	4	5
64-40RHY	2	19866.65				
64-40RG	2	34122.36	34122.36			
ARLR	2	36696.78	36696.78			
AZ	2	45101.71	45101.71	45101.71		
ARTL	2	54266.38	54266.38	54266.38		
LA	2	54322.67	54322.67	54322.67		
ROG	2	63149.28	63149.28	63149.28	63149.28	
TXWF	2		68612.36	68612.36	68612.36	
OK	2		79482.66	79482.66	79482.66	
TXBryan	2			87307.23	87307.23	
NMBingham	2				102166.5	
NMVado	2					293705.53
Significance		0.07	0.06	0.08	0.09	1.00

Table C.10. Grouping of Data Based on G* /sin δ at 1 Hz, 40°C (APA Mixes).

Mix Type	N	1	2	3
ARLR	2	11028.05		
64-40RG	2	15789.73		
AZ	2	16421.16		
64-40RHY	2	17958.03		
ARTL	2	18236.02		
LA	2	20062.19		
ROG	2	25508.06		
TXWF	2	26654.79		
TXBryan	2	33293.30		
OK	2	39865.09	39865.09	
NMBingham	2		62170.52	
NMVado	2			162842.36
Significance		0.05	0.08	1.00

Table C.11. Grouping of Data Based on Flow Number (APA Mixes).

Mix Type	N	1	2	3
ARLR	2	169		
64-40RG	2	197		
ROG	2	202		
ARTL	2	218		
LA	2	428		
AZ	2	534		
64-40RHY	2	1617		
TXWF	2	3159	3159	
OK	2	3559	3559	
TXBryan	2		5807	
NMBingham	2			15000.5
NMVado	2			15001
Significance		0.07	0.12	1.00

Table C.12. Grouping of Data Based on Flow Number Slope (APA Mixes).

Mix Type	N	1	2	3	4	5	6
64-40RHY	2	0.218					
NMBingham	2	0.293	0.293				
OK	2	0.312	0.312	0.312			
NMVado	2	0.315	0.315	0.315			
TXBryan	2		0.356	0.356	0.356		
64-40RG	2		0.373	0.373	0.373		
TXWF	2			0.401	0.401		
LA	2				0.433		
ARTL	2				0.434		
AZ	2				0.445	0.445	
ARLR	2					0.542	0.542
ROG	2						0.579
Significance		0.068	0.128	0.094	0.094	0.050	0.426

Table C.13. Grouping of Data Based on Flow Time (APA Mixes).

Mix Type	N	1	2
ROG	2	8	
ARLR	2	22	
ARTL	2	47.5	
LA	2	90.5	
64-40RG	2	110	
64-40RHY	2	113	
AZ	2	297.5	
TXWF	2	743	
OK	2	1536.5	
TXBryan	2	2966	
NMBingham	2		25697.5
NMVado	2		28263.5
Significance		0.22	0.24

Table C.14. Grouping of Data Based on Flow Time Intercept (APA Mixes).

Mix Type	N	1
OK	2	0.007465
TXBryan	2	0.00765
NMBingham	2	0.00785
NMVado	2	0.00875
TXWF	2	0.0092
64-40RG	2	0.01095
LA	2	0.0111
ROG	2	0.01175
AZ	2	0.01185
ARLR	2	0.01295
64-40RHY	2	0.01345
ARTL	2	0.0136
Significance		0.1091309

Table C.15. Grouping of Data Based on Flow Time Slope (APA Mixes).

Mix Type	N	1	2	3	4	5	6
NMBingham	2	0.152					
NMVado	2	0.159	0.159				
TXBryan	2	0.185	0.185				
TXWF	2	0.203	0.203	0.203			
OK	2	0.207	0.207	0.207			
64-40RHY	2	0.211	0.211	0.211			
AZ	2	0.232	0.232	0.232	0.232		
ARTL	2		0.263	0.263	0.263	0.263	
64-40RG	2			0.303	0.303	0.303	
LA	2				0.314	0.314	
ARLR	2					0.351	
ROG	2						0.619
Significance		0.123	0.052	0.056	0.102	0.082	1.000

Table C.16. Grouping of Data Based on Hamburg Rut Depth (Hamburg Mixes).

Mix ID	N	Subset for alpha = .05				
		1	2	3	4	5
TXCO	2	2.17				
TXYK	2		3.72			
TXBR	2		4.60	4.60		
64-40RHY	2			5.44		
TXWF	2				8.94	
64-40RG	2				9.21	
ROG	2					12.07
Significance		1.000	0.119	0.130	0.601	1.000

Table C.17. Grouping of Data Based on E* at 10 Hz, 54.4°C (Hamburg Mixes).

Mix ID	N	Subset for alpha = .05			
		1	2	3	4
64-40RG	2	221			
64-40RHY	2	456	456		
ROG	2		689		
TXWF	2			1078	
TXBR	2			1229	
TXYK	2				2031
TXCO	2				2077
Significance		0.109	0.112	0.276	0.732

Table C.18. Grouping of Data Based on E* at 1 Hz, 54.4°C (Hamburg Mixes).

Mix ID	N	Subset for alpha = .05		
		1	2	3
64-40RG	2	149		
64-40RHY	2	265		
ROG	2	277		
TXWF	2		487	
TXBR	2		516	
TXCO	2		562	
TXYK	2			949
Significance		0.188	0.422	1.000

Table C.19. Grouping of Data Based on E* /sin ϕ at 10 Hz, 54.4°C (Hamburg Mixes).

Mix ID	N	Subset for alpha = .05		
		1	2	3
64-40RG	2	801		
64-40RHY	2	1462		
ROG	2	1477		
TXBR	2		2469	
TXWF	2		2682	
TXCO	2		3160	
TXYK	2			4592
Significance		0.136	0.129	1.000

Table C.20. Grouping of Data Based on E* /sin ϕ at 1 Hz, 54.4°C (Hamburg Mixes).

Mix ID	N	Subset for alpha = .05	
		1	2
ROG	2	517	
64-40RG	2	569	
64-40RHY	2	737	
TXWF	2	979	
TXBR	2	990	
TXCO	2	1037	
TXYK	2		1732
Significance		0.064	1.000

Table C.21. Grouping of Data Based on Flow Number (Hamburg Mixes).

Mix ID	N	Subset for alpha = 0.05	
		1	2
64-40RG	2	197	
ROG	2	202	
64-40RHY	2	1617	1617
TXWF	2	3159	3159
TXBR	2		5807
TXCO	2		6033
TXYK	2		6755
Significance		0.219	0.055

Table C.22. Grouping of Data Based on Flow Number Slope (Hamburg Mixes).

Mix ID	N	Subset for alpha = 0.05			
		1	2	3	4
64-40RHY	2	0.22			
TXYK	2	0.24	0.24		
TXCO	2	0.28	0.28	0.28	
TXBR	2		0.36	0.36	
64-40RG	2		0.37	0.37	
TXWF	2			0.40	
ROG	2				0.58
Significance		0.304	0.059	0.073	1.000

Table C.23. Grouping of Data Based on Flow Time (Hamburg Mixes).

Mix ID	N	Subset for alpha = 0.05		
		1	2	3
TXCO	2	0.16		
TXYK	2	0.17		
TXBR	2	0.19		
TXWF	2	0.20		
64-40RHY	2	0.21	0.21	
64-40RG	2		0.30	
ROG	2			0.62
Significance		0.257	0.058	1.000

Table C.24. Grouping of Data Based on Flow Time Intercept (Hamburg Mixes).

Mix ID	N	Subset for alpha = 0.05		
		1	2	3
TXYK	2	0.0051		
TXCO	2	0.0061		
TXBR	2	0.0077	0.0077	
TXWF	2	0.0092	0.0092	
64-40RG	2		0.0110	0.0110
ROG	2		0.0118	0.0118
64-40RHY	2			0.0135
Significance		0.054	0.055	0.196

Table C.25. Grouping of Data Based on Flow Time Slope (Hamburg Mixes).

Mix ID	N	Subset for alpha = 0.05		
		1	2	3
TXCO	2	0.16		
TXYK	2	0.17		
TXBR	2	0.19		
TXWF	2	0.20		
64-40RHY	2	0.21	0.21	
64-40RG	2		0.30	
ROG	2			0.62
Significance		0.257	0.058	1.000

APPENDIX D:
CORRELATIONS OF DIFFERENT TEST PARAMETERS WITH APA PARAMETERS

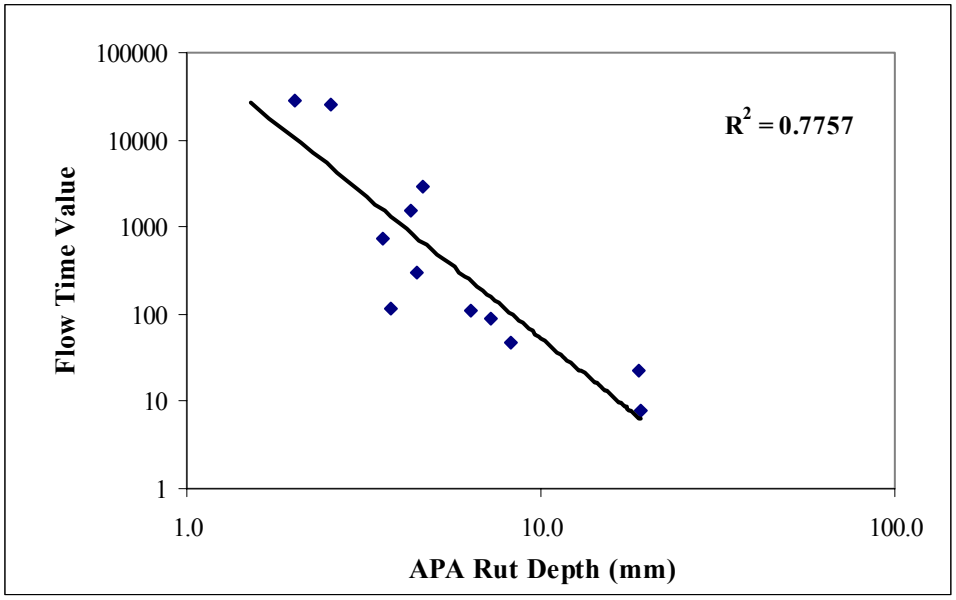

Figure D.1. APA Rut Depth versus Flow Time Value.

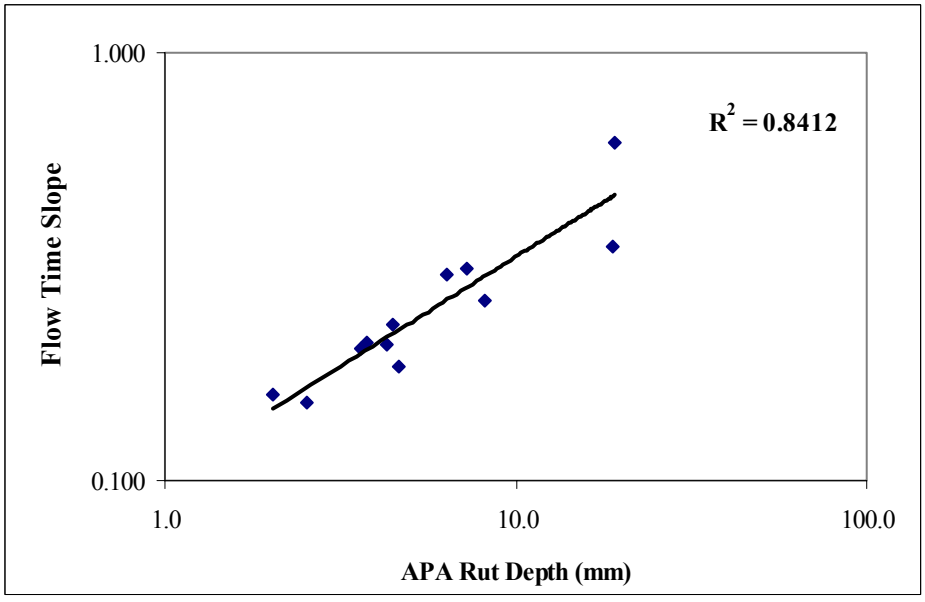

Figure D.2. APA Rut Depth versus Flow Time Slope.

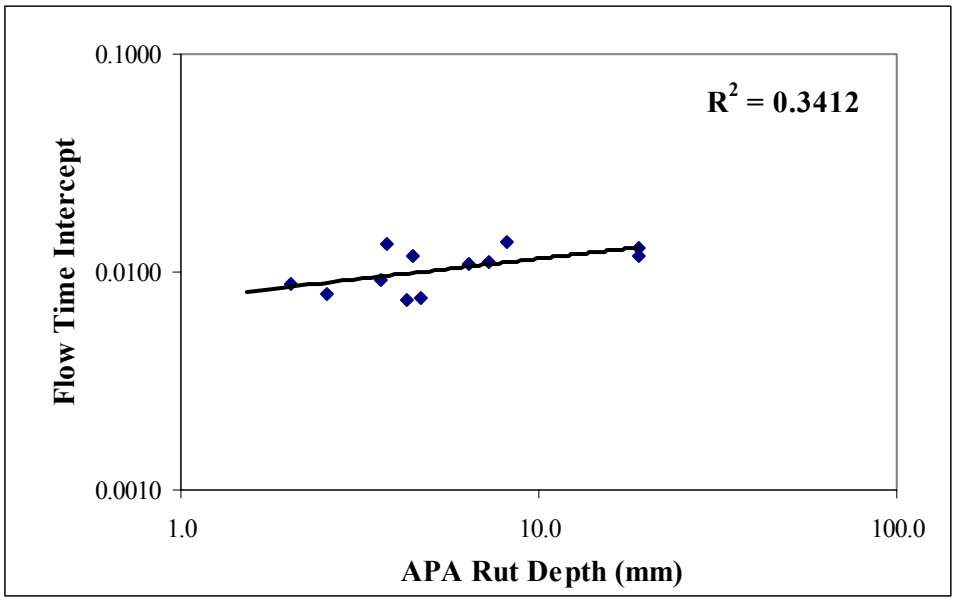

Figure D.3. APA Rut Depth versus Flow Time Intercept.

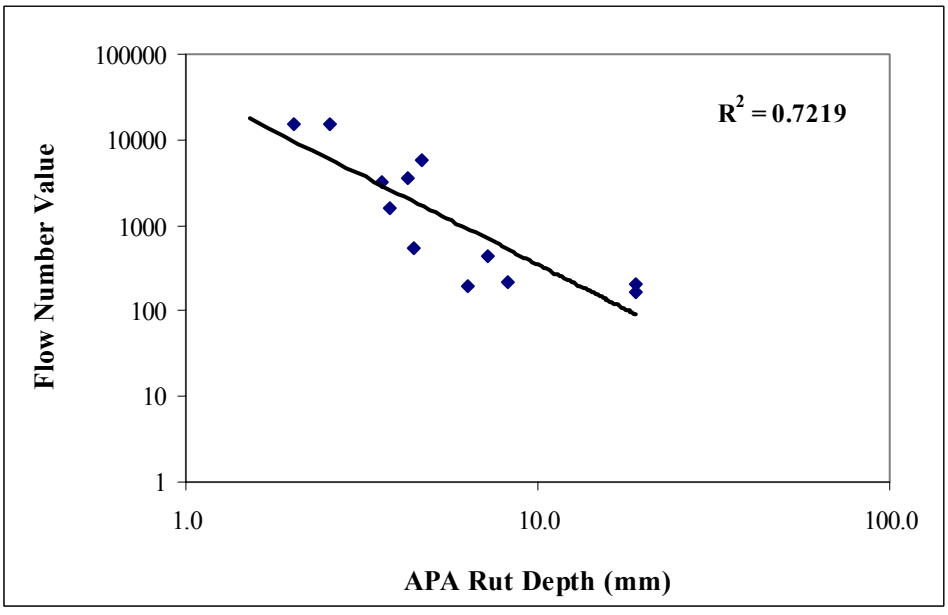

Figure D.4. APA Rut Depth versus Flow Number Value.

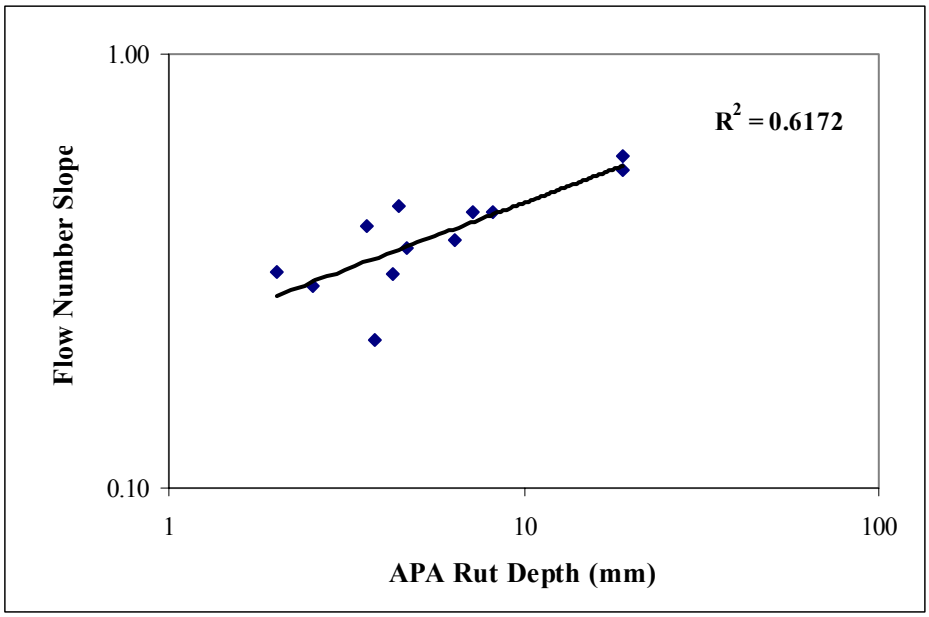

Figure D.5. APA Rut Depth versus Flow Number Slope.

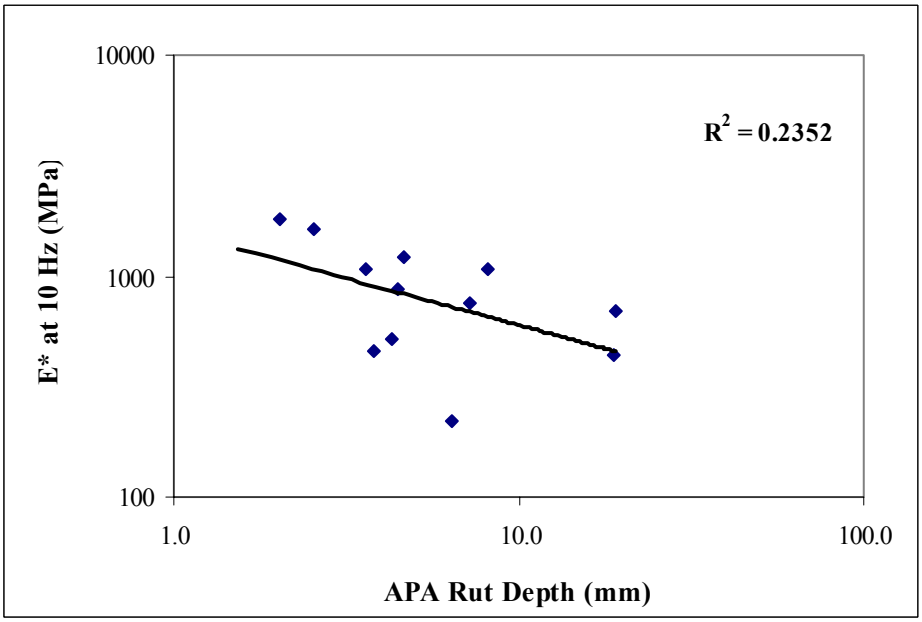

Figure D.6. APA Rut Depth versus E* at 10 Hz.

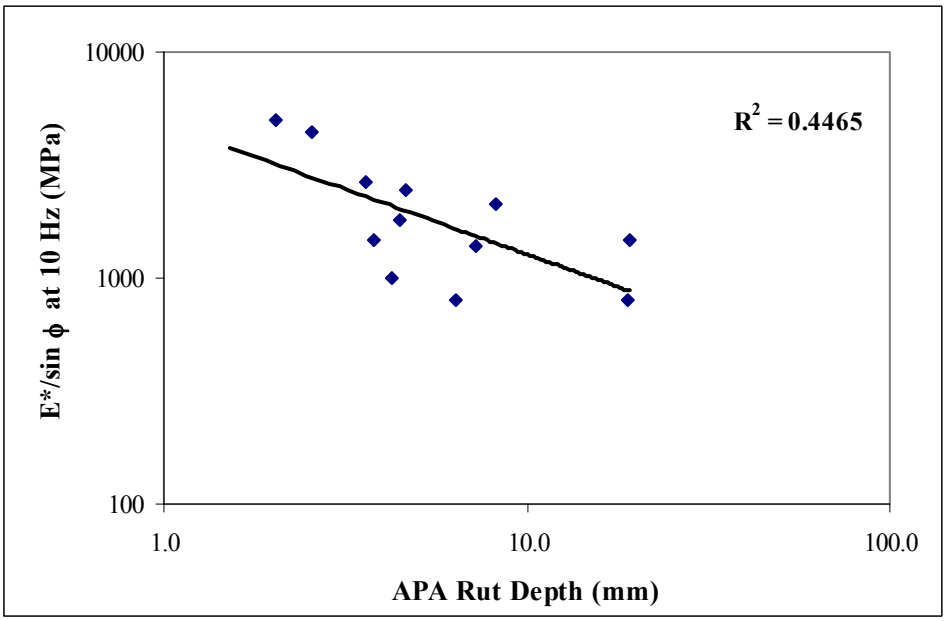

Figure D.7. APA Rut Depth versus E*/sin ϕ at 10 Hz.

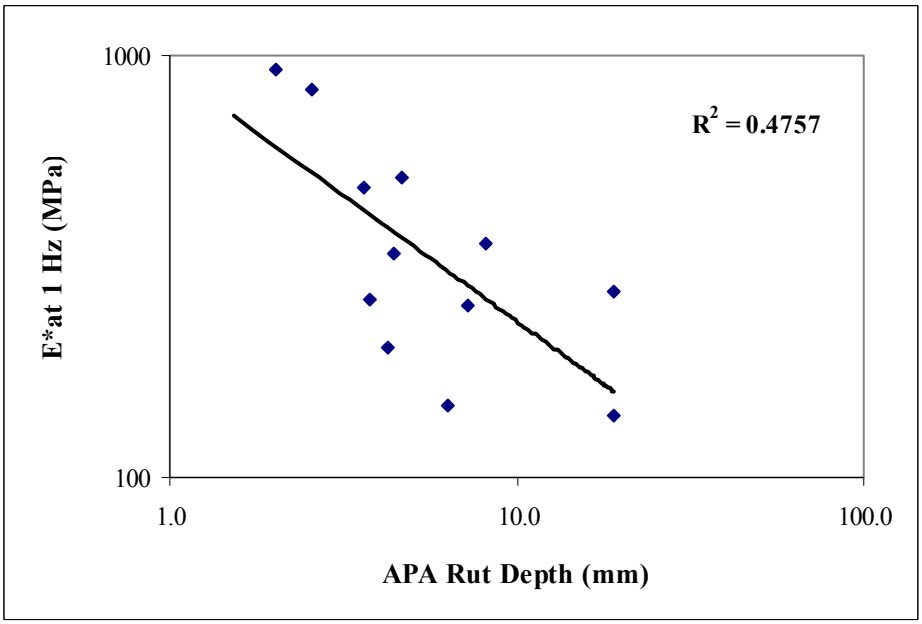

Figure D.8. APA Rut Depth versus E* at 1 Hz.

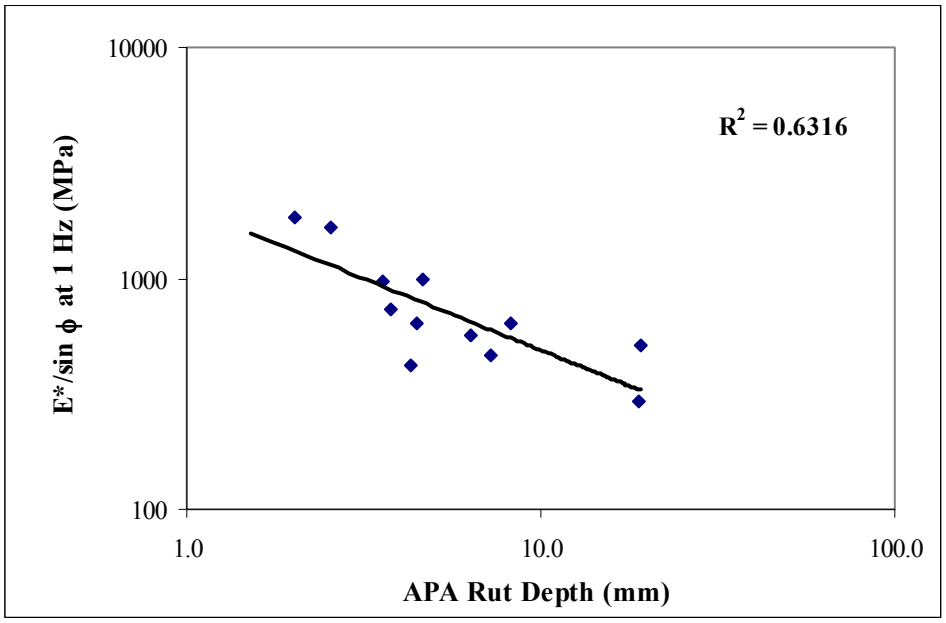

Figure D.9. APA Rut Depth versus E*/sin ϕ at 1 Hz.

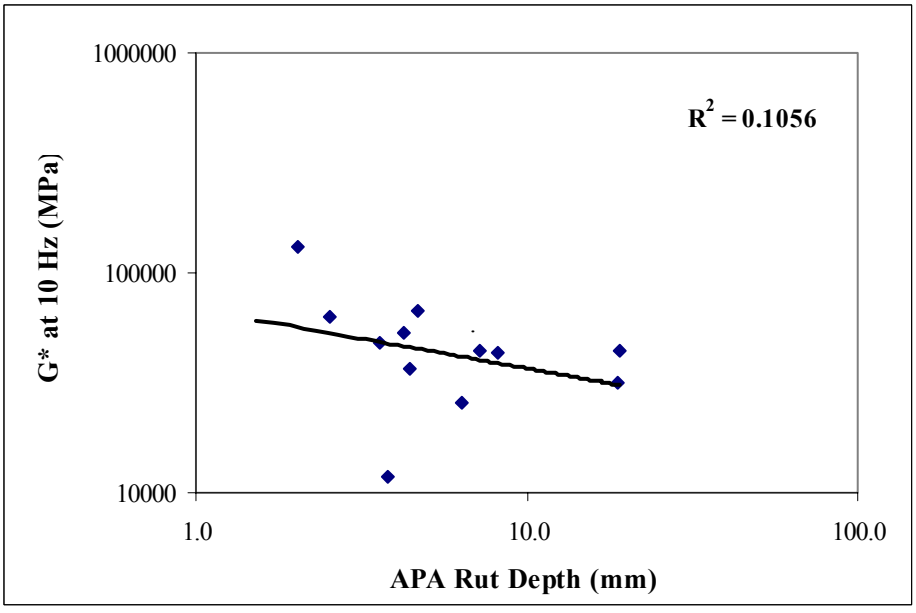

Figure D.10. APA Rut Depth versus G* at 10 Hz.

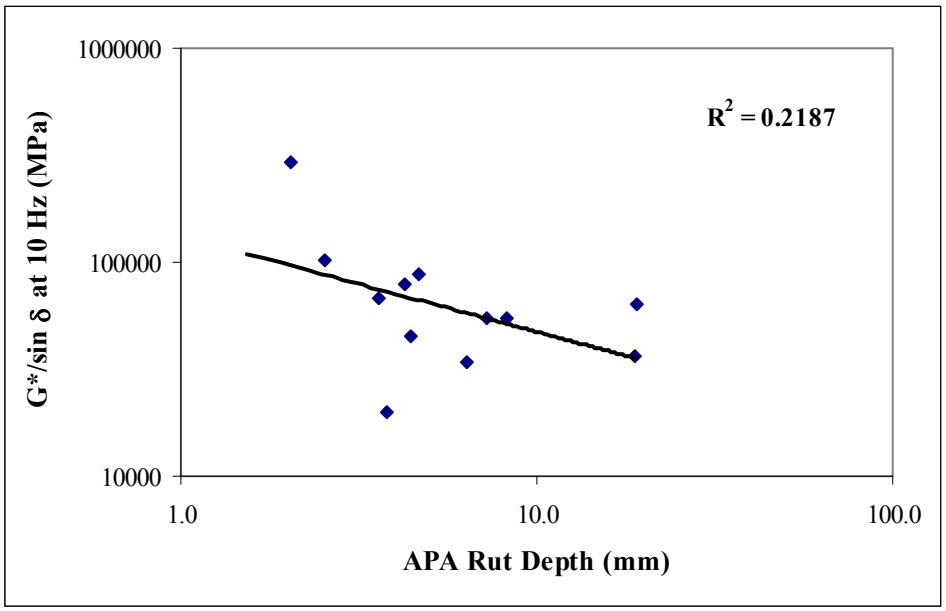

Figure D.11. APA Rut Depth versus G*/sin δ at 10 Hz.

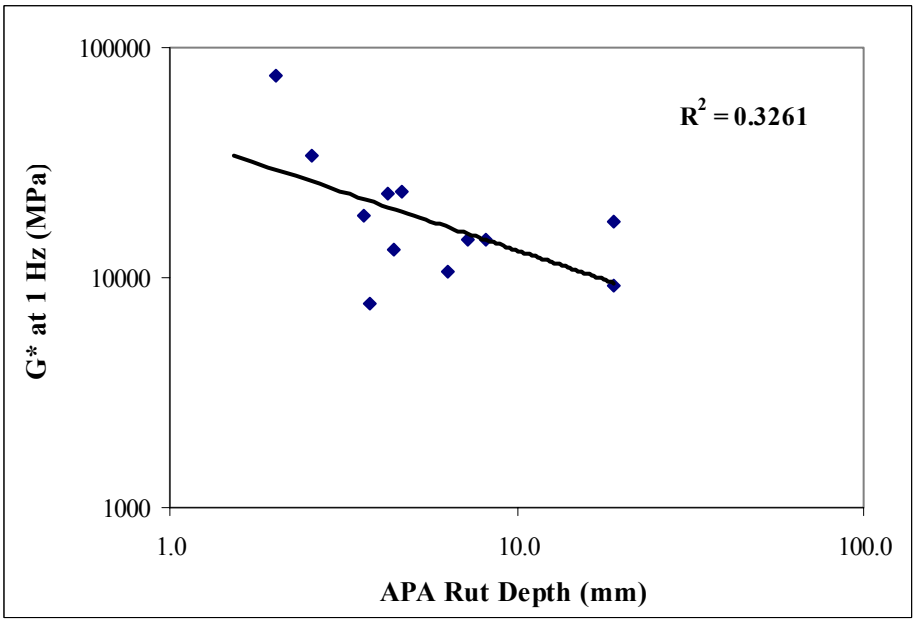

Figure D.12. APA Rut Depth versus G* at 1 Hz.

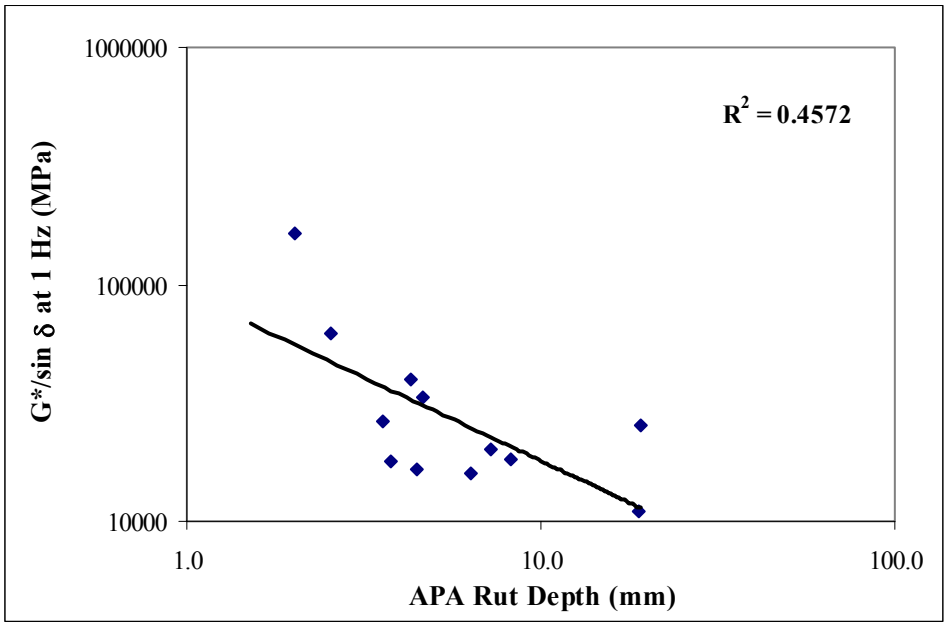

Figure D.13. APA Rut Depth versus G*/sin δ at 1 Hz.

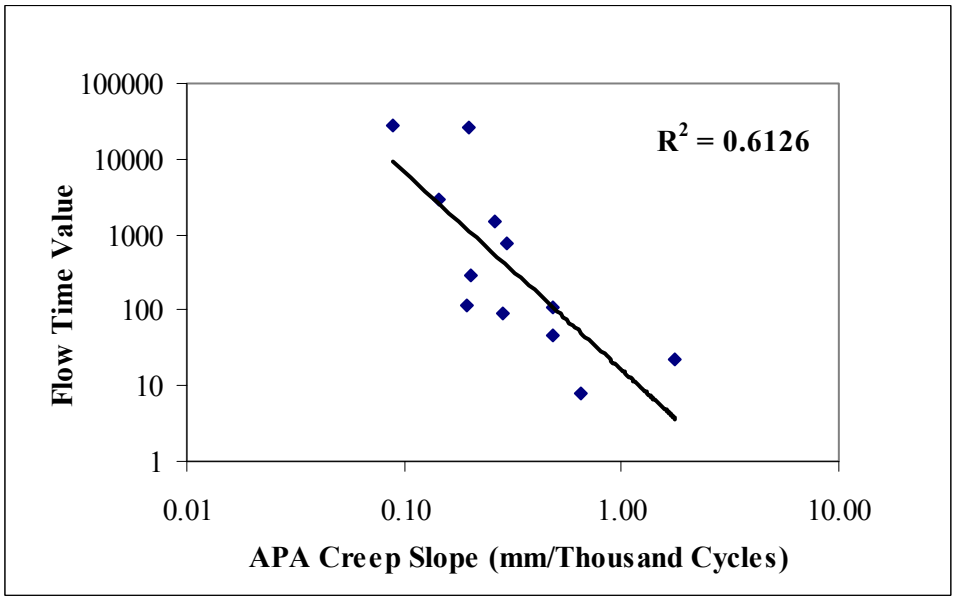

Figure D.14. APA Creep Slope versus Flow Time Value.

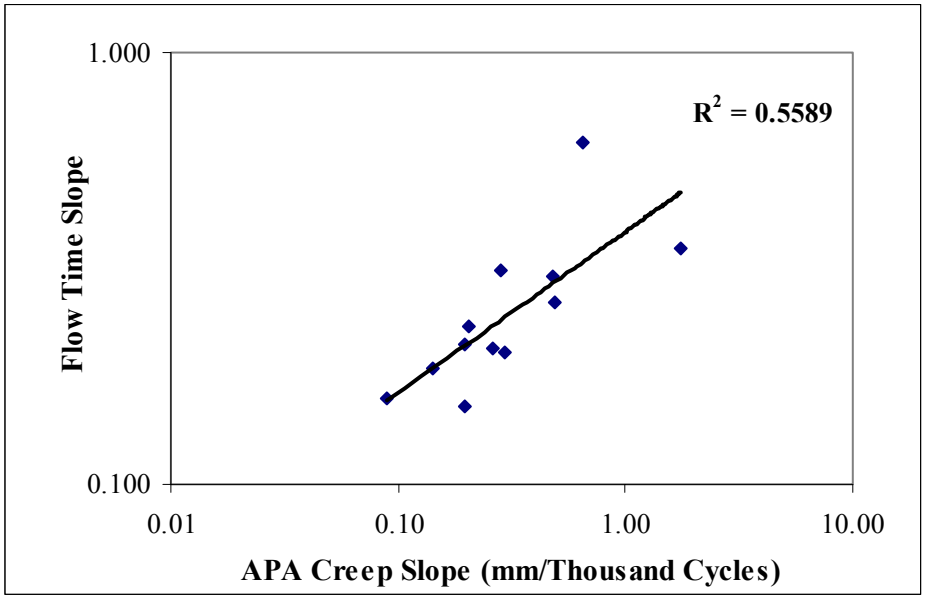

Figure D.15. APA Creep Slope versus Flow Time Slope.

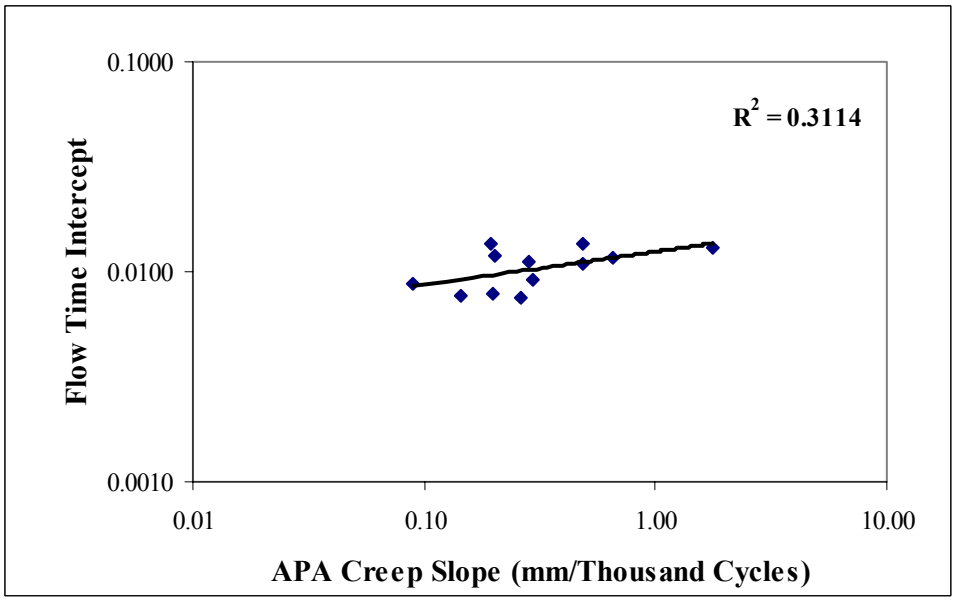

Figure D.16. APA Creep Slope versus Flow Time Intercept.

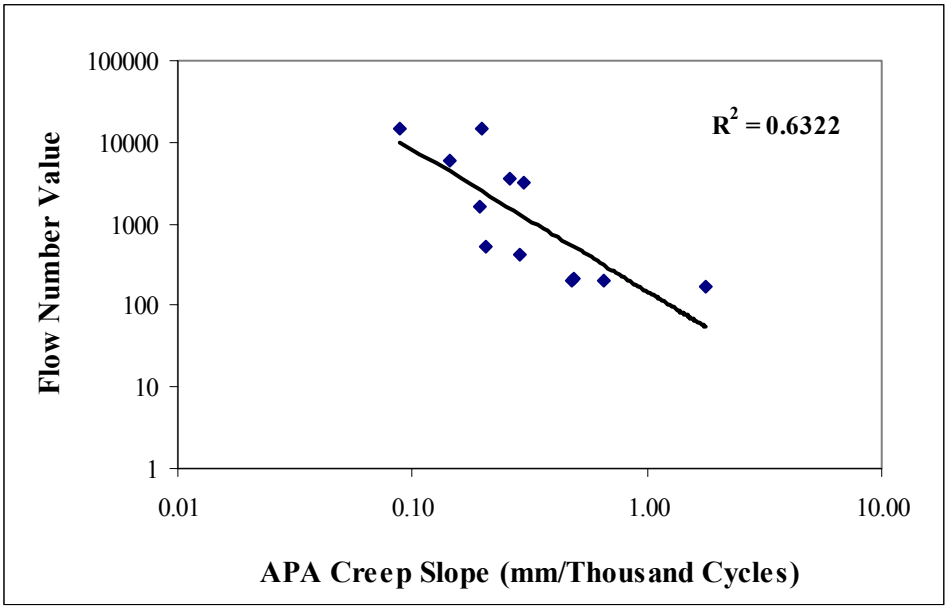

Figure D.17. APA Creep Slope versus Flow Number Value.

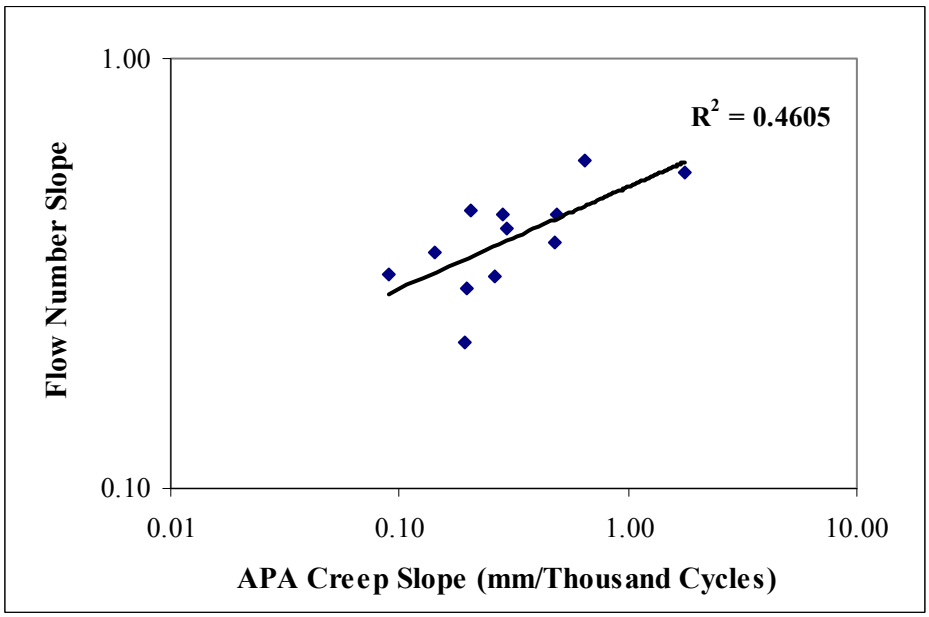

Figure D.18. APA Creep Slope versus Flow Number Slope.

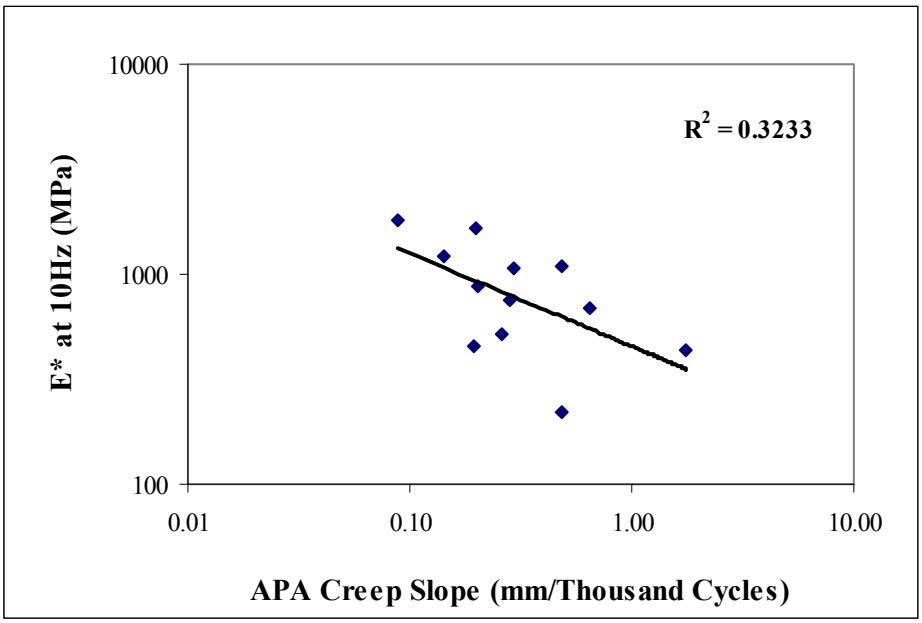

Figure D.19. APA Creep Slope versus E* at 10 Hz.

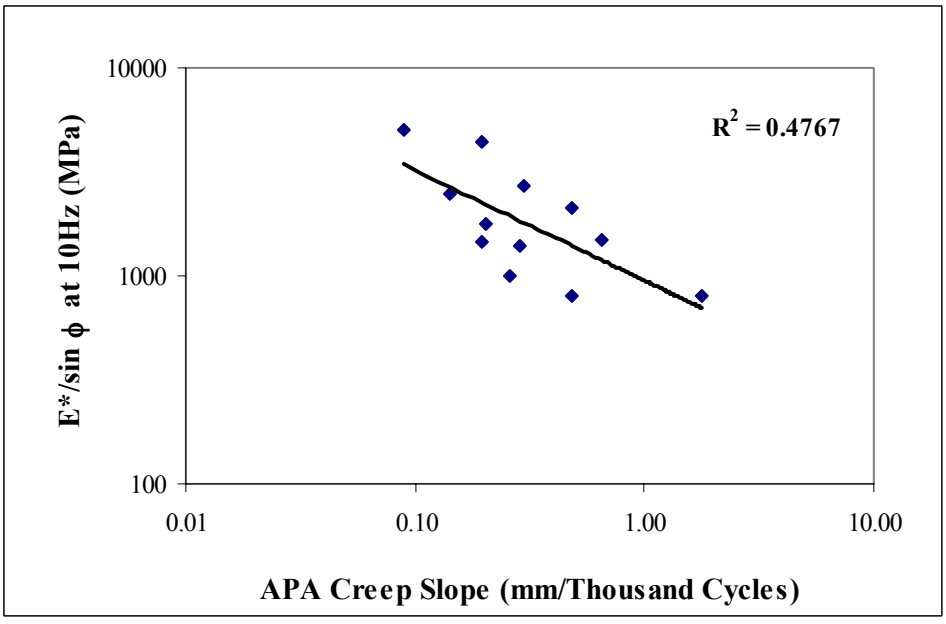

Figure D.20. APA Creep Slope versus E*/sin ϕ at 10 Hz.

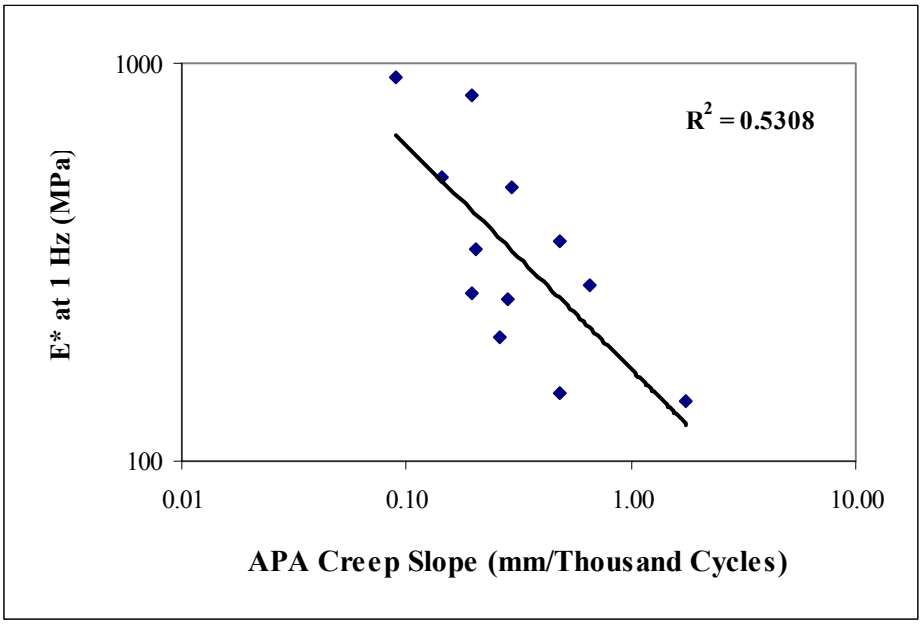

Figure D.21. APA Creep Slope versus E* at 1 Hz.

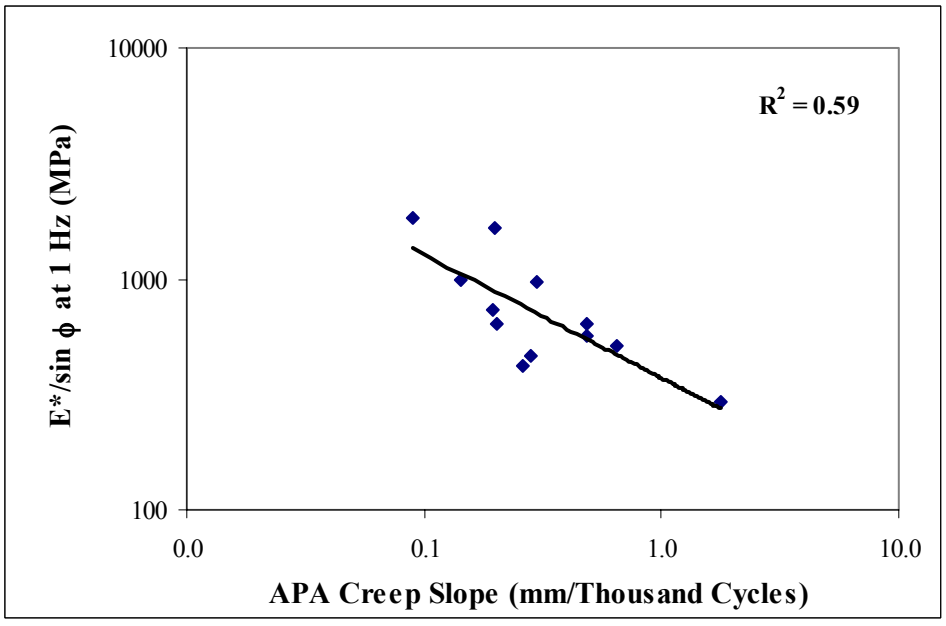

Figure D.22. APA Creep Slope versus E*/sin ϕ at 1 Hz.

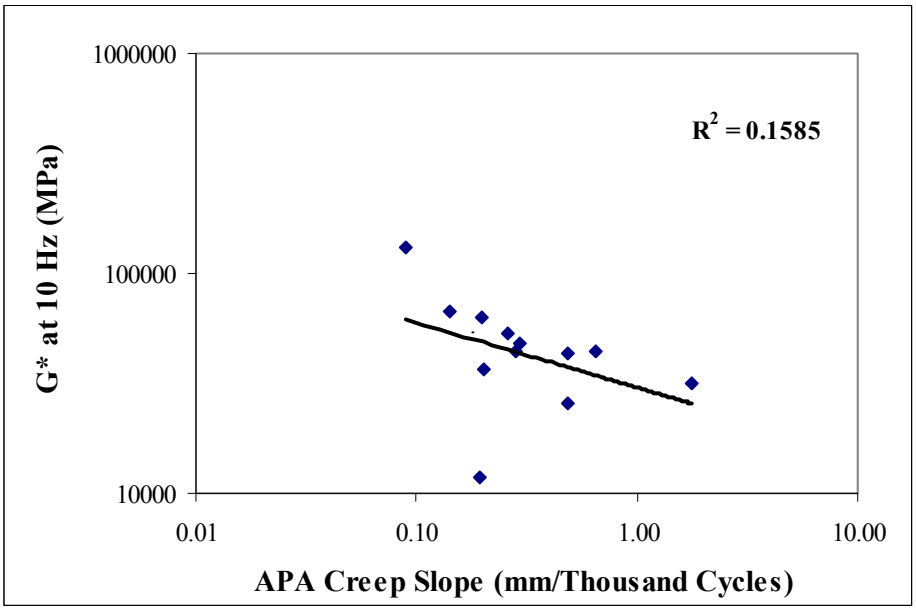

Figure D.23. APA Creep Slope versus G* at 10 Hz.

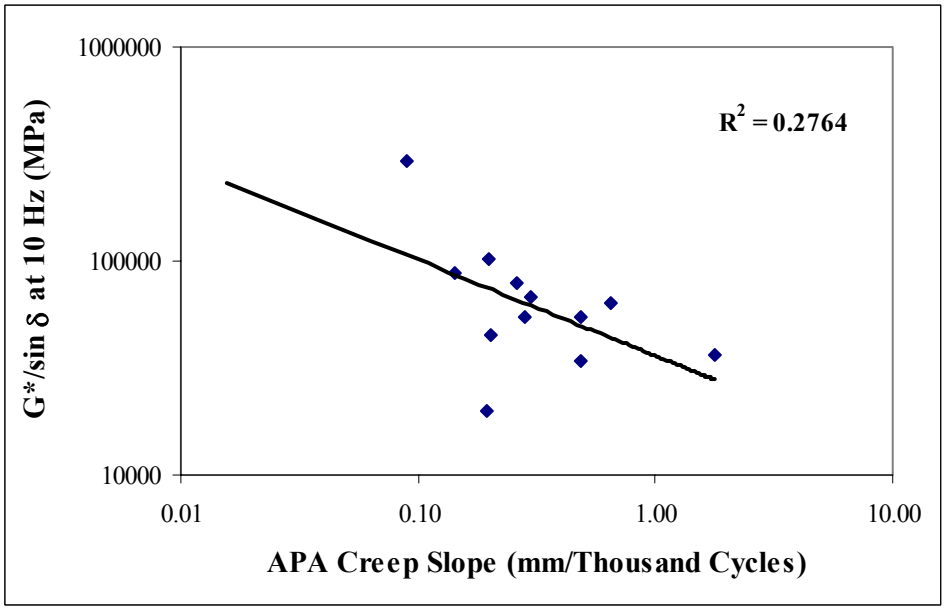

Figure D.24. APA Creep Slope versus G*/sin δ at 10 Hz.

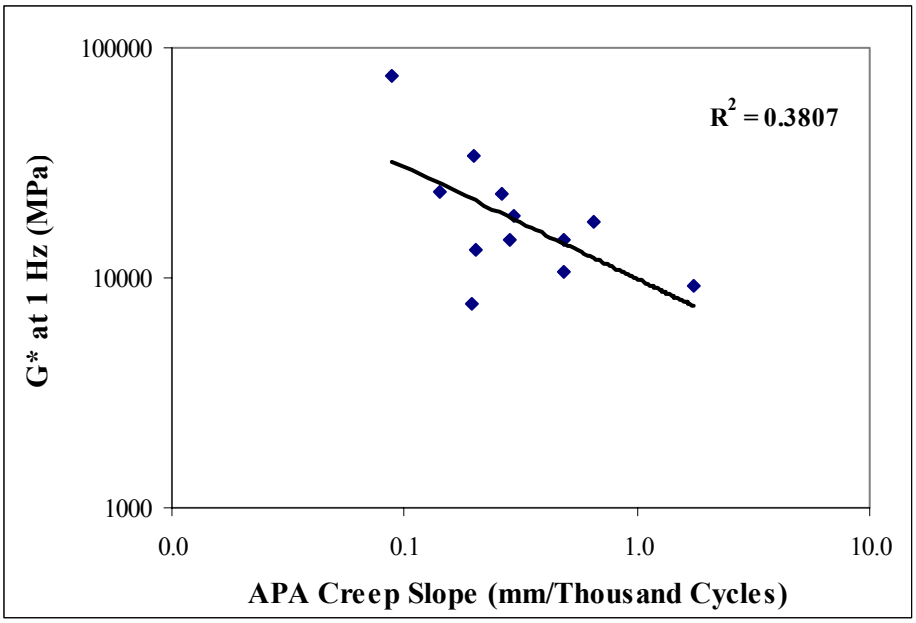

Figure D.25. APA Creep Slope versus G* at 1 Hz.

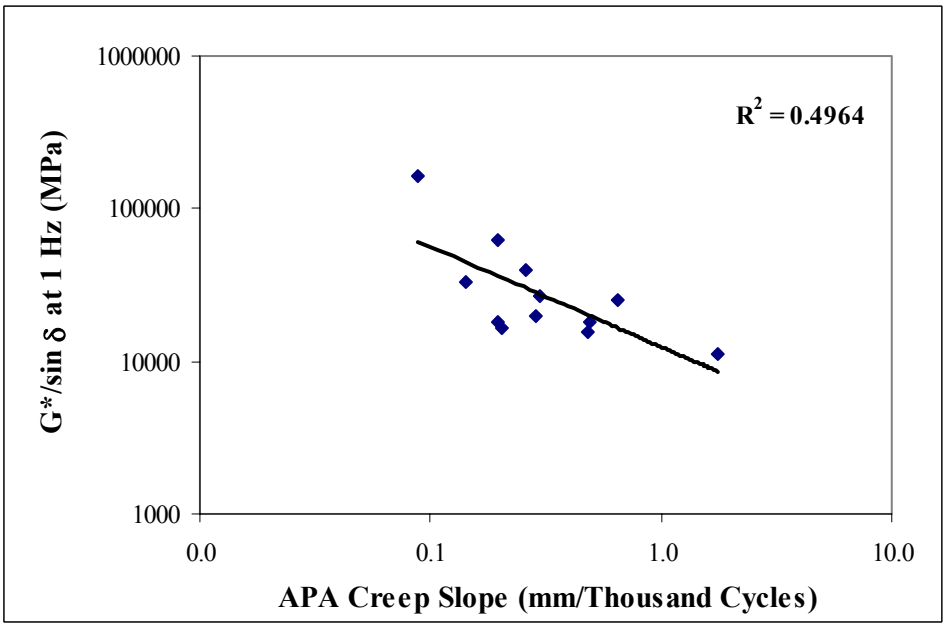

Figure D.26. APA Creep Slope versus G*/sin δ at 1 Hz.

APPENDIX E:
CORRELATIONS OF DIFFERENT TEST PARAMETERS WITH HAMBURG RUT DEPTH

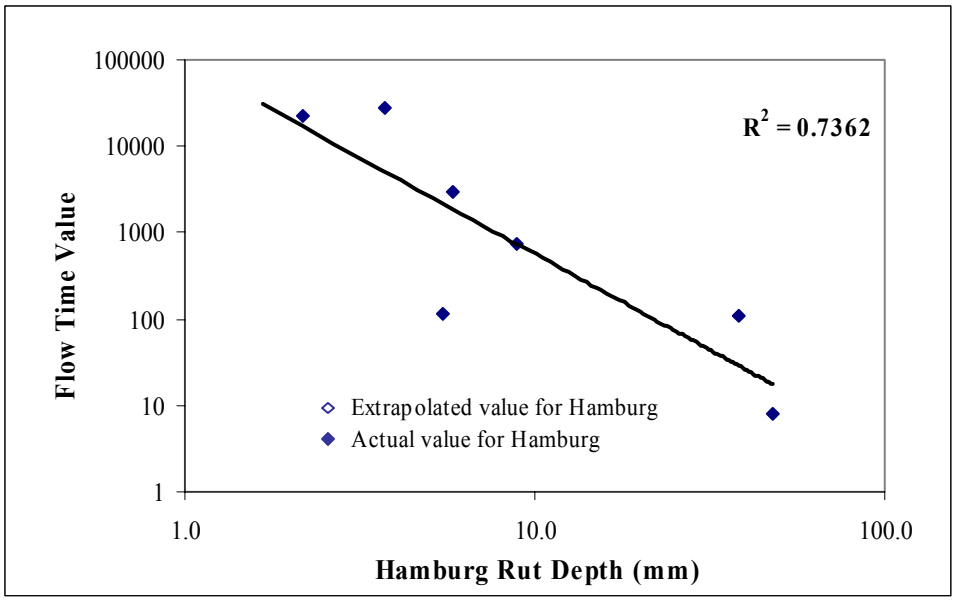

Figure E.1. Hamburg Rut Depth versus Flow Time Value.

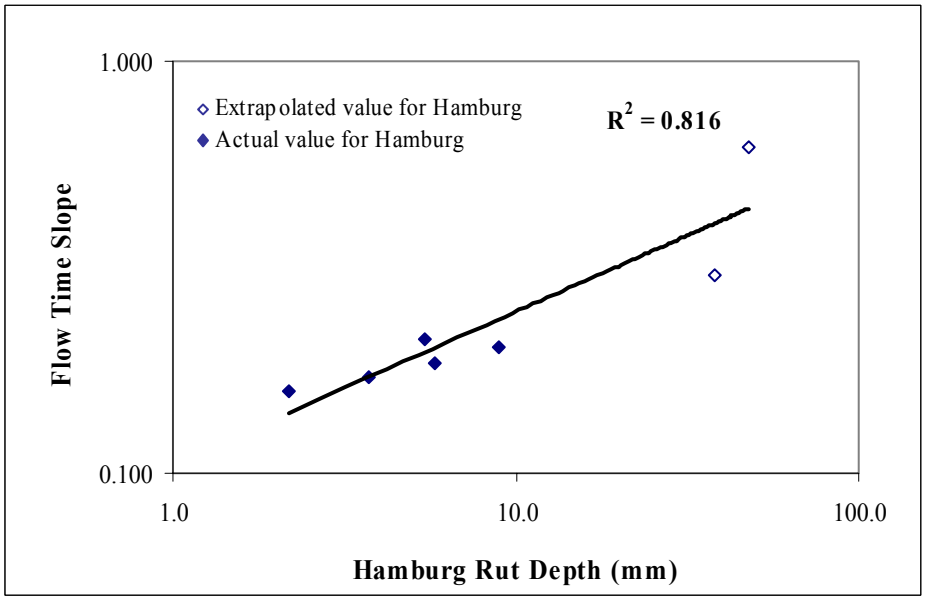

Figure E.2. Hamburg Rut Depth versus Flow Time Slope.

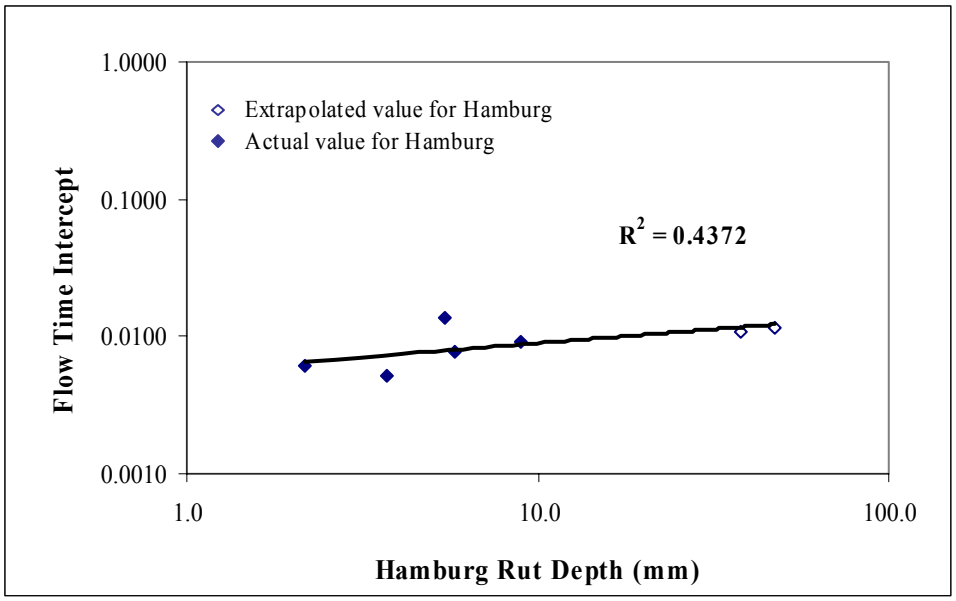

Figure E.3. Hamburg Rut Depth versus Flow Time Intercept.

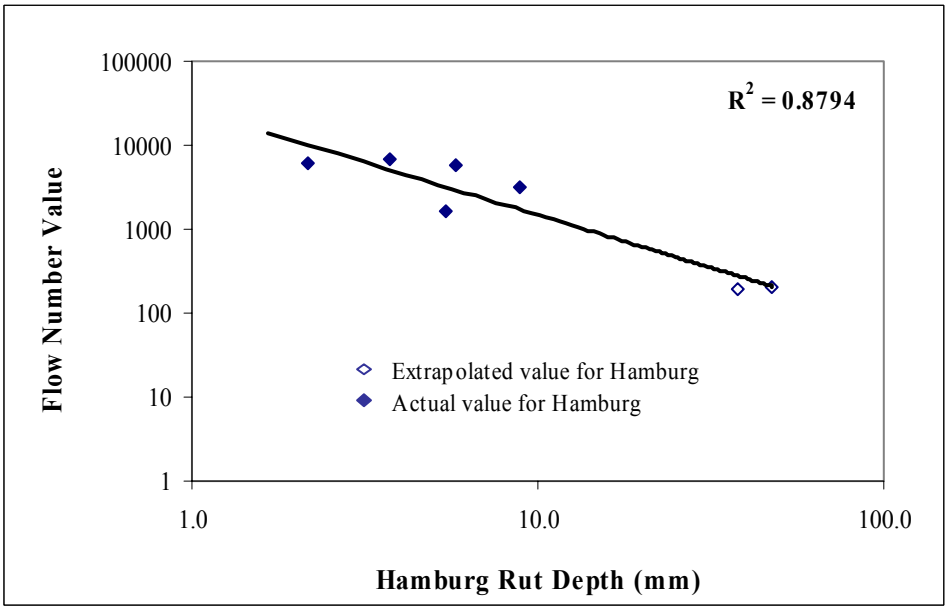

Figure E.4. Hamburg Rut Depth versus Flow Number Value.

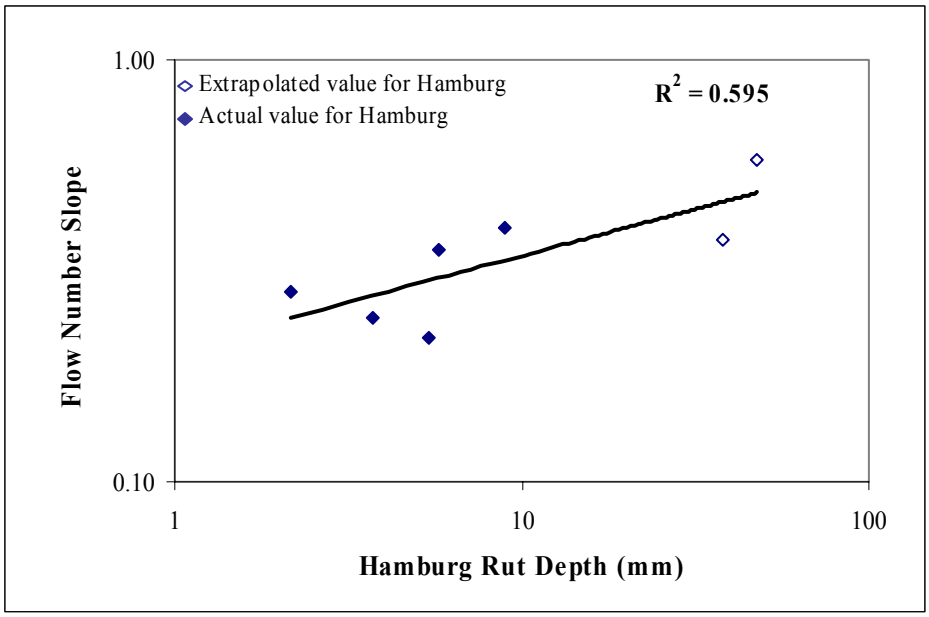

Figure E.5. Hamburg Rut Depth versus Flow Number Slope.

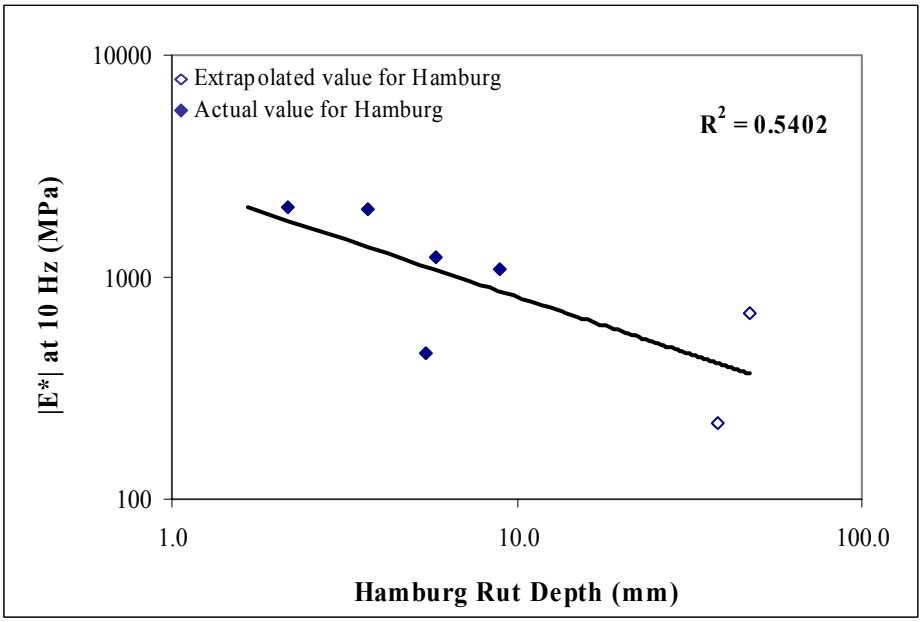

Figure E.6. Hamburg Rut Depth versus E* at 10 Hz.

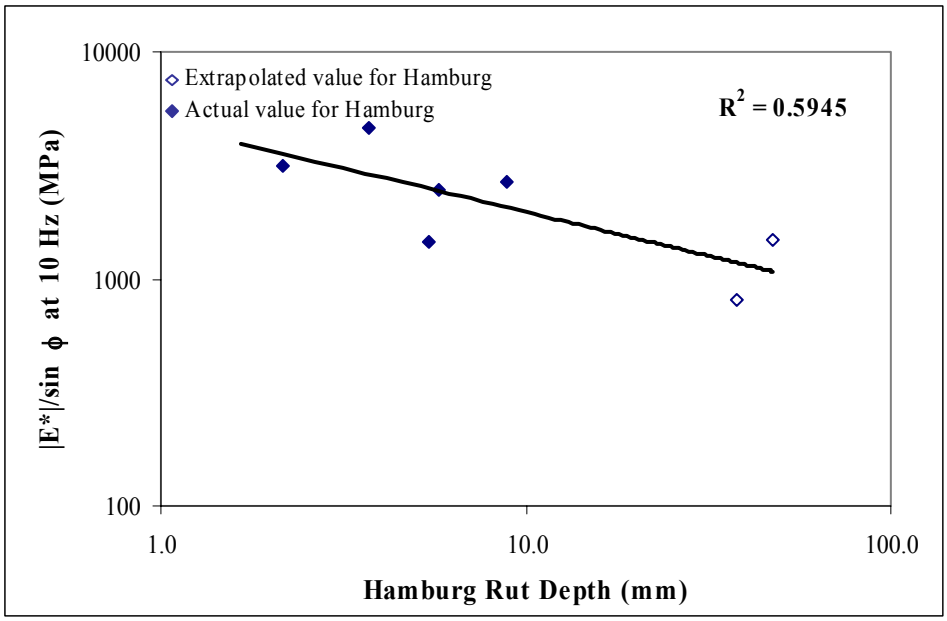

Figure E.7. Hamburg Rut Depth versus E*/sin ϕ at 10 Hz.

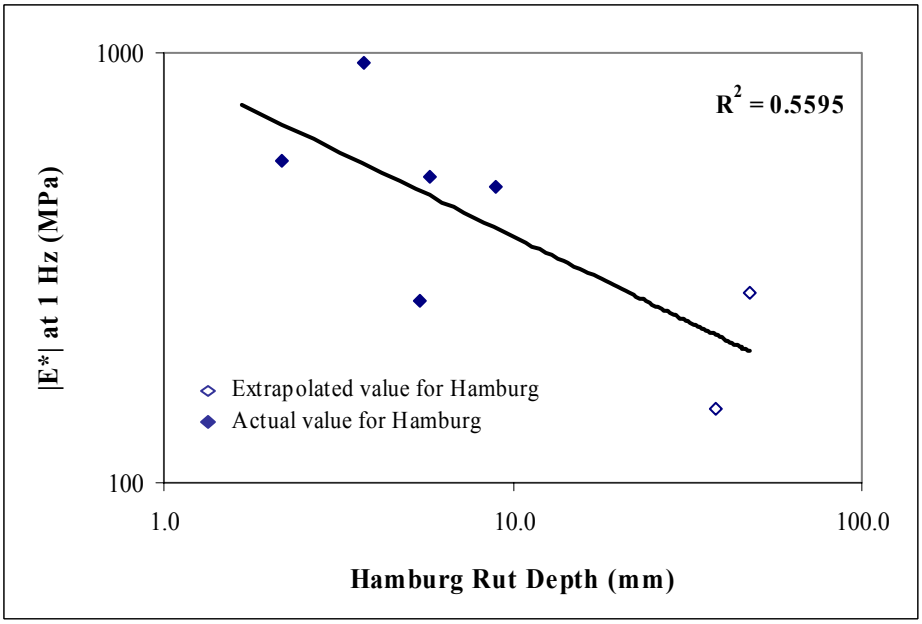

Figure E.8. Hamburg Rut Depth versus E* at 1 Hz.

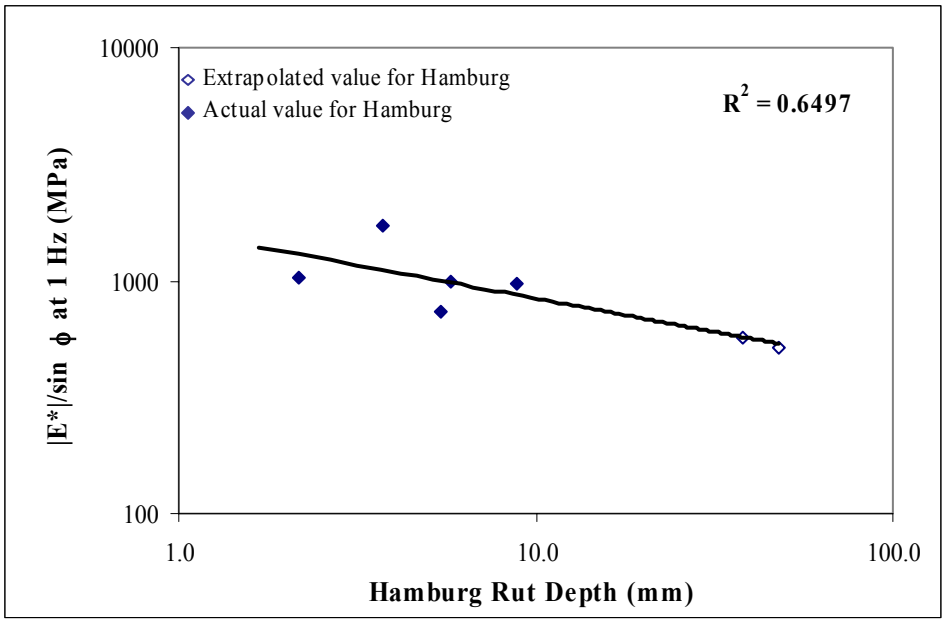

Figure E.9. Hamburg Rut Depth versus E*/sin ϕ at 1 Hz.

APPENDIX F:
GRADATIONS OF SELECTED MIXES FOR MOISTURE SUSCEPTIBILITY EXPERIMENT

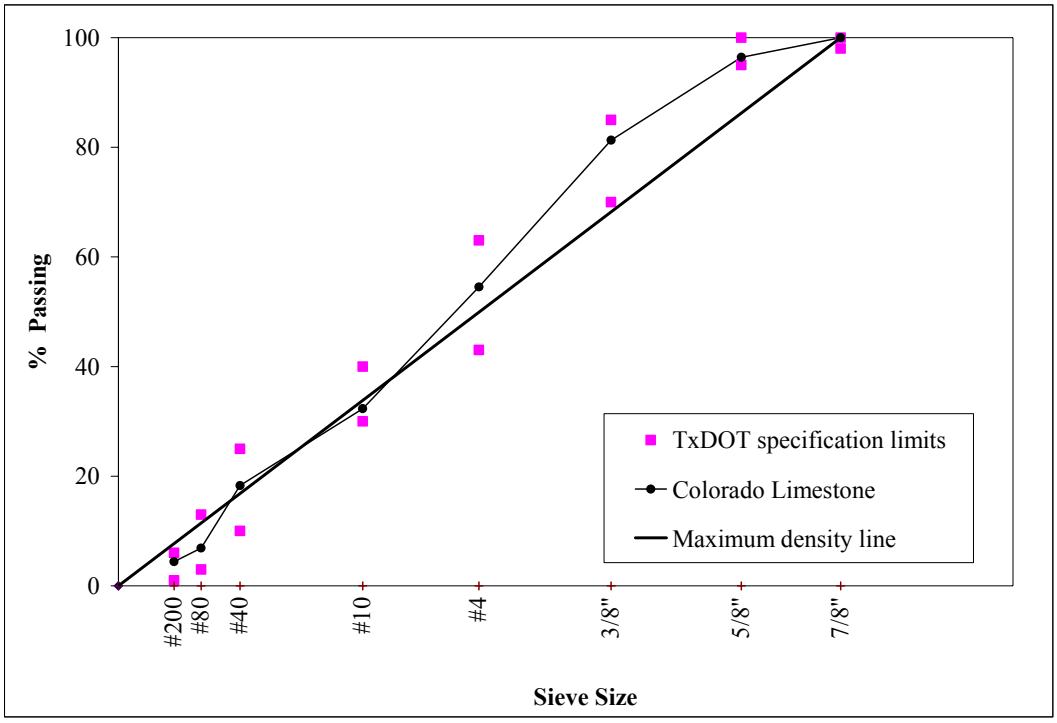

Figure F.1. Gradation of Mix Design Using Limestone from Colorado Materials.

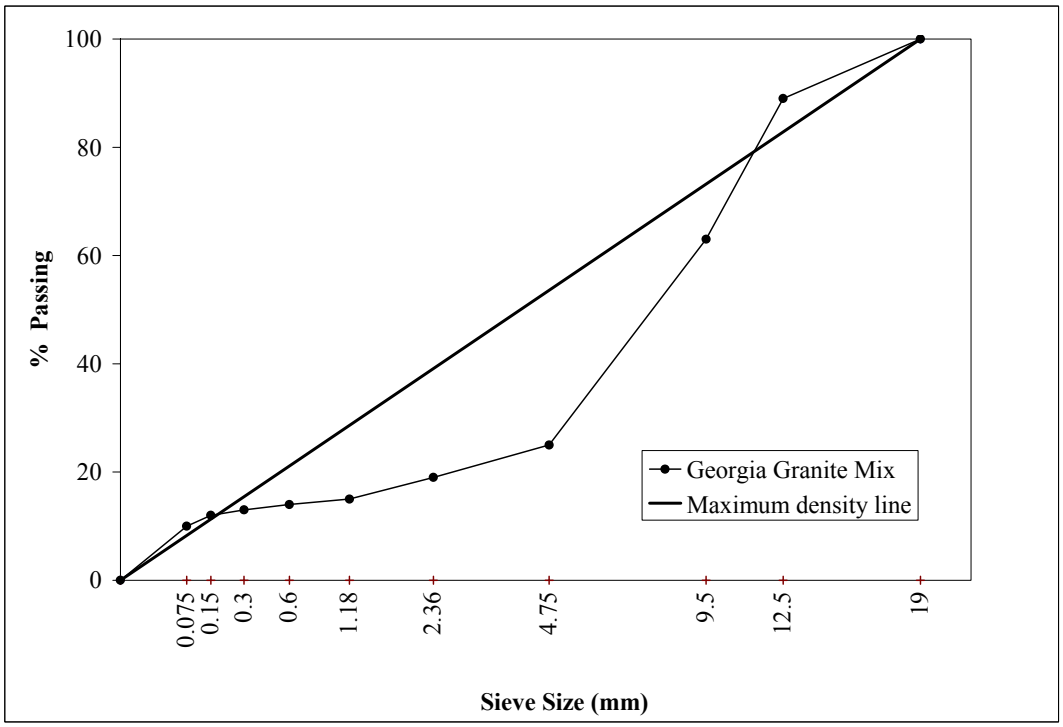

Figure F.2. Gradation of Mix Design Using Granite from Georgia.

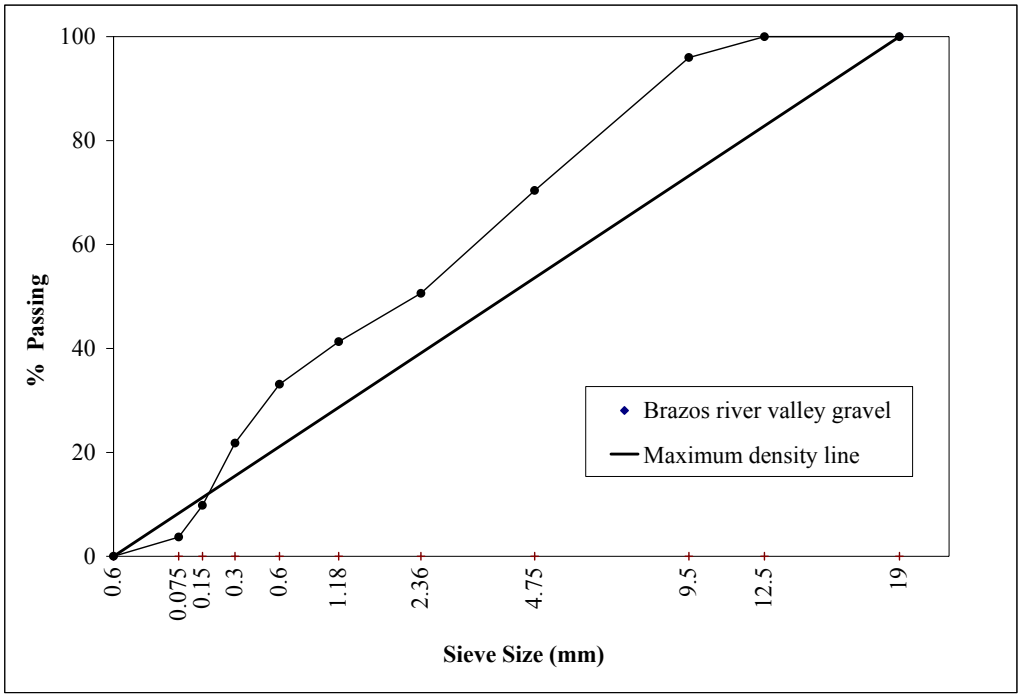

Figure F.3. Gradation of Mix Design Using Gravel from Brazos River Valley.

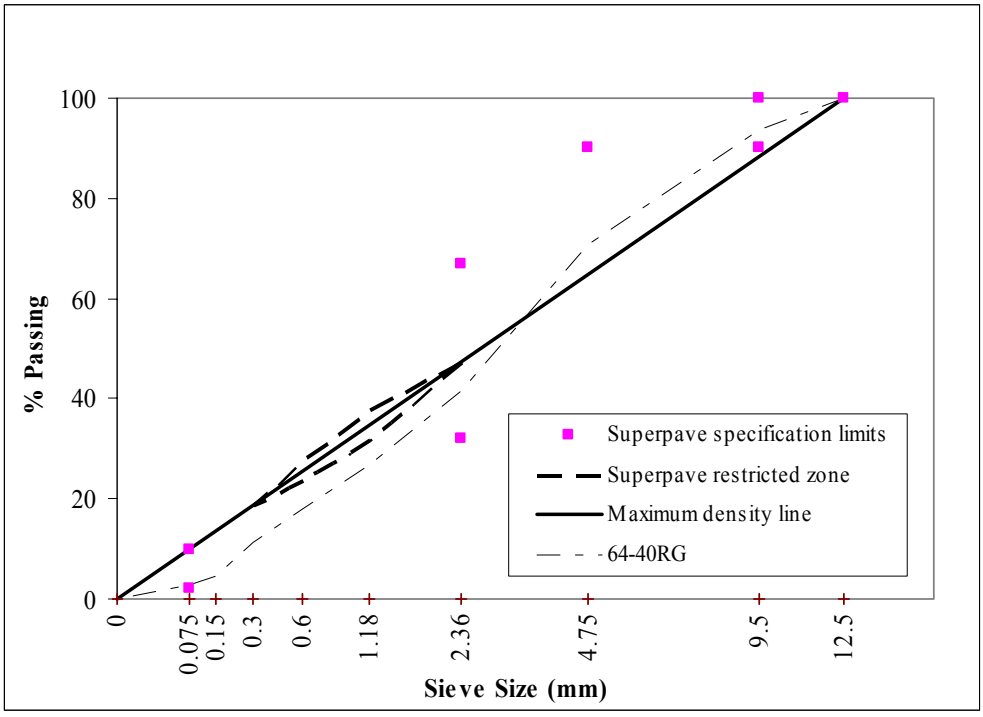

Figure F.4. Gradation of Mix Design Using Gravel from Fordyce.

Note: Specification limits on graphs shown only where available.

APPENDIX G:
HAMBURG TEST DATA

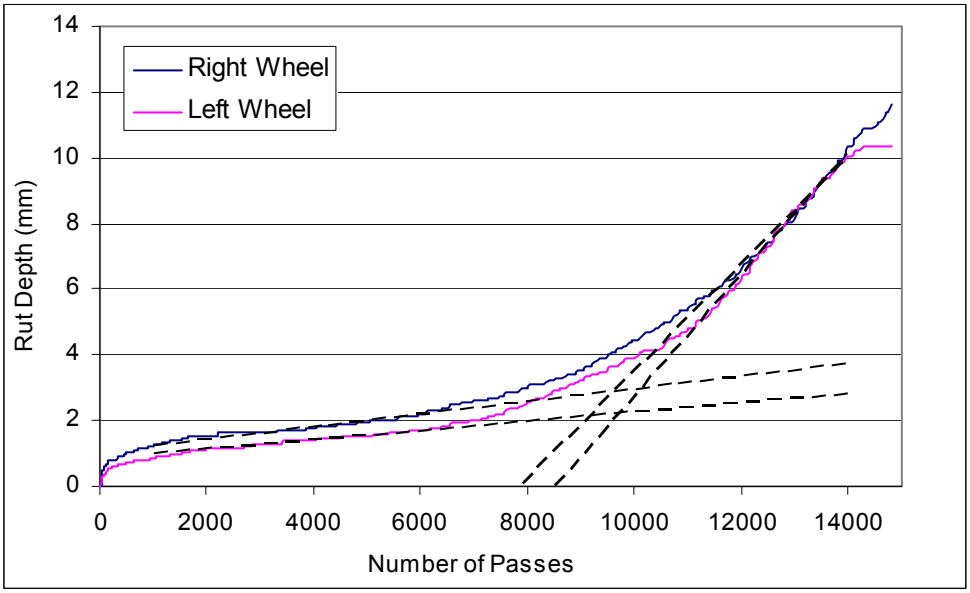

Figure G.1. Hamburg Test Result for Colorado Limestone Mix.

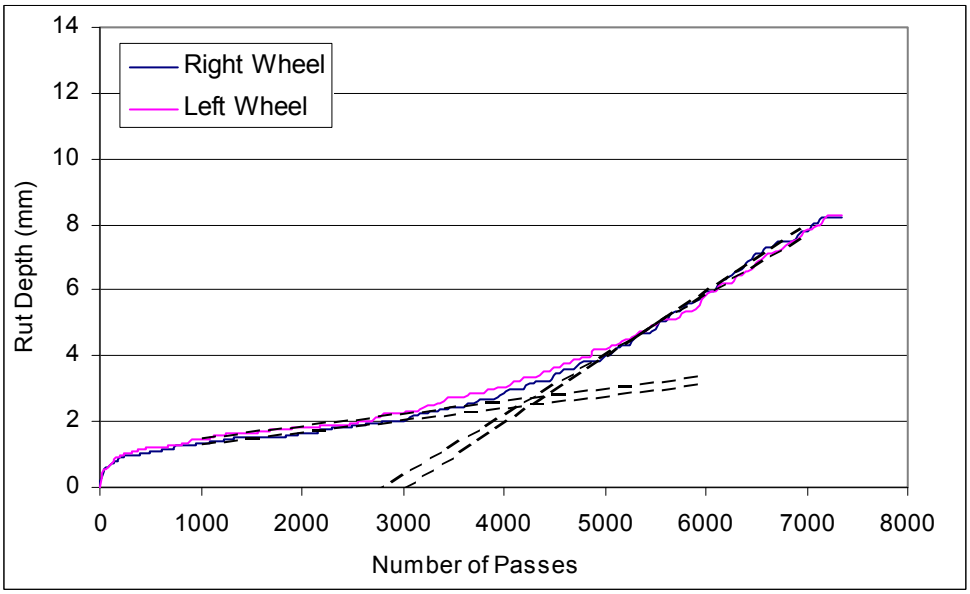

Figure G.2. Hamburg Test Result for Colorado Limestone Mix + 1% Hydrated Lime.

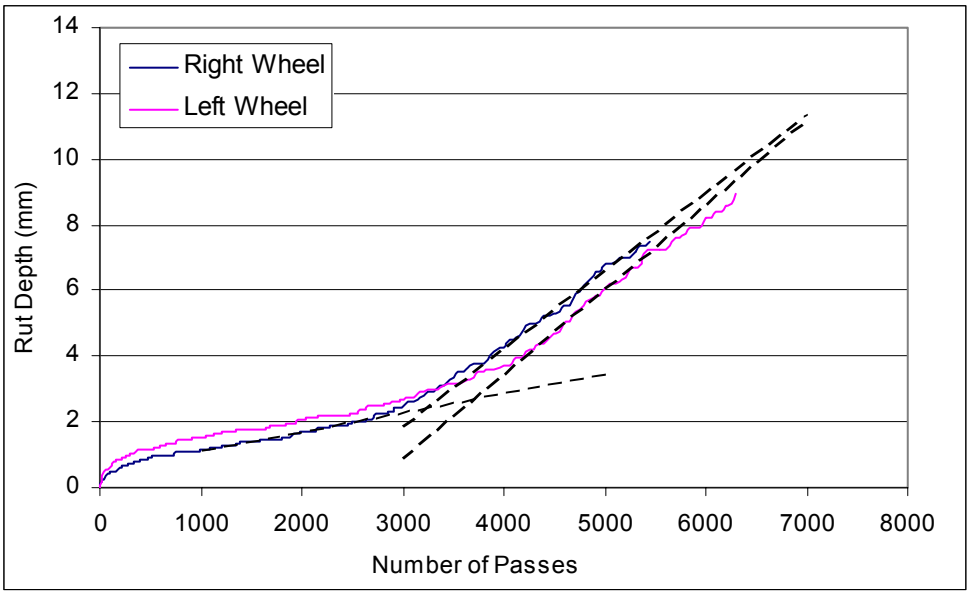

Figure G.3. Hamburg Test Result for Colorado Limestone Mix + 1.5% Perma-Tac.

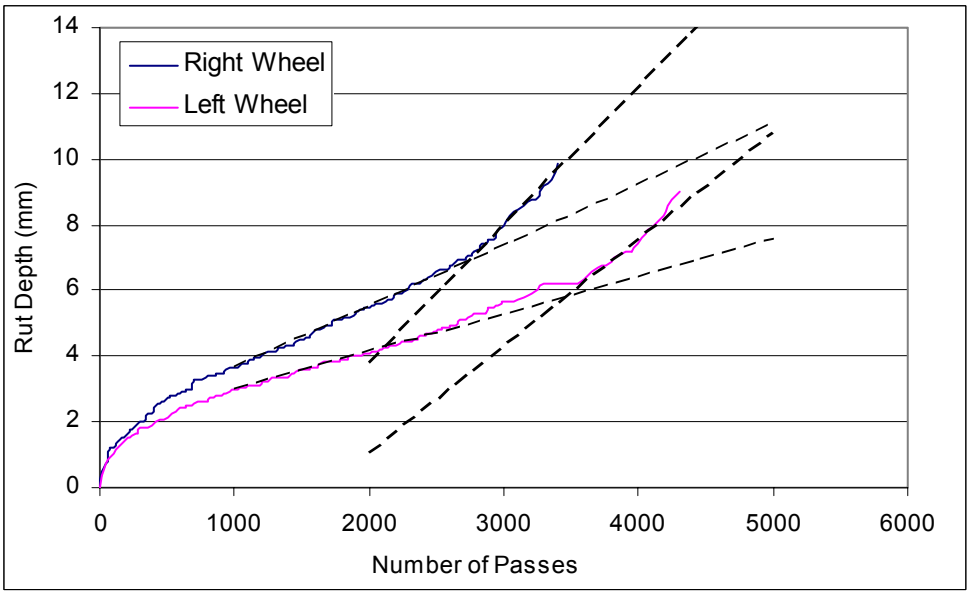

Figure G.4. Hamburg Test Result for Fordyce Gravel Mix.

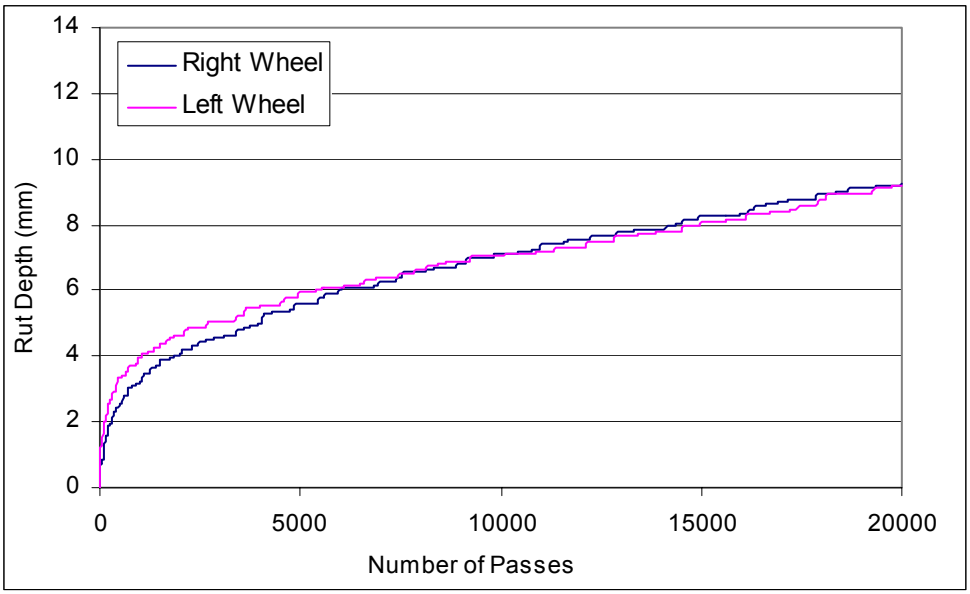

Figure G.5. Hamburg Test Result for Fordyce Gravel Mix + 1% Hydrated Lime.

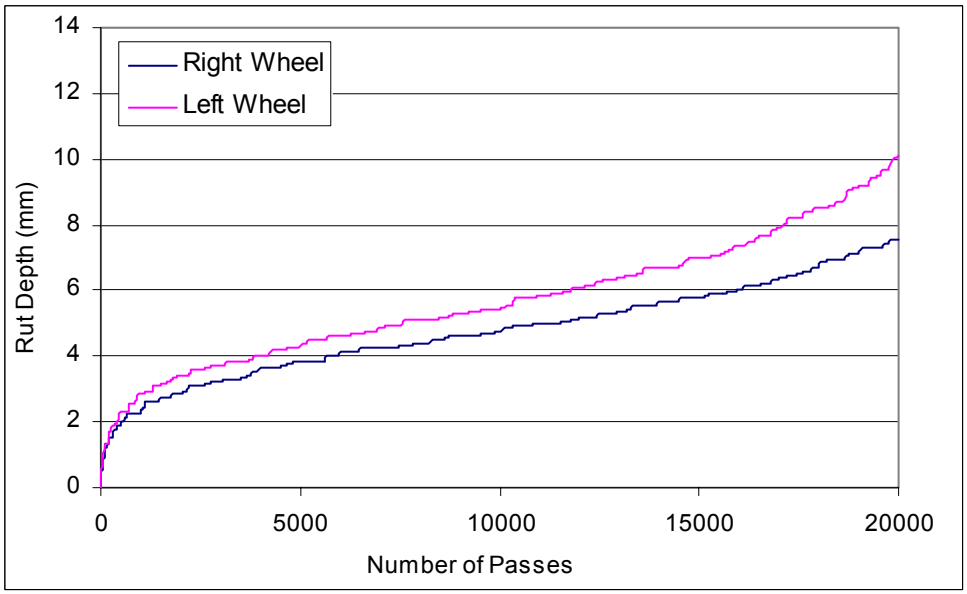

Figure G.6. Hamburg Test Result for Fordyce Gravel Mix + 1.5% Perma-Tac.

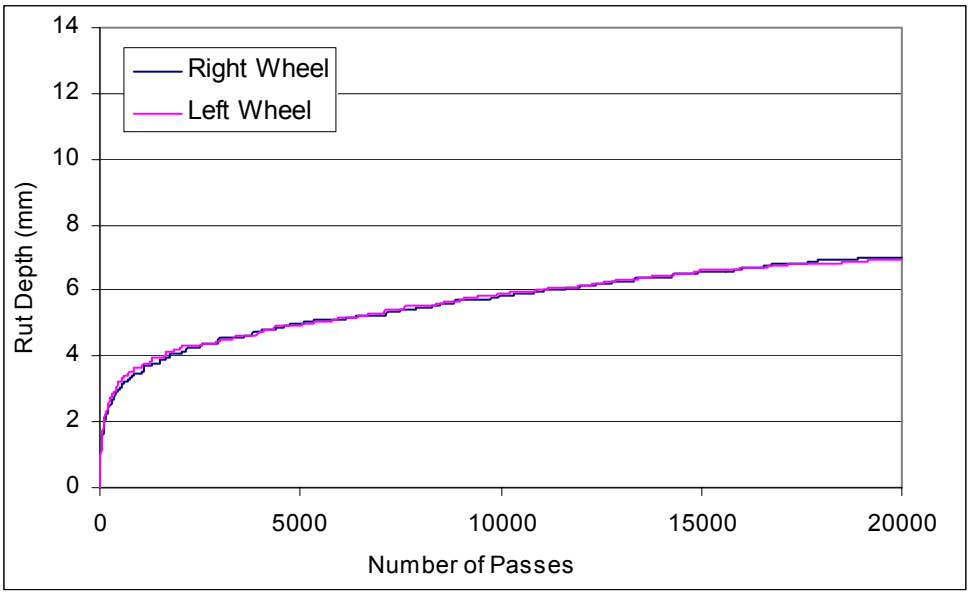

Figure G.7. Hamburg Test Result for Georgia Granite Mix.

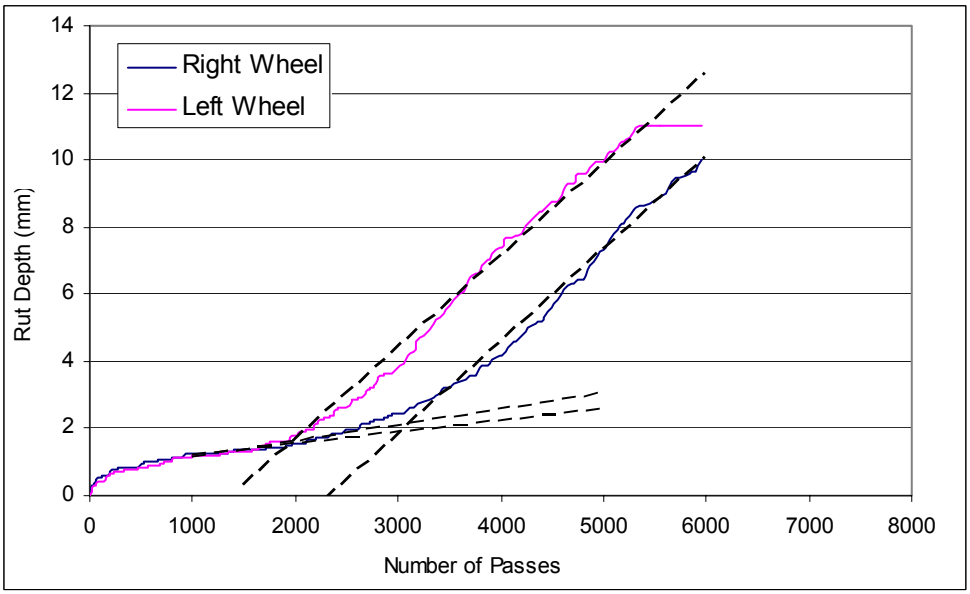

Figure G.8. Hamburg Test Result for Brazos Valley Rounded Gravel Mix.

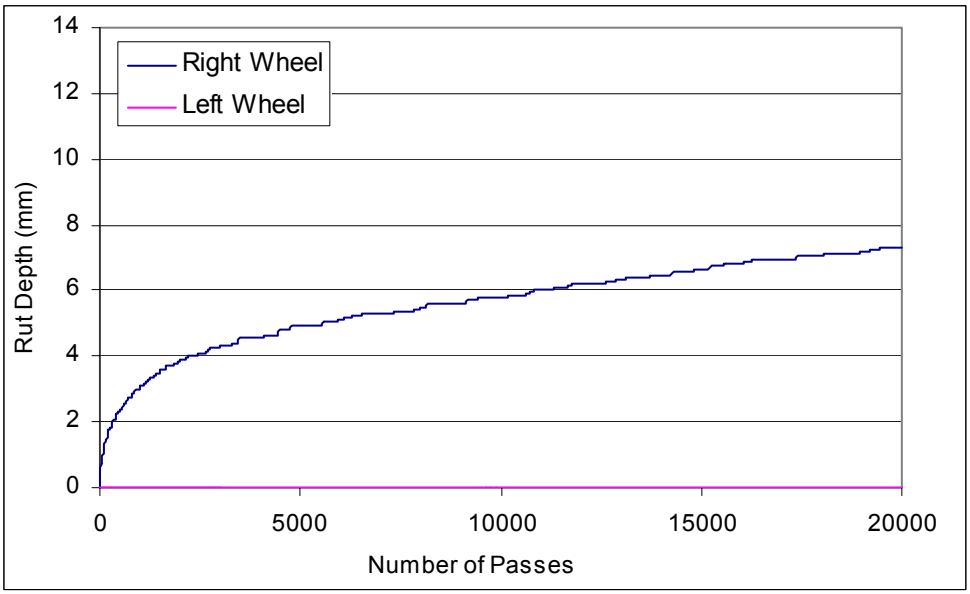

Figure G.9. Hamburg Test Result for Brownwood Limestone Mix.

APPENDIX H:
THEORETICAL BASIS AND TEST PROCEDURES FOR THE UNIVERSAL SORPTION DEVICE AND WILHELMY PLATE METHOD

Universal Sorption Device

Theoretical Background

Surface energy of aggregates is calculated using spreading pressures of three probe vapors on the aggregate surface. The spreading pressure is calculated from an isotherm, which is a plot of the mass of vapor adsorbed on the aggregate surface versus the partial vapor pressure of the probe. The USD that was used in this research project has indigenous software that performs all necessary calculations to provide specific surface area of the aggregate particles and spreading pressure of any given vapors on the aggregate surface. Data generated by the USD for various vapors is compiled in a Microsoft Excel spreadsheet that calculates the surface energy components of the aggregate. The following theoretical background is for information only and, as mentioned earlier, most of the calculations are built into the system software.

Work of adhesion based on total surface of the probe vapor and its spreading pressure on the aggregate is given by:

$$W_a = \pi_e + 2\Gamma_l^T \quad (1)$$

where,

W_a = the work of adhesion,

π_e = spreading pressure at saturation vapor pressure of the solvent, and

Γ^T_l = the total surface energy of the probe vapor.

The work of adhesion is also related to the surface energy of the solid and probe vapor as follows:

$$W_a = 2\sqrt{\Gamma_s^{LW}\Gamma_l^{LW}} + 2\sqrt{\Gamma_s^{+}\Gamma_l^{-}} + 2\sqrt{\Gamma_s^{-}\Gamma_l^{+}} \quad (2)$$

where,

W_a = the work of adhesion,

Γ = the surface energy,

subscript s refers to aggregate,

subscript l refers to probe vapor,

superscript LW refers to the Lifschitz van der Waals or dispersive component,

superscript + refers to the acid component, and

superscript – refers to the base component.

From the above two relationships, the following equality can be established:

$$\pi_e + 2\Gamma_l^T = 2\sqrt{\Gamma_s^{LW}\Gamma_l^{LW}} + 2\sqrt{\Gamma_s^+\Gamma_l^-} + 2\sqrt{\Gamma_s^-\Gamma_l^+} \quad (3)$$

where the various terms are as described earlier.

The adsorbed mass of a vapor on the aggregate surface is related to the spreading pressure using Gibbs equation as follows:

$$\pi_e = \frac{RT}{A}\int_0^{p_0}\frac{n}{P}dP \quad (4)$$

where,

π_e = spreading pressure at saturation vapor pressure of the solvent,

R = universal gas constant,

T = absolute temperature,

A = specific surface area of absorbent,

P = the vapor pressure of the probe vapor, and

n = the mass of the adsorbed vapor on the aggregate surface.

Spreading pressures of three probe vapors with known surface energy values will generate a set of three linear equations based on Equation 3, which can be solved to obtain the three surface energy components of the aggregates.

Description of Test Equipment

A process and instrumentation diagram of the latest test setup is shown in Figure H.1. This setup was developed as a part of the ongoing NCHRP Project 9-37, "Using Surface Energy Measurements to Select Materials for Asphalt Pavements."

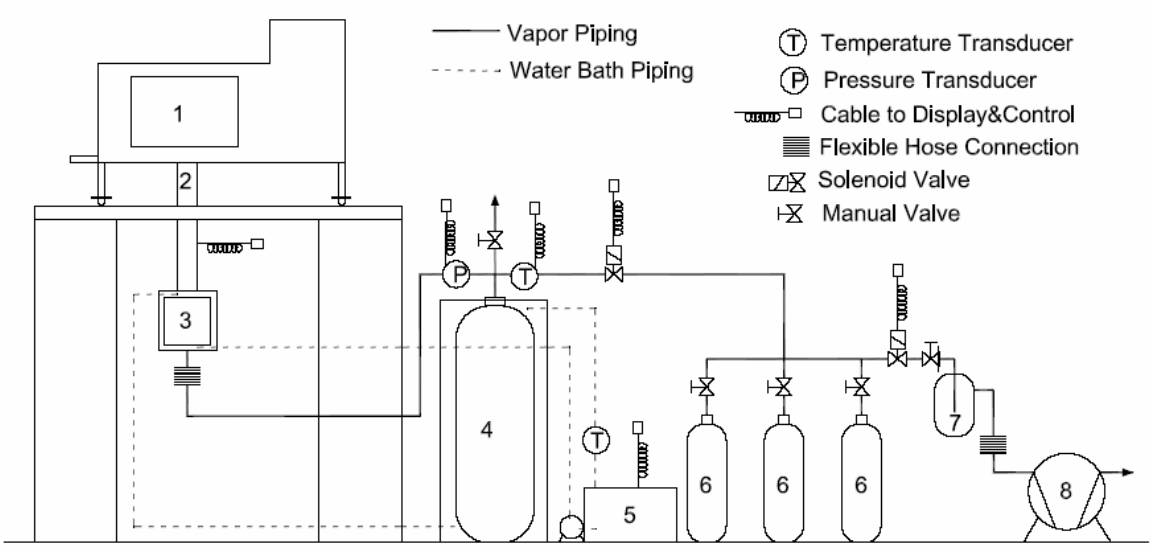

Figure H.1. Layout of Universal Sorption Device System.

1. Microbalance
2. Magnetic suspension
3. Sample cell
4. Buffer Tank
5. Water bath
6. Probe vapor containers
7. Knock out tank
8. Vacuum pump

The mass of probe vapor that is adsorbed on to the aggregate surface is measured using a magnetic suspension balance. The aggregate sample itself is in an airtight cell beneath the balance. The advantage of a magnetic suspension balance is that it uses magnetic force to measure the sample mass and is therefore physically separate from the microbalance.

The test is conducted at a temperature of 77°F (25°C). A water bath is used to circulate water through a jacket of tubing that encloses the main sample cell and the buffer tank vapor pressure during the test procedure is controlled using a solenoid valve with feedback control.

Sample Preparation

About 25 gm of sample is required for each test. The sample is cleaned with distilled water and heated in a conventional oven at 248°F (120°C) for about four to six hours. The sample is then allowed to cool in a desiccator with anhydrous calcium sulfate crystals that prevent adsorption of moisture on the aggregate surface.

Test Procedure

A sample container basket is used to suspend the sample in the balance. This basket is rinsed and air-dried with acetone prior to use. The preconditioned aggregate sample is poured in the basket and suspended from the balance. The test cell is raised and bolted with the top flange using six hexagonal bolts to ensure that the sample is in an airtight environment. The temperature controlling steel jacket is raised to enclose the entire cell assembly. The sample is degassed until the mass of the sample does not show any change indicating that most of the physically adsorbed vapors are removed from the surface. This procedure typically requires about four hours. During the first two hours of degassing, the sample cell and buffer tank are heated to 140°F (60°C) to facilitate removal of any condensate or adsorbed vapors in the system. The temperature is then brought back to 77°F (25°C) for the remainder of the degassing. Once degassing is complete, the adsorption test is performed with the required vapor. The test may proceed for five to 14 hours depending on the aggregate specific surface area. The test sequences are mostly computer controlled. The user is required only at two stages in the test: 1) to load the sample, center the balance, and start degassing; and 2) to start the test after degassing.

Wilhelmy Plate Method

Theoretical Basis

Surface energy components of asphalt are calculated using the contact angles of different probe liquids on the asphalt surface. The Wilhelmy plate method is used for measuring the contact angle of a liquid on the asphalt surface. The WP method is based on kinetic force equilibrium when a very thin plate, suspended from a highly accurate balance, is immersed or withdrawn from a liquid solvent at a very slow and constant speed. The contact angles that develop between an asphalt-coated glass plate and solvent liquids are obtained. The basic principle is schematically illustrated in Figure H.2. The dynamic contact angle between the asphalt-coated plate and the probe liquid, measured during the immersion process, is called the advancing contact angle.

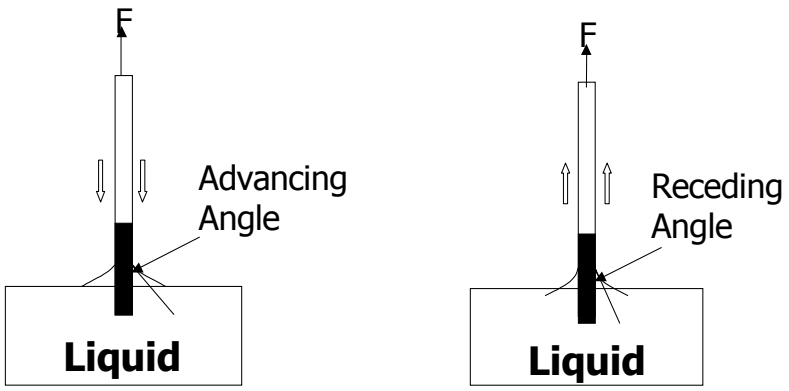

Figure H.2. Schematic Illustration of Wilhelmy Plate Method.

The basic principles of this method that are used to obtain the contact angles and the surface energy components of semi-liquid asphalt are summarized in the following paragraphs. When a plate is suspended in air, Equation 5 is valid:

$$F = Wt_{plate} + Wt_{asphalt} - V.\rho_{air}.g \qquad (5)$$

where,

F is the force measured with the Cahn balance of the DCA (Figure H.3), which is also the force required to hold the plate,

Wt_{plate} and $Wt_{asphalt}$ are the weight of the glass plate and weight of the coated asphalt film, respectively,

V is the volume of the asphalt plate,

ρ_{air} is the density of the air, and

g is the local acceleration of gravity.

When a plate is partially immersed in a fluid, the balance measures the force using equation 6:

$$F = Wt_{plate} + Wt_{asphalt} + P_t\Gamma_L Cos\theta - V_{im}\rho_L g - (V - V_{im})\rho_{air} g \qquad (6)$$

where,

P_t = the perimeter of the asphalt coated plate,

Γ_L = the total surface energy of the liquid,

θ = the dynamic contact angle between the asphalt and the liquid, and

V_{im} = the volume of the immersed plate.

By subtracting Equation 5 from Equation 6, Equation 7 is obtained:

$$\Delta F = P_t \Gamma_L Cos\theta - V_{im}\rho_L g + V_{im}\rho_{air} g \qquad (7)$$

Equation 8 is obtained by rearranging terms in Equation 7, and the contact angle can be calculated from all the parameters on the right hand side, which are determined during the test.

$$Cos\theta = \frac{\Delta F + V_{im}(\rho_L - \rho_{air})g}{P_t \Gamma_L} \qquad (8)$$

The Good-van Oss-Chaudhury (GvOC) equation (2), is used to relate contact angle to surface energy components.

$$\Gamma_l(1 + Cos\theta) = 2\sqrt{\Gamma_s^{LW}\Gamma_l^{LW}} + 2\sqrt{\Gamma_s^{-}\Gamma_l^{+}} + 2\sqrt{\Gamma_s^{-}\Gamma_l^{-}} \qquad (9)$$

where, Γ_l, Γ_l^+, and Γ_l^- are the surface free energy components of the liquid.

This equation is similar to Equation 3 with the difference that, instead of spreading pressure, the contact angle of three probe liquids on the asphalt surface is measured and used for calculating the three surface energy components.

Description of Test Equipment

The Dynamic Contact Angle (DCA) equipment from Cahn was used for this test. Figure H.3 shows a schematic of the test.

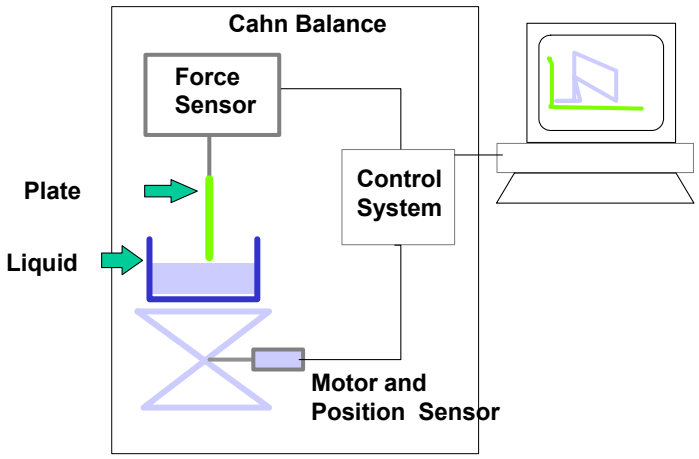

Figure H.3. The Cahn Dynamic Contact Angle Analyzer.

On the left side is the Wilhelmy plate sample chamber in which the asphalt coated glass plate is suspended from the Cahn Balance, and on the right is the data acquisition and processing system using the DCA software. The DCA software directly acquires data from the Cahn Balance and automatically calculates the advancing and receding contact angles.

A typical output of the DCA is shown in Figure H.4. The advancing stage is represented by the bottom part of the hysteresis loop. When the plate advances to the liquid surface and touches it, a meniscus forms, and the force increases substantially. As the plate is immersed, the advancing angle builds up with a corresponding decrease in slope due to buoyancy. As the direction of travel is reversed, the receding angle is measured and, again, a slope due to buoyancy is observed. As mentioned earlier, this force due to buoyancy is accounted for in the equations for determining the contact angle.

Sample Preparation

Glass slides (50 mm by 24 mm by 0.15 mm thick) are used as a substrate for preparing the asphalt specimens. The glass slides are rinsed with distilled water and acetone prior to use. A sample of asphalt is heated in a small container at 194°F to 275°F (90°C - 135°C) depending on the viscosity of the asphalt for about two hours in a conventional oven. Once the asphalt is ready for preparing slides, it is placed over a hot plate set at a sufficiently high temperature to prevent cooling of asphalt. The glass slides are then dipped at about half their length in the asphalt. Excess asphalt is allowed to drain from the slide.

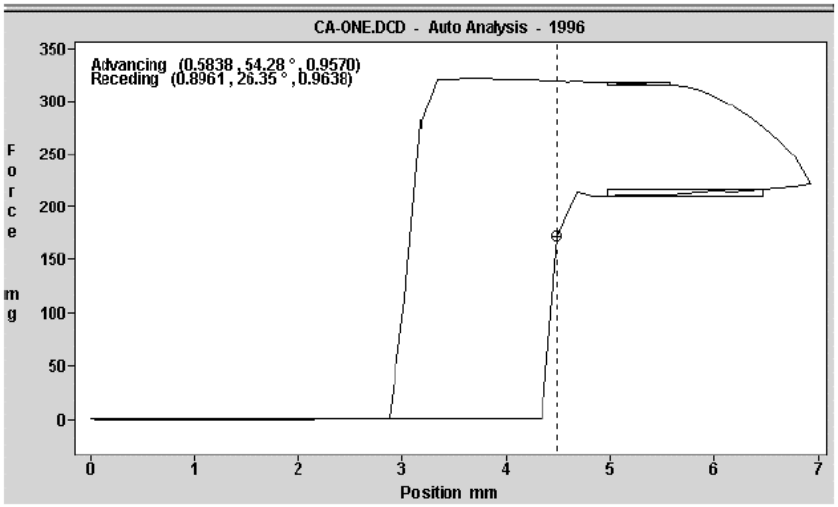

Figure H.4. Cahn Dynamic Contact Angle Analyzer Output.

The slide may be held upside down for a few seconds to promote the formation of a smooth thin film. Six such slides are prepared so that at least two slides are tested with each probe liquid. Once the slides are prepared they are stored in a vacuum desiccator for about 24 hours prior to testing to remove any adsorbed moisture. The dimensions of the test slide are measured and recorded.

Test Procedure

A fresh sample of the probe liquid (99%+ purity) is taken in a 3.05-in^3 (50-cc) glass beaker and placed on the balance base. The asphalt slide is suspended from the top hook of the balance. The WinDCA software is used to control the test and acquire and analyze the data and provide the contact angles. Once the contact angles are obtained, the surface energy components can be calculated using the equations described earlier. Researchers at the Texas Transportation Institute have developed software, CASE, as a part of ongoing NCHRP Project 9-37. This software is useful for selecting appropriate probe liquids for the WP test and for calculating the surface energy components from the contact angle data.

APPENDIX I:
HMA MIXTURE TESTING

Table I.1. Summary of Texas Mixtures Tested (Plant Produced).

Mix No.	Dis-trict	County	High-way	CSJ No.	Mix Type	Asphalt Type	Aggregate	Test Result					Comment
								DM	FT	FN	Hamburg	APA	
1	ATL	Harrison	IH-20	IM-20-7(57)	12.5 mm Superpave	PG 76-22	Quartzite	Link			Link	Link	Surface Course
2	ATL	Harrison	IH-20	IM-20-7(57)	12.5 mm Superpave	PG 76-22	Sandstone	Link			Link	Link	Surface Course
3	ATL	Harrison	IH-20	IM-20-7(57)	12.5 mm Superpave	PG 76-22	Siliceous River Gravel	Link			Link	Link	Surface Course
4	ATL	Harrison	IH-20	IM-20-7(57)	Type C	PG 76-22	Quartzite	Link			Link	Link	Surface Course
5	ATL	Harrison	IH-20	IM-20-7(57)	Type C	PG 76-22	Sandstone	Link			Link	Link	Surface Course
6	ATL	Harrison	IH-20	IM-20-7(57)	Type C	PG 76-22	Siliceous River Gravel	Link			Link	Link	Surface Course
7	ATL	Harrison	IH-20	IM-20-7(57)	CMHB-C	PG 76-22	Quartzite	Link			Link	Link	Surface Course
8	ATL	Harrison	IH-20	IM-20-7(57)	CMHB-C	PG 76-22	Sandstone	Link			Link	Link	Surface Course
9	ATL	Harrison	IH-20	IM-20-7(57)	CMHB-C	PG 76-22	Siliceous River Gravel	Link			Link	Link	Surface Course
10	ATL	Harrison	IH-20	IM-20-7(57)	Type B	PG 76-22	Limestone	Link			Link	Link	Base Course
11	AUS	Travis	-	-	Type D	PG 64-22	Limestone	Link	Link	Link	Link	Link	TxAPT Surface
12	AUS	Travis			Type B	PG 64-22	Limestone	Link			Link		Base Course
13	AUS	Travis			Type C	PG 76-22	Limestone (Centex Mat)	Link			Link		Surface
14	CRP	Various			Type B	PG 76-22	Gravel (Wright)	Link			Link		Base Course
15	CRP	Various			Type C	PG 76-22	Limestone + Gravel	Link			Link		Surface Course
16	LBB	Lubbock		006801052	CMHB-C	PG 70-28	Granite	Link			Link		Surface Course

DM: Dynamic Modulus FT: Flow Time FN: Flow Number Link to test result

Table I.1. Summary of Texas Mixtures Tested (Plant Produced) (continued).

Mix No.	Dis-trict	County	High-way	CSJ No.	Mix Type	Asphalt Type	Aggregate	Test Result					Comment
								DM	FT	FN	Hamburg	APA	
17	LBB	Lubbock		078301079	Type B	PG 70-28	Limestone	Link					Base Course
18	LRD	Webb	US 359	0086-02-019	Type D	PG 76-22		Link					Surface Course
19	SAT	Medina	US 90	0024-06-060	Type C	PG 70-22	Trap Rock & Limestone	Link					
20	WAC	McClennan	IH-35	0015-01-164	Superpave	PG 70-22	Igneous	Link					Perpetual Pavement Project
21	WAC	McClennan	IH-35	0015-01-164	3/4" Stone-Filled	PG 76-22		Link					
22	WAC	McClennan	IH-35	0015-01-164	1" Stone-Filled	PG 76-22		Link					
23	WAC	McClennan	IH-35	0015-01-164	SMA	PG 76-22		Link					Test on two lots
24	WAC	Bell	US 190	0185-01-032	Type C	PG 76-22		Link			Link		
25	YKM	Various			Type D	PG 70-22	Gravel	Link			Link		

DM: Dynamic Modulus FT: Flow Time FN: Flow Number Link to test result

Table I.2. Summary of Texas Mixtures Tested (Lab Mixed).

Mix No.	Dis-trict	County	High-way	CSJ No.	Mix Type	Asphalt Type	Aggregate	Test Result					Comment
								DM	FT	FN	Hamburg	APA	
1	ATL	Harrison	IH-20	IM-20-7(57)	12.5 mm Superpave	PG 76-22	Quartzite	Link			Link		
2	ATL	Harrison	IH-20	IM-20-7(57)	12.5 mm Superpave	PG 76-22	Sandstone	Link			Link		
3	ATL	Harrison	IH-20	IM-20-7(57)	12.5 mm Superpave	PG 76-22	Siliceous River Gravel	Link			Link		
4	ATL		IH-30										Corey
5	ATL				CMHB-C		Gravel						
6													
7	AUS				Type D		Limestone						TxAPT Surface
8	AUS				Type B		Limestone	Link					Base Course
9	AUS				Type C		Limestone (Centex Mat)						Surface
10	BRY	Wash-ington	US 290		Type C	PG 64-22	Limestone	Link					
11	BRY				CMHB-C	PG 64-22	Limestone						Task 3
12	CRP				Type B		Gravel	Link	Link	Link	Link		Task 6
13	CRP				Type C		Gravel	Link	Link	Link	Link		Task 6
14	CRP				Type D		Gravel	Link	Link	Link	Link		Task 6
15	CRP				Type B								
16	CRP				Type C								
17	Fujie							Link					
18	FTW	Wise	SH-114	0350-01-026	19 mm SHHMAC	PG 64-22	Bridgeport	Link			Link		Rich Bottom

DM: Dynamic Modulus FT: Flow Time FN: Flow Number Link to test result

Table I.2. Summary of Texas Mixtures Tested (Lab Mixed) (continued).

Mix No.	Dis-trict	County	High-way	CSJ No.	Mix Type	Asphalt Type	Aggregate	Test Result					Comment
								DM	FT	FN	Hamburg	APA	
19	FTW	Wise	SH-114	0350-01-026	25 mm SFHMAC	PG 70-22	Bridgeport	Link			Link		Base Course
20	FTW	Wise	SH-114	0350-01-026	19 mm SPHMAC	PG 76-22	Bridgeport	Link			Link		Level-up Course
21	LRD				Type B		Gravel	Link	Link	Link	Link		Task 6
22	LRD				Type C		Gravel	Link	Link	Link	Link		Task 6
23	LRD				Type D		Gravel	Link	Link	Link	Link		Task 6
24	LRD		IH-35		19 mm SMA	PG 70-22	Traprock	Link	Link	Link	Link	Link	Task 3
25	LRD				Type C			Link					
26	LRD				Type D			Link					
27	PHR				19 mm Superpave		Gravel	Link	Link	Link	Link		Task 6
28	PHR				12.5 mm Superpave		Gravel	Link	Link	Link	Link		Task 6
29	PHR				9.5 mm Superpave		Gravel	Link	Link	Link	Link		Task 6
30	YKM		US 59		12.5 mm Superpave	PG 76-22	Gravel	Link					0-4468
31	YKM				Type A	PG 64-22	Gravel	Link					Task 2B
32	YKM				Type B	PG 64-22	Limestone	Link					Task 2B
33	YKM				Type B	PG 70-22	Gravel	Link					Task 2B
34	YKM				Type C	PG 70-22	Limestone	Link					Task 2B
35	YKM				Type C	PG 70-22	Gravel	Link					Task 2B
36	YKM				Type D	PG 64-22	Limestone	Link					Task 2B

DM: Dynamic Modulus FT: Flow Time FN: Flow Number Link to test result

Table I.2. Summary of Texas Mixtures Tested (Lab Mixed) (continued).

Mix No.	Dis-trict	County	High-way	CSJ No.	Mix Type	Asphalt Type	Aggregate	Test Result					Comment
								DM	FT	FN	Hamburg	APA	
37	YKM				Type D	PG 64-22	Gravel	Link					Task 2B
38	YKM				Type C	PG 76-22	Limestone	Link	Link	Link	Link	Link	Task 3
39	YKM				Type D		Limestone	Link					
40	WAC		IH-35		12.5 mm Superpave			Link					
41	WAC				3/4" Stone-Filled			Link					
42	WAC				1" Stone-Filled			Link					
43	WAC				SMA			Link					
44	WAC		IH-35		SMA			Link					
45	WAC		US 190		Type C			Link					
46	WFS				12.5 mm Stone-Filled	PG 76-22	Limestone	Link					Task 3
47	LBB				CMHB-C			Link					
48	LBB				Type B			Link					
49	BWD				Type C	PG 64-22	Limestone	Link			Link		0-4523

DM: Dynamic Modulus FT: Flow Time FN: Flow Number Link to test result